

Forest Fire Modelling

Luca Malangone



Unione Europea



*Ministero dell'Istruzione,
dell'Università e della Ricerca*



UNIVERSITÀ DEGLI
STUDI DI SALERNO

FONDO SOCIALE EUROPEO

Programma Operativo Nazionale 2007/2013

“Ricerca Scientifica, Sviluppo Tecnologico, Alta Formazione”

Regioni dell’Obiettivo 1 – Misura III.4

“Formazione superiore ed universitaria”

Department of Industrial Engineering

*Dottorato di Ricerca in Scienza e Tecnologie per
l’Industria Chimica, Farmaceutica e Alimentare
(XI Cycle-New Series)*

FOREST FIRE MODELLING

Supervisor

Prof. Salvatore Vaccaro

Ph.D. student

Luca Malangone

Scientific Committee

Prof. Paola Russo

Prof. Domingos Xavier Viegas

Ph.D. Course Coordinator

Prof. Paolo Ciambelli

To my parents

Acknowledgments

Over the past three years, several people have contributed in different ways to shape my research work. First of all, I would like to express my deepest gratitude to my supervisor, prof. Salvatore Vaccaro for giving me the opportunity to accomplish such a complex and very interesting field of study offering me support, encouragement, positive discussion, criticism and motivation to finish it.

I would like to truly thank prof. Paola Russo, my second supervisor, for the positive discussions and recommendations for my work and for patiently sharing my ups and down throughout this time

Special thanks to prof. Domingos X. Viegas for approving and positively assessing my work, giving me support and a great deal of encouragement.

Thanks to prof. Paolo Ciambelli for his support and coordination activity.

I would also like to thank all the present and former members of the department of Industrial Engineering for creating a very dynamic and positive working experience.

Last, but not least, my deepest gratitude goes to my family for supporting and lifting me up during the hard moments

List of References

1. Malangone L., Russo P., Vaccaro S., Viegas, DX (2012): *Fire Behaviour in Canyons due to symmetric and asymmetric ignitions*. International Congress "Fire Computer Modeling" October 18-19th, Santander (Spain) ISBN 978-84-86116-69-9.
2. Malangone L., Russo P., Vaccaro S.(2012): *Simulation by a physical model of fire spread within a relatively large domain with complex geometry*. XXXV Meeting of the Italian Section of the Combustion Institute, Milano, 10-12 Ottobre. doi:10.4405/35proci2012.III1, ISBN: 978-88-88104-14-0.
3. Malangone L., Russo P., Vaccaro S. (2011): *Effects of wind and terrain slope on flames propagation in a vegetative fuel bed*. XXXIV Event of the Italian Section of the Combustion Institute Roma, 24-26 October. doi:10.4405/34proci2011.III22, ISBN: 978-88-88104-13-3.
4. Malangone L., Russo P., Vaccaro S. (2011): *Ruolo del carico di combustibile superficiale nella propagazione di un incendio forestale*. Convegno Scientifico Nazionale Sicurezza nei Sistemi Complessi, VI Edizione, Bari 18-19-20 ottobre.
5. Malangone L., Russo P., Vaccaro S. (2011): *The role of the terrain geometry on the flames propagation through a vegetative fuel bed*. In MCS 7, Mediterranean Combustion Symposium, Chia Laguna, Cagliari, Sardinia, Italy, September 11-15, ISBN: 978-88-88104-12-6
6. Ciambelli P., Malangone L., Russo P., Vaccaro S. (2010): *Preliminary Modelling Study of Wildland Fires by WFDS*. In: VI International Conference on Forest Fire Research. Coimbra, 15-18 November, 2010.
7. Ciambelli P., Malangone L., Russo P., Vaccaro S. (2010). *Preliminary Study of Wildland Fires*. In: Processes and Technologies for a Sustainable Energy. Ischia, June 27-30, 2010, vol. unico. p. IV-3,1-IV-3,6, ISBN: 978-88-88104-11-9, doi: 10.4405/ptse2010.IV3

Contents

Chapter I - Forest fires and fire management

I.1 Wildland fires as agents of damage of wooded areas	1
I.1.1 European statistics	3
I.1.2 Global emissions of selected pyrogenic species	6
I.2 Management activities over fire prevention and suppression	7
I.3 Role of fire behaviour modelling	8
I.2 Aim of the work	9
I.3 Outline of the thesis	9
I.4 References	10

Chapter II - Literature review and main characteristics of the prediction tools used for surface vegetation fires

II.1 Fundamentals of fire and combustion phenomenon	13
II.1.1 Fuel chemistry	15
II.1.2 Solid phase reactions: competing processes	16
II.1.3 Gas phase reactions	18
II.2 Physics of combustion	18
II.2.1 Advection or Fluid transport	19
II.2.2 Buoyancy, convection and turbulence	19
II.2.3 Radiant heat transfer	20
II.2.4 Firebrands (solid fuel transport)	20
II.2.5 Atmospheric interactions	21
II.2.6 Topographic interactions	21
II.3 Physical Models	21
II.3.1 Weber (1991)	22
II.3.2 AIOLOS-F (CINAR S.A., Greece)	23
II.3.3 FIRETEC (Los Alamos National Laboratory, USA)	23
II.3.4 Forbes (1997)	24
II.3.5 Grishin (Tomsk State University, Russia)	24
II.3.6 IUSTI (Institut Universitaire des Systemes Thermiques Industriels, France)	25
II.3.7 PIF97	26

II.3.8 LEMTA (Laboratoire d'Énergétique et de Mécanique Théorique et Appliquée, France)	27
II.3.9 UoS (University of Salamanca, Spain)	27
II.3.10 WFDS (National Institute of Safety Technology, USA)	28
II.4 Discussion and summary	29
II.5 References	32

Chapter III - Forest fire modelling: basic equations and numerical constraints

III.1 Physical mechanisms and characteristic length scales	37
III.2 Fundamental equations	41
III.3 Simulation conditions	43
III.3.1 Domain meshing	44
III.4 References	46

Chapter IV- Fire propagation on flat and sloped surface. Role of the surface fuel in generating a crown fire

IV.1 Introduction	49
IV.2 Simulation conditions	50
IV.2.1 Flat and sloped terrain	50
IV.2.2 Forest stand domain	51
IV.3 Results and discussion	53
IV.3.1 Flat and sloped terrain	53
IV.3.2 Forest stand domain	61
IV.4 Conclusions	67
IV.5 References	68

Chapter V - Fire propagation across double-slope and canyon configurations

V.1 Introduction	69
V.2 Simulation conditions	71
V.2.1 Double-slope domain	71
V.2.2 Canyon configuration	73
V.3 Results and discussion	73
V.3.1 Double-slope domain	73
V.3.2 Canyon configuration	77

V.3.2.1 Effect of the position of the ignition source	81
V.3.2.1.1 Symmetric vs. asymmetric ignition: qualitative comparison	82
V.3.2.1.2 Symmetric vs. asymmetric ignition: quantitative comparison	83
V.4 Conclusions	89
V.5 References	90
Chapter VI - Simulation of fire spread within a relatively large scale domain with complex geometry	
VI.1 Introduction	93
VI.2 Simulation conditions	94
VI.3 Results and discussion	96
VI.4 Conclusions	97
VI.5 References	98
Chapter VII - Conclusions	99

Index of figures

Figure I.1 Total area of fires burned in North America, Europe and CIS – countries IFFN (2002).	2
Figure I.2 Burnt area in the Southern Member States	3
Figure I.3 Number of fires in the Southern Member States	3
Figure I.4 Average fire size in the Southern Member States	4
Figure I.5 The wildland fire triangle.	7
Figure II.1 Schematic of chemical structure of portion of neighbouring cellulose chains, indicating some of the hydrogen bonds (dashed lines) that may stabilise the crystalline form of cellulose (Source: Ball et al. (1999))	15
Figure II.2 Degradation of wood by low-temperature and high-temperature pathways	17
Figure II.3 Mass fraction and time derivative of the mass fraction as functions of temperature for several softwoods	17
Figure III.1 Mechanisms of thermal degradation of vegetation	41
Figure III.2 Experimental fire and simulation (using WFDS) carried out in a tall Douglas fir (Mell et al., 2009)	44
Figure IV.1 Configuration of the computational forest domain. d is the distance between the tree trunks. Wind is constant at the boundary surface (\rightarrow) and blows along x at 5 m/s.	51
Figure IV.2 Fire spreading on flat and sloped terrains in the absence of wind. Colourbar for the temperatures in the gas phase (in correspondence of $y=0$) is reported on the right.	53
Figure IV.3 Fire spreading on flat and slope terrains for wind blowing at 5 m/s along x . Colourbar for the temperatures in the gas phase (in correspondence of $y=0$) is reported on the right.	54
Figure IV. 4a (left column) Surfaces (m^2) spanned by the fire in time (s) at fixed domain inclinations (α) for different wind velocities (v in m/s)	56
Figure IV.4b (right column) Surfaces (m^2) spanned by the fire in time (s)	

at fixed wind velocities (v) for different domain inclinations (slope)	56
Figure IV.5a (left) Influence of the terrain slope on the rate of spread (ROS= R_l) in (m/s) at different wind velocities.	58
Figure IV.5a (right) Influence of wind velocity on the rate of spread (ROS= R_l) in (m/s) at different terrain slopes. Symbols stand for results of simulations while curves are calculated by Eq. IV.6.	58
Figure IV.6a (left) Influence of the terrain slope on the rate of spread (ROS _i) in (m/s) at different wind velocities.	59
Figure IV.6b (right) Influence of wind velocity on the rate of spread (ROS _i) in (m/s) at different terrain slopes. Symbols stand for results of simulations. Lines represent the interpolating curves.	59
Figure IV.7 Time evolution of HRR for flat domain under calm ($v=0$ m/s) and windy ($v=4$ m/s) conditions.	60
Figure IV.8a Distance spanned by the fire front at the ground level at different d for fixed ρ_F (1: $\rho_F=0.90$; 2: $\rho_F=1.80$; 3: $\rho_F=2.70$) (cfr. Table IV.2). Black lines mark the separation ($x=5$ in Figure IV.1) between the zone where only surface fuel existed and that where both fuels were present.	61
Figure IV.8b Distance spanned by the fire front at the ground level at different ρ_F for a fixed d (1: $d=0$; 2: $d=-1$; 3: $d=1$) (cfr. Table 2). Black lines mark the separation ($x=5$ in Figure 1) between the zone where only surface fuel existed and that where both fuels were present.	61
Figure IV.9 Time evolution of the temperature space profiles on the $y=0$ plane, for the case A1 of Table IV.2, during a surface to crown fire transition. Colourbar on the top is the same for each time step	62
Figure IV.10 Temperature space profiles at $t=143.4$ s on the $y=0$, $y=-1$ and $y=-2$ planes (cfr. Figure IV.1) for the case C2 of Table 2. Solid lines represent the sections of the tree stand cut by the y planes	63
Figure IV.11 x -component of the velocity field at 80 s in correspondence of the base of the tree canopies ($z=1$ m). (left): $d= 3$ m (case A1 of Table IV.3), (centre): $d= 2$ m (case B1 of Table IV.3) and (right): $d= 4$ (case C1 of Table IV.3).	64
Figure IV.12 Time evolution of the temperature space profiles on the $z=0$ plane. $d=3$ m. (left) $\rho_F =0.90$ kg/m ³ (case A1 of Table IV.3) and (right) $\rho_F=2.70$ kg/m ³ (case A3 of Table IV.3).	66

Figure IV.13 Time evolution of HRR. $d=3$ m. (blue line) $\rho_F=0.90$ kg/m ³ (case A1 of Table IV.3) and (red line) $\rho_F=2.70$ kg/m ³ (case A3 of Table IV.3)	66
Figure V.1 Double-slope plane configuration.	71
Figure V.2 Dihedral plane during a fire test (Viegas 2010b)	72
Figure V.3 Canyon Configuration ($\beta=\delta= 40^\circ$)	73
Figure V.4 Comparison between the experimental and simulated rate of spread for flames moving on plane b	74
Figure V.5 Comparison between the experimental and simulated rate of spread for flames moving on plane a	74
Figure V.6 Evolution in time of the fire profiles. Red line marks the changing in slope between the two faces forming the dihedral table. Time in seconds is reported for each profile.	75
Figure V.7 Heat Release Rate (HRR) vs. time on the plane a for $\beta=-20^\circ$ and -40° .	76
Figure V.8. Heat Release Rate (HRR) vs. time on the plane a, at $\beta= 20^\circ$ and 40° . Plane a ignition time: 30s and 75s at $\beta= 40^\circ$ and 20° , respectively	76
Figure V.9 Comparison between experimental and simulation results (MC=0.13). Dotted lines, at 78, 107 and 124 s, evidence the different fire contours between the experimental and simulation results.	77
Figure V.10 Comparison of burnt area growth in canyon configuration between the experimental tests and the simulated results at different moisture contents. Exponential fitting curves are represented by solid lines.	78
Figure V.11 Heat release rate profiles for canyon geometry at different moisture content (MC)	79
Figure V.12 Pinus needles: Comparison between experimental (solid line) and simulated results (solid+squares line)	80
Figure V.13 Fire simulation for the symmetric ignition. Frame times: 5s; 20s; 40s; 60s; 80s; 100s; 120s; 140s	82
Figure V.14 Fire simulation for the asymmetric ignition. Frame times: 50s; 130s; 210s; 280s; 320s; 340s; 380s; 400s; 420s; 460s; 500s; 550s.	82

Figure V.15 Time profiles of HRR for the cases of symmetric (right) and asymmetric (left) ignition source.	83
Figure V.16 Fire shape evolution in time for symmetric ignition (grey dot). Time step between lines is 20 s	84
Figure V.17 Fire shape evolution in time for asymmetric ignition (grey dot). Time step between lines is 40 s. First fire profile is at 20 s	85
Figure V.18 Surface evolution in time for symmetric ignition ($\beta=40^\circ$ top, $\beta=40^\circ$ bottom)	86
Figure V.19 Surface evolution in time for the asymmetric ignition ($\beta=40^\circ$ top, $\beta=40^\circ$ bottom)	87
Figure V.20 HRR time evolution for the asymmetric ignition ($\beta=40^\circ$)	88
Figure VI.1 Aerial view of the Lousã area (left), its visualization in SURGE software (top) and its conversion in WFDS code (right).	94
Figure VI.2 Time shape profiles. Dashed line: canyon water line	96
Figure VI.3 Area growth in the field experiment compared with the modelled results	96

Index of tables

Table I.1 Number of fires and burnt area in the five Southern Member States in the last 32 years (FFEMA, 2011)	4
Table I.2: Global emissions of selected pyrogenic species in the late 1990s (In mass of species per year; Tg/a) (IFFN 2004).	6
Table II.1 Outline of the major biological, physical and chemical components and processes occurring in a wildland fire and the temporal and spatial (vertical and horizontal) scales over which they occur (Sullivan, 2008)	14
Table II.2 Approximate analysis of some biomass species (Shafizadeh, 1982)	16
Table II.3 Summary of the physical models (1990-present) discussed	22
Table II.5 Summary of the physical models (adapted from Sullivan, 2008)	30
Table III.1 Typical attenuation length scale for various ecosystems	40
Table IV.1 Physical properties of the fuel families in the forest domain	52
Table IV.2 Numerical simulations set in the forest domain	52
Table IV.3 Parameters of Equations IV.2 to IV.5 obtained through linear and quadratic fitting	57

Summary

Wildland fires have always been undesired and dangerous events. The danger includes the destruction of a renewable natural resource, damage of the atmospheric environment through the emissions of pollutant gases, which contribute to the greenhouse effect, and threat to the lives of people living in the areas surrounding the place where fire occurs and of the members of firefighting teams. To cope with all this, it is necessary to know the behaviour of the fire in order to be able to make adequate and proper decisions that will assist activities implemented in fire suppression and prevention. In this context, fire behaviour modelling is utilized to determine these characteristics and to simulate fire propagation in a variety of vegetations, under diverse climatic and topographic conditions.

In this context the aim of the thesis work was to study and describe the fire propagation under different fuel features and boundary conditions with particular attention to terrain configurations where fire propagation may be characterized by abrupt variations in intensity and propagation rate. These areas include double-slope domain and canyons where such a phenomena (commonly identified as eruptive behaviour) occurs without any change in the main factors governing the fire propagation (i.e. atmospheric condition, vegetative fuel, domain topography). This work aims to provide an increase of knowledge in the fire spreading, currently still limited, thanks to the adoption of a physically-based code (WFDS) to model flame propagation; in fact, through the numerical resolution of the fundamental balance equation describing the fire phenomenon, it offers a way to analyze the fire behaviour on a scientific basis. To pursue this target different aspects, reported in different chapters, were considered in this work.

The first part examines shortly the social, economical and ecological impact of wildland fires on a global scale and for the countries of the Euro-Mediterranean region. The role of fire behaviour modelling as a tool for fire fighting activities and prevention management is put in evidence and discussed.

In the second part the role of fire behaviour modelling as a tool for fire fighting activities and prevention management is put in evidence and discussed. Such a part endeavours to shortly review the main surface fire spread models developed since 1990 with particular attention to physically-based codes. These models are alternative to empirical or quasi-empirical models, which do not have physical basis and are only statistical in nature or make use of some form of physical framework upon which to base the statistical modelling chosen. A comparison between the most frequently used simulation codes is accomplished and the advantages to consider a

physical code - for instance *WFDS* - rather than an empirical or quasi-empirical one is highlighted.

The subsequent section presents an outline of the physical mechanisms and length scales governing the propagation of wildfires, which have to be considered when a physical modelling approach is employed. In this context, the literature highlights two regimes in the propagation of surface fires, i.e. wind-driven fires and plume-dominated fires, which are governed by radiation and convective heat transfer, respectively. In this part a short outline of the mathematical background, which is used to describe the physical and chemical aspects involved in the fire phenomena along with its numerical implications, is also provided.

The fourth chapter discuss about the way by which the wind and the terrain inclination affect the fire propagation across a homogeneous fuel; in this case also the possibility for the occurrence of a transient regime even under constant geometric and ambient conditions is also addressed. Furthermore, the role played by the understorey vegetation on the development of a crown fire is investigated by considering a domain made of a heterogeneous surface fuel under a linear stand of trees.

The fifth part deals with the description of fire behaviour across double-slope terrains and canyon configuration. Simulations, performed by the *WFDS* code, help, in the first case, to understand the main parameters affecting the variation of fire propagation in correspondence of the domain slope change. In the second case, the numerical approach provides insights in the understanding and description of the so-called eruptive behaviour, characterized by an exponential increase in the fire propagation rate, promoted by the particular domain configuration.

In the sixth section the numerical code *WFDS* is used to study the behaviour of a fire propagating over a relatively large area with a real surface configuration. In particular, the code provides information to deduce the fire front shape profiles and terrain area burned in time.

Finally, part seven discusses the findings of this thesis and summarizes the main conclusions. The potentiality of the numerical code in providing reliable and detailed predictions of the behaviour and effects of fire over a wide range of conditions is highlighted. However information about the limitations of the code is also provided.

Chapter I

Forest fires and fire management

The two main aspects in examining wildland fires involve the damage caused by such natural disasters and the activities involved in fire prevention and suppression. This section presents some forest fire data for a global scale and countries of the Euro–Mediterranean region. Additionally, a short review of basic activities encompassed by scientific research for fire prevention and wildland suppression is provided. Section 1.2 presents the main objectives of fire management while section 1.3 introduces the role of fire behaviour modelling as a tool for fire fighting activities and prevention. Next sections report the aim of the work and the outline of the thesis work.

I.1 Wildland fires as agents of damage of wooded areas

Wildland fires have always been undesired and dangerous events throughout the world. The damages caused by them can be classified into three major groups:

- Destruction of a renewable natural resource used as an energy source and also as a source for a number of products of substantial economic and social significance.
- Environmental damage resulting from the emissions into atmosphere of contaminant gases thus contributing to the greenhouse effect. Additional damage results from contamination of fertile soils, deforestation, contamination of underground water, activation of erosion and landslide processes, desertification of large land areas, etc.
- Human injuries and/or deaths both among the population living in the fire affected areas, and among members of firefighting teams. Moreover, material damage is caused affecting the way of life of local population living in the areas where the fire events occurred.

Wildfire incidences have been increasing worldwide, with adverse effects on economies, livelihoods, and human health and safety that are comparable to those associated with other natural disasters as earthquakes, floods, droughts and volcanic eruptions (ISDR 2003). Main global vegetation zones

are considered to be the northern boreal forest, the temperate forest, the Mediterranean, the tropical rainforest and the tropical/savanna regions.

International forest fires news (2004) indicated that within 1997–1998 fires have destroyed twenty million hectares of rainforest in Latin America and Southeastern Asia. During the same period five million hectares were destroyed in Borneo and another 9.5 in East Kalimantan, Indonesia. Brazil has lost as a result of fires 15 million forest hectares in the period 1988–1997 (ISDR Working Group of Wildland Fire 2003). These data become even more significant when it is realised that these fires are not natural phenomena in tropical rainforests and they do not facilitate any vegetation regeneration.

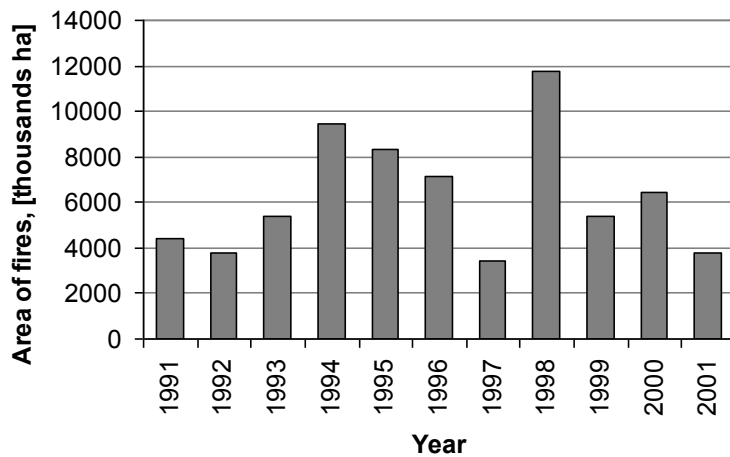


Figure I.1 Total area of fires burned in North America, Europe and CIS – countries IFFN (2002).

Figure I.1 illustrates the distribution of the total area affected by forest fires that have occurred on the territory of the US, Canada, European countries and the countries of the Commonwealth of Independent States (CIS) in the period 1991–2001. These fires have occurred in areas of the northern boreal forest and in the part of the temperate forest (USA, Mediterranean basin and the Balkans). It is apparent that the average surface area of forests devastated by fires is about 6 million hectares and in 1998 this figure reached 12 million hectares. It should be noted here that this maximum was due to the high temperatures experienced that year (one of the hottest in the 20th century) and also to the El-Nino phenomenon. Despite of the fact that no data is presented for other regions (such as Australia, African savannas), from all said above it is obvious that wildland fires represent a serious problem globally, burning millions of hectares of vegetation each year.

1.1.1 European statistics

For the period 1980–2011 the number of forest fires in five southern member - (Portugal, Spain, France, Italy, and Greece) varied greatly (Fig. I.2). The statistics vary considerably from one year to the next, which clearly indicates how much the burnt area depends on seasonal meteorological conditions.

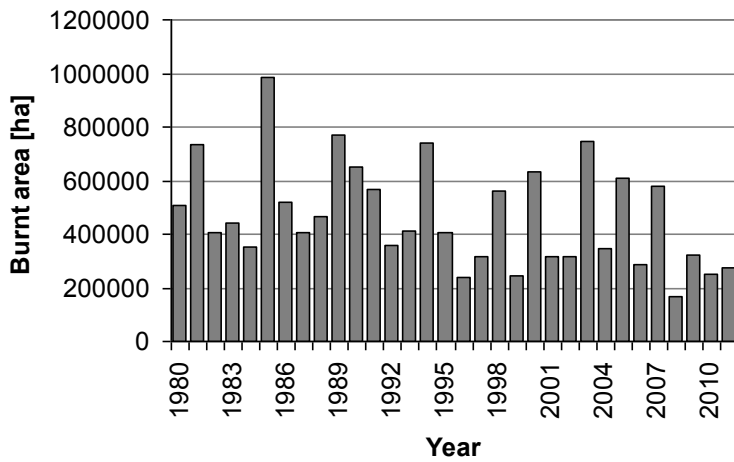


Figure I.2 *Burnt area in the Southern Member States*

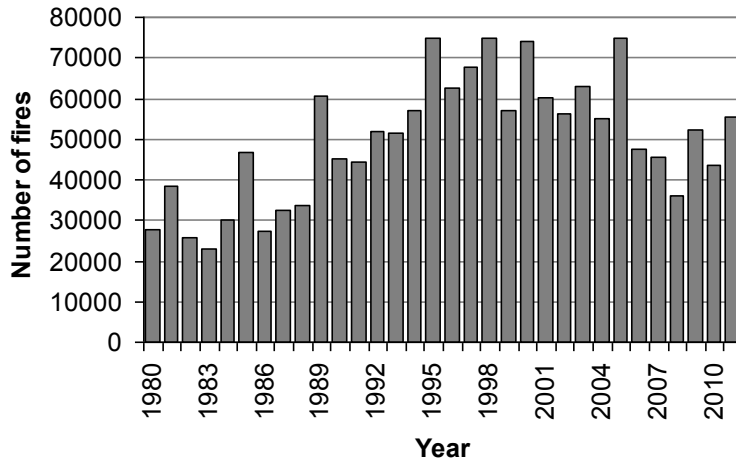


Figure I.3 *Number of fires in the Southern Member States*

Overall, the total burnt area for all 5 countries in 2011 is around 62% of the average for the last decade and 58% of the long term average (32 years;

Table I.1). During 2011 fires in these 5 countries burned a total area of 269 081 ha. This is slightly higher than the area burnt in 2010, but among the lowest values since 1980 (only 1996, 1999, 2008 and 2010 were lower). The number of fires that occurred (55 543) is also higher than the number registered in 2010, but slightly below the average of the last 2 decades (see Table I.1 for details). Figure I.3 shows the yearly number of fires in the five southern member states listed above since 1980. After the increasing trend during the 1990s, which was also partly due to the improvement in recording procedures, the number of fires was stable for around one decade, and in the last decade a decrease was observed. However, in the last 5 years the trend has been slightly upward. Overall, 2011 was an average year in terms of number of fires. In 2011 the number of fires was 27% more than that recorded in 2010, but the total burnt area increased by only 6%.

Figure I.4 shows the yearly average fire size in the 5 countries since 1980. There is a clear difference in average fire size before and after 1990. This is a similar trend to that observed in the number of fires and is also partly due to the same reasons (the additional fires that are recorded thanks to the improvements in the statistical systems are the smallest ones). But it is also largely due to the improvements of the fire protection services of the countries.

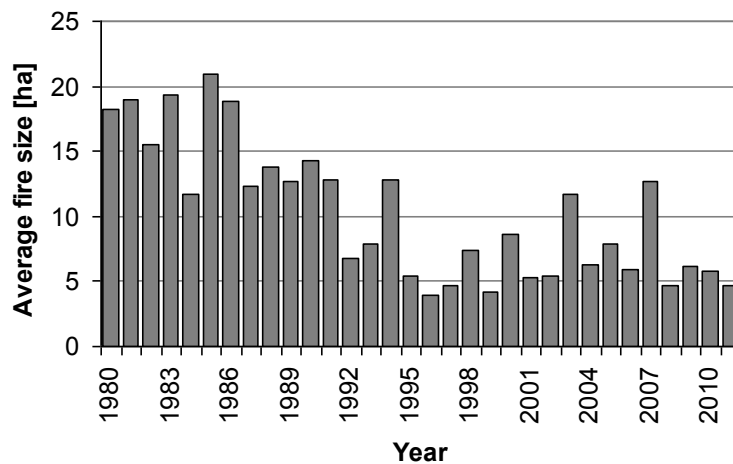


Figure I.4 Average fire size in the Southern Member States

Forest fires in Italy in 2011 occurred much more in comparison to the previous three years. In 2011, there were 8 181 fires recorded, burning a total area of 72 004 hectares, 38 428 of which were wooded. In Italy forest fires occur in all regions. In winter they are located mostly in the Alpine regions (especially the North-western regions), while in summer they are mostly concentrated in the Mediterranean regions (Southern regions and

islands). In Liguria fires occur both in summer and winter at about the same frequency. In 2011 the number of fires was about 68% more than in 2010, while the wooded burned area was about 99% more. As usually, forest fires mainly occurred in southern regions. As far as the number of fires is concerned, Campania was the most affected region with 1 435 fires, but the worst burned area occurred in Calabria (total: 14 437 ha; wooded: 8 174 hectares)

Table I.1 *Number of fires and burnt area in the five Southern Member States in the last 32 years (FFEMA, 2011)*

NUMBER OF FIRES	PORTUGAL	SPAIN	FRANCE	ITALY	GREECE ^(*)	TOTAL
2011	25 221	16 028	4 500	8 181	1 613	55 543
% of total in 2011	45%	29%	8%	15%	3%	100%
Average 1980-1989	7 381	9 515	4 910	11 575	1264	34 645
Average 1990-1999	22 250	18 152	5 538	11 164	1748	58 851
Average 2000-2009	24 949	18 337	4 406	7 259	1695	56 645
Average 2010-2011	23 624	13 875	4 200	6 533	1333	49 564
Average 1980-2011	18 533	15 243	4 904	9 783	1554	50 017
Total (1980-2011)	593 052	487 788	156 931	313042	49723	1 600 536

BURNT AREAS (ha)	PORTUGAL	SPAIN	FRANCE	ITALY	GREECE ^(*)	TOTAL
2011	73 813	84 490	9 630	72 004	29 144	269 081
% of total in 2011	27%	31%	4%	27%	11%	100%
Average 1980-1989	73 484	244 788	39 157	147 150	52417	556 995
Average 1990-1999	102 203	161 319	22 735	118 573	44108	448 938
Average 2000-2009	150 101	125 239	22 342	83 878	49238	430 798
Average 2010-2011	103 452	69 630	9 965	59 271	19056	261 373
Average 1980-2011	108 275	170 397	26 946	112 955	46742	465 314
Total (1980-2011)	3 464 789	5 454 717	862 262	3 614 546	1495735	14 890 049

^(*) Number of fires are incomplete since 2009

Despite the reduction in number of fires and forest fires, Italy is among the European countries where the phenomenon is particularly serious. In many Italian regions, the majority of fires are detected and extinguished when the fires are of minimal size, so that only few fires escape control. However, these few fires are those determining the greater part of the burned area and often also affect urban areas and infrastructures, causing serious damage and particular concern.

The phenomenon of forest fires is not generalized throughout the country, as about 50 out of the 110 provinces are most affected and therefore these should receive special attention. The fire fighting system, which in some regions has reached levels of excellence, is overall fragile. In Italy the

Regions have primary responsibility in the field of forest fires and, through conventions and programme agreements, empower the Italian Forest Corps in prevention, preparedness, coordination in the regional operations rooms and in the survey of burned areas, and the National Service of Fire Brigades in active firefighting and coordination in the regional operations rooms. The Italian Forest Corps also submits the forest fire prevention plans of national and regional parks and protected natural areas for examination.

1.1.2 Global emissions of selected pyrogenic species

Scientific interest on biomass smoke as a pollutant grew when early estimates of pyrogenic emissions suggested that, for some atmospheric pollutants, biomass burning could rival fossil fuel use as a source of atmospheric pollution. These emissions could affect large world areas, especially in the tropics (IFFN 2004). Table I.2 presents data for assumed emission levels for gases causing the heaviest atmospheric pollution.

From these data it is clear that gaseous emissions released into atmosphere during fires and contributing to the greenhouse effect exceed the emissions released from burning biofuels and reach up to 30% of all emissions resulting from burning fossil fuels. The aerosols emitted from vegetation fires influence climate directly and indirectly. Direct effects are (a) backscattering sunlight into space, resulting in an increased albedo and a cooling effect and, (b) absorption of sunlight which leads to cooling of the Earth's surface and atmospheric warming (ISDR 2003). Gaseous emissions in atmosphere from Latin America fires are estimated at roughly total carbon cost of \$10–15 billion as per the Kyoto Protocol. Smoke resulting from the burning of vegetation contains a large amount of various chemicals many of them have adverse health impacts (Goh *et al.*, 1999). Devastating South-eastern Asia fires in 1997–1998 caused respiratory health problems, which along with transport disorder were estimated at US\$ 9.3 billion (ISDR 2003).

Table I.2: *Global emissions of selected pyrogenic species in the late 1990s (In mass of species per year; Tg/a) (IFFN 2004).*

	Savanna and grassland	Tropical forest	Extra - tropical forest	Biofuel burning	Fossil fuel burning
CO ₂	5096	2101	1004	4128	23100
CO	206	139	68	206	650
CH ₄	7.4	9.0	3.0	16.2	110
NO	12.2	2.2	1.9	2.9	45

I.2 Management activities over fire prevention and suppression

Fire suppression involves all activities associated with the control and final suppression of a wildland fire after it is initially started. In order to visualize the basic principles of fire suppression the fire triangle is usually used (Figure I.5).

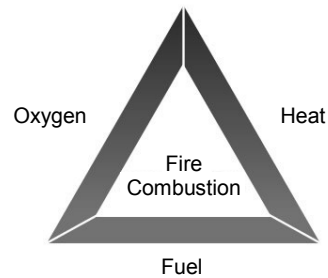


Figure I.5 *The wildland fire triangle.*

To stop the free-burning fire it must be either (1) removed by removing the fuels ahead of the spreading combustion zone, (2) reduce the temperature of burning fuels, or (3) exclude oxygen by reaching the combustion zone by smothering (Alexander, 2000). From a practical viewpoint, most generally this means to create a physical barrier by removing the vegetation material, to cool down fire flames using water, or to reduce fire intensity by soil covering, suppressants like foam, or chemical fire retardants, which could be sprayed over from ground level or from the air above.

Scientific research involved with assisting activities for wildland fire management is basically focused into several fields (Lampin *et al.*, 2004; Rodriguez y Silva & Moreno Robles 2005; Marzano *et al.*, 2006; Xanthopoulos *et al.* 2006):

- *Determination of wildland fire risk, ignition danger, propagation danger and vulnerability.* Ignition danger is the danger that arises due to combination of factors that lead to wildfire inception. Propagation can be defined also as the fire spread danger. This type arises due to the combined existence or factors emergence that favour wildfire spread. Vulnerability is related to the potential fire impact or else potential damages on environmental and socio-economic elements and is defined by the factors that can favour such a process.
- *Developing Decision Support Systems (DSS).* These systems should meet various needs: observation and predicting of weather data, risk assessment, early fire detection, determination of fire behaviour, advising and pre-suppression planning, and suppression decision support.

- *Fuel management by reducing fuels through mechanical or physical means or through the use of prescribed burning.* Management objectives must satisfy legal requirements, be thoroughly planned, and when conducted, be in accordance with clearly defined procedures providing for safe work practices and manageable fire behaviour. They should also be environmentally sensitive and have their outcomes recorded.
- *Developing new methods and means for fighting fires and providing for their efficient application in real conditions.* Work in this field comprises creating the material resources, training of fire-fighting crews and efficient interaction between individual departments involved in activities for fire prevention and suppression.
- *Creating models that will assist the identification of social and economic impacts of forest fires and of basic risk factors:* forestry profitability, demographic pressure, social tension, forestry culture and organisational logic.

I.3 Role of fire behaviour modelling

Fire behaviour is generally defined as the manner in which fuel ignites, flame develops, fire spreads as determined by the interaction of fuels, weather, and topography. The more important fire characteristics from the practical standpoint of fire suppression are: forward rate of spread, fire intensity, flame front dimensions, spotting pattern, fire size and shape, rate of perimeter increase, burn out time (Alexander, 2000). Various resource types in fighting forest fires usually feature efficiency limitations. Therefore, it is necessary to be aware of the characteristics and the behaviour of the fire in order to be able to make adequate and proper decisions that will assist activities involved in fire suppression. For example, Alexander (2000) considered that ‘...Direct attack on fire perimeters with excess of 4,000 kW/m intensities is generally not possible. Backfiring is possible, though not always successful up to around 10,000 kW/m...’. Fire behaviour modelling is utilized to determine these characteristics and to simulate fire propagation in a variety of vegetations, under diverse climatic and topographic conditions. These models are used as a tool to assist activities involved in fire prevention, detection and suppression. The main application fields for these models comprise:

- *Predicting a risk.* The applicability of fire behaviour modelling is linked to determining the risk of ignition of the vegetation and the fire spread danger. Based on identifying the fire hazard and risk it is possible to make decisions to carry out activities involved in the prevention and early detection of wildland fires.
- *Mathematical reconstruction of a fire.* Using theoretical models for testing various hypothesis associated with the occurrence and spreading

of wildland fires. The results of such simulations can find practical application in all fields of fire management.

- *Interpolation between or extrapolating beyond experimental results.* Laboratory and field experiments feature limitations (financial, time-related, etc.) related to the number and parameter values describing vegetation and external conditions. Using fire models, based on experiments allows to test in practice an unlimited combination of external conditions.
- *As part of a decision support system.* In this case the application of fire behaviour modelling is associated with reducing the time span between the fire discovering and the actual action putting of firefighting crews based on options for activity plans developed in advance.
- *Evaluation of effectiveness of fire suppression.* Using the developed models it is possible to test the application of various means / techniques for suppressing fires and to determine the most efficient approach for given characteristics of fire behaviour.

I.2 Aim of the work

The aim of this thesis work was to increase the level of knowledge of the physical phenomena occurring during a fire spreading across a domain under different fuel and boundary conditions.

Accordingly, several fire configurations and scenarios have been considered. Preliminary investigation addressed the effect of wind and terrain inclination on fire propagation and the interaction between surface and vertical fuel in originating a crown fire. Furthermore, particular attention was focused to some terrain configurations which have not been particularly considered in the literature such as slope-changing domains and canyons where fire propagation may be characterized by abrupt variations in intensity and propagation rate. Study of fire spreading across a real heterogeneous terrain has also been accomplished.

The *WFDS* code has been employed to study and describe the fire propagation in the conditions listed above in order to put the basis to carry out a risk analysis of fire spreading taking into account specific terrain features and vegetative characteristics of a given geographic area. When available, clues from the literature have been considered in order to validate the code and put in evidence the main related aspects.

I.3 Outline of the thesis

To accomplish the aims summarized above different topics, organized in separated section were considered.

The second part endeavours to shortly review the main surface fire spread models developed since 1990 with particular attention to physically-based

codes. A comparison between the most frequently used simulation codes was accomplished and the advantages to consider a physical code - for instance *WFDS* - to study the fire propagation and behaviour respect to a an empirical or quasi-empirical one was highlighted.

The subsequent section presents an outline of the physical mechanisms and length scales governing the propagation of wildfires which have to be considered when a physical modelling approach is considered. In this part a short outline of the mathematical background, which is used to describe the physical and chemical aspects involved in the fire phenomena along with its numerical implications, is also provided.

The fourth chapter discusses about the way by which the wind and terrain inclination affect the fire propagation across a homogeneous fuel; in this case also the possibility for the occurrence of a transient regime even under constant geometric and ambient conditions was addressed. Furthermore, the role played by the understory vegetation on the development of a crown fire was , investigated by considering a domain made of a heterogeneous surface fuel under a linear stand of trees.

The fifth part deals with the study and description of fire behaviour across double-slope and canyon configurations. Simulations, performed by the *WFDS* code, helps, in the first case, to understand the main parameters affecting the variation of fire propagation in correspondence of the domain slope change . In the second case, the numerical approach provides insights in the understanding and description of the so-called eruptive behaviour, characterized by an exponential increase in the fire propagation rate promoted by the particular domain configuration.

In the sixth chapter the numerical code is used to study the behaviour of a fire propagating over a relatively large area having a real surface configuration. Model results are compared with data, available in the literature, showing a good agreement.

Finally, part seven discusses the findings of this thesis and summarizes the main conclusions. Potentiality of the numerical code to provide reliable and detailed information on the fire behaviour is reported. However, it also stressed how for now long calculation times and difficulty of use and handling are serious limits to its use as a real-time tool for fire safety and emergency management

I.4 References

Alexander, M., 2000. *Fire behaviour as a factor in forest and rural fire suppression*. Forest research, Rotoria, in association with the New Zealand Fire Service Commission and National Rural Fire Authorities, Wellington. Forest research bulletin No. 197, Forest and Rural Fire Scientific and Technical Series, Report No. 5, p.28.

- Forest Fires in Europe Middle East and North Africa (FFEMA), 2011, European Commission – Joint Research Centre – Institute for Environment and Sustainability . Scientific and technical Research series – ISSN 1018-5593 (print), ISSN 1831-9424 (online)
- Goh, K., Schwela, D., Goldammer, J. & Simpson, O., 1999, *Health guidelines for vegetation fire events. Background paper*. Published on behalf of UNEP, WHO, and WMO. Institute of Environmental Epidemiology, Ministry of the Environment, Singapore. Namic Printers, Singapore, p.498.
- International Forest Fires News (IFFN), 2002. *Forest fires in Europe 1961–1998* [online]. Available at: http://www.fire.unifreiburg.de/iffn/country/global/Europe_1.htm.
- International Forest Fires News (IFFN), 2004 *Assessment of Global missions from Vegetation Fires* [online]. Available at: http://www.fire.unifreiburg.de/iffn/iffn_31/18-iffn-31-Emissions.pdf
- ISDR Working Group of Wildland Fire, 2003. *Background paper: An overview of vegetation fires globally*. International Wildland fire summit. Australia, 8 October 2003.
- Lampin, C., Molina, D., Martin, P. & Caballero, D., 2004. *The Interest of Socio-Economical Sciences in Wildland Fires: a State of the Art* [online]. Available at: http://eufirelab.org/prive/directory/units_section_5/D-05-01/D-05-01.pdf.
- Marzano, R. et al., 2006. *Wildland Fire Danger and Hazards: a state of the art, final version* [online]. Available at: http://www.eufirelab.org/prive/directory/units_section_8/D-08-05/D-08-05.pdf
- Rodriguez y Silva, F. & Moreno Robles, A., 2005. Towards methods for wildland fire suppression planning (intermediate) [online]. Available at: http://www.eufirelab.org/prive/directory/units_section_9/D-09-02/D-09-02.pdf
- Xanthopoulos, G. et al., 2006. *Methods to study fire impacts on plants (forest stands, shrubs, herbaceous taxa), soil and fauna* [online]. Available at: http://www.eufirelab.org/prive/directory/units_section_4/D-04-10/D-04-10.pdf

Chapter II

Literature review and main characteristics of the prediction tools used for surface vegetation fires

This part of the work shortly reviews the main surface fire spread models developed since 1990 with particular attention to physically-based codes. These models are based on the fundamental chemistry and/or physics of combustion and fire spread and have become in the last years a promising tool to investigate the forest fire behaviour in a less subjective way. This approach, promoted by improvement in computer potentialities, aims to substitute or limit the use of empirical or quasi-empirical model: the former contains no physical basis at all (generally only statistical in nature) while the latter uses some form of physical framework upon which to base the statistical modelling chosen. Furthermore, the basics of the physic and chemical aspects of fire and combustion phenomena are provided to better explain the assumptions the models are based on.

II.1 Fundamentals of fire and combustion phenomenon

Wildland fire is the complicated combination of energy, in the form of heat, produced by chemical combustion, its transport to surrounding unburnt fuel and the subsequent ignition of this fuel. The former is the domain of chemistry (more specifically, *chemical kinetics*) and occurs on the scale of molecules, and the latter is the domain of physics (more specifically, *heat transfer* and *fluid mechanics*) and occurs on scales ranging from millimetres up to kilometres (Table II.1).

It is the interaction of these processes over the wide range of temporal and spatial scales that makes the modelling of wildland fire behaviour a considerable problem. According to Grishin (1997), several steps need to be

considered in order to develop a physical model able to describe the fire behaviour:

1. Physical analysis of the phenomenon and isolation of the mechanism governing the heat transport from the fire front to the surrounding;
2. Determination of the physical and reaction properties of the medium and deduction of the basic system of equations with corresponding boundary conditions;
3. Selection of a method of numerical solution of the problem;
4. Programming and test check of the program; .
5. Validation of the code through comparison with results obtained from real systems.

Stages one and two represent considerable sources of contention for the best method to represent the phenomenon of wildland fire. In fact, even if great advances in the understanding of what is going on in these processes, uncertainties still remains (di Blasi, 1998). The chemistry of combustion involved in wildland fire is really complex both because of the nature of the fuel itself and the wide range of conditions over which the combustion can occur.

Table II.1 *Outline of the major biological, physical and chemical components and processes occurring in a wildland fire and the temporal and spatial (vertical and horizontal) scales over which they occur (Sullivan, 2008)*

TYPE	TIME SCALE (s)	VERTICAL SCALE (m)	HORIZONTAL SCALE (m)
Combustion reactions	0.0001 – 0.01	0.0001 – 0.01	0.0001 – 0.01
Fuel particles	–	0.001 – 0.01	0.001 – 0.01
Fuel complex	–	1 – 20	1 – 100
Flames	0.1 – 30	0.1 – 10	0.1 – 2
Radiation	0.1 – 30	0.1 – 10	0.1 – 50
Conduction	0.01 – 10	0.01 – 0.1	0.01 – 0.1
Convection	1 – 100	0.1 – 100	0.1 – 10
Turbulence	0.1 – 1000	1 – 1000	1 – 1000
Spotting	1 – 100	1 – 3000	1 – 10000
Plume	1 – 10000	1 – 10000	1 - 100

II.1.1 Fuel chemistry

Wildland fuel is composed of live and dead plant material consisting primarily of leaf litter, twigs, bark, wood, grasses, and shrubs, (Beall and Eickner, 1970). The primary chemical constituent of biomass fuel is cellulose (of chemical form $(C_6O_5H_{10})_n$), which is a polymer of a glucosan (variant of glucose) monomer, $C_6O_6H_{12}$ (Shafizadeh, 1982; Williams, 1982). Cellulose (Figure II.1) is a linear, unbranched polysaccharide of $\approx 10,000$ D-glucose units in $\beta(1,4)$ linkage¹.

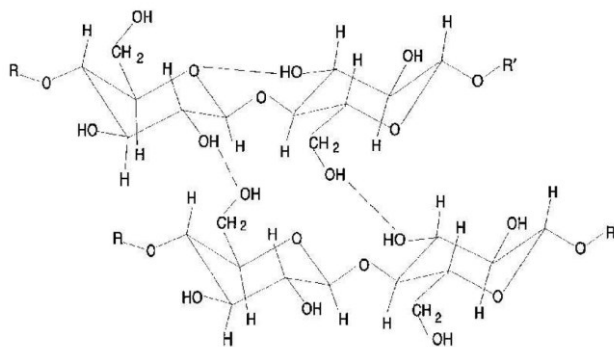


Figure II.1 Schematic of chemical structure of portion of neighbouring cellulose chains, indicating some of the hydrogen bonds (dashed lines) that may stabilise the crystalline form of cellulose (Source: Ball *et al.* (1999))

The parallel chains are held together by hydrogen bonds (Ball *et al.*, 1999). Other major chemical components of wildland fuel include hemicelluloses (copolymers of glucosan and a variety of other possibly monomers) and lignin (a phenolic compound) in varying amounts, depending upon the species, cell type and plant part (Table II.2).

The cellulose is the same in all types of biomass, except for the degree of polymerisation (i.e. the number of monomer units per polymer). A lot of studies have been performed on the combustion of this component, but very few on the degradation of hemicelluloses and lignin (di Blasi, 1998), due perhaps to the relative thermal instability of these compounds.

The degradation of biomass is generally considered as the sum of the contribution of its main components (cellulose, hemicelluloses and lignin)

¹ The D- prefix refers to one of two configurations around the chiral centre of carbon-5. The β (1, 4) refers to the configuration of the covalent link between adjacent glucose units, often called a glycosidic bond.

but the extrapolation of the thermal behaviour of the main biomass components to describe the kinetics of such a complex fuels is only a rough approximation (di Blasi, 1998). The presence of inorganic matter in the biomass structure can act as a catalyst or an inhibitor for the degradation of cellulose making the description of the degradation process an even more complex process to study.

Table II.2 *Approximate analysis of some biomass species (Shafizadeh, 1982)*

SPECIES	CELLULOSE (%)	HEMI-CELLULOSE (%)	LIGNIN (%)	OTHER (%)
Softwood	41.0	24.0	27.8	7.2
Hardwood	39.0	35.0	19.5	6.5
Wheat straw	39.9	28.2	16.7	15.2
Rice straw	30.2	24.5	11.9	33.4
Bagasse	38.1	38.5	20.2	3.2

II.1.2 Solid phase reactions: competing processes

When wood is exposed to elevated temperatures, changes can occur in its chemical structure. The extent of the changes depends on the temperature level and the length of time of the exposure.

At temperatures below 100°C, permanent reductions in strength can occur. The magnitude of the reduction depends on the moisture content, heating medium, exposure period and species. The strength degradation is probably due to depolymerization reactions, although little research has been done on the chemical mechanism. (Gerhards 1979, 1982, 1983; Koch, 1985).

At temperatures above 100°C, chemical bonds begin to break. Between 100°C and 200°C, non-combustible products, such as carbon dioxide, traces of organic compounds and water vapour, are produced. Above 200°C the celluloses break down, producing tars and flammable volatiles that can diffuse into the surrounding environment. If the volatile compounds are mixed with air and heated to the ignition temperature, combustion reactions occur. The energy from these exothermic reactions radiates to the solid material, thereby propagating combustion, or pyrolysis, reactions. If the burning mixture accumulates enough energy to emit radiation in the visible spectrum, the phenomenon is known as flaming combustion. Above 450°C all volatile material is gone. The residue that remains is char that can be oxidized to carbon dioxide, carbon monoxide and water vapour.

The thermal degradation of wood can be represented by two pathways (Figure II.2), one occurring at high temperatures ($>300^{\circ}\text{C}$), the other at lower temperatures. These two competing reactions occur simultaneously.

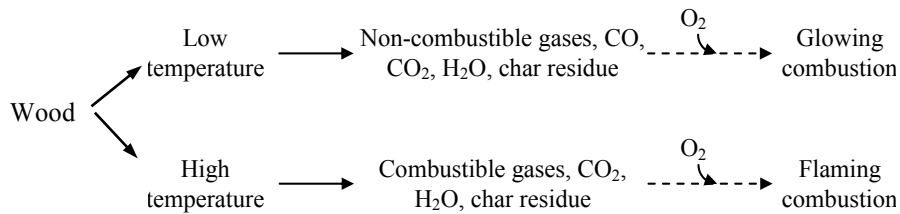


Figure II.2 Degradation of wood by low-temperature and high-temperature pathways

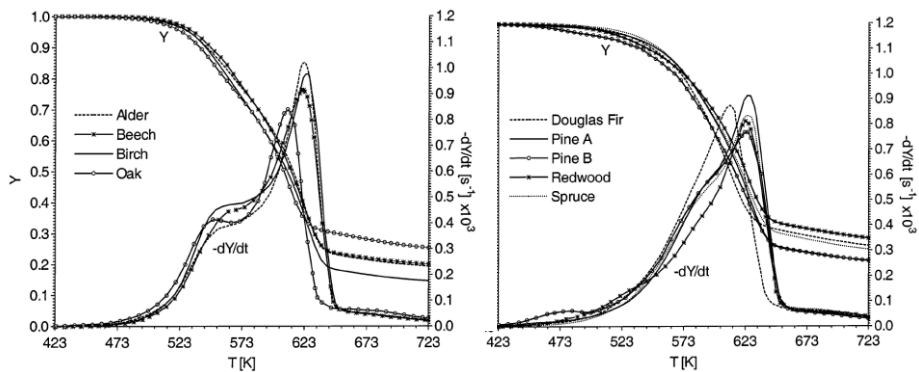


Figure II.3 Mass fraction and time derivative of the mass fraction as functions of temperature for several softwoods (left) and hardwoods (right)(Morten *et al.*, 2002)

The thermal degradation of wood can be represented as the sum of the thermal degradation reactions of the individual components, namely cellulose, hemicellulose and lignin. The influence of these individual components on the thermal degradation reactions of wood can be seen by plotting the wood weight loss as a function of temperature (Figure II.3). The mass fraction, Y , and the time derivative of the mass fraction, $-dY/dt$ (TG and DTG curves, respectively) are reported as functions of temperature in Figures II.3 for the hardwoods and softwoods (Morten *et al.*, 2002). The DTG curves show two main regions. Because the temperature intervals of hemicellulose and cellulose decomposition partially overlap each other, the hemicellulose decomposition (first region) usually appears as a more or less pronounced “shoulder” instead of a well-defined peak. The second region is

associated with the attainment of the maximum, mainly because of cellulose decomposition, followed by a rapid decay and a long tail. The wide range of temperatures, where lignin decomposes, hinders the appearance of a peak attributable to this component. Quantitative methods can be applied to the thermogravimetric analysis curves to obtain the kinetic parameters of the thermal degradation which are highly dependent on the experimental conditions - such as heating rates, sample size – adopted in the tests. However, the comparison between the thermal degradation pathway in Figure II.3 shows a similar behaviour for different vegetative species, justifying the use of a single kinetic expression to model the pyrolysis kinetic of many vegetable fuels (Porterie *et al.*, 2005; Morvan and Dupuy, 2004).

II.1.3 Gas phase reactions

Gas phase combustion of levoglucosan, the main tracer of wood pyrolysis, is highly complex and simplified as:



This assumes that all intermediate reactions, consisting of oxidation reactions of derivative products are mostly complete. However, the number of reaction and their pathways is quite large: for example Williams (1982) gives a non-exhaustive list of 14 possible pathways for the combustion of CH_4 , one of the possible intermediates of the thermal degradation of levoglucosan, to H_2O and CO_2 . Intermediate species include CH_3 , H_2CO , HCO , CO , OH and H_2 .

At any stage in the reaction process, any pathway may stop (through loss of energy or reactants) and its products may be rejected to take no further part in combustion: these partially combusted components form the smoke. The faster and more turbulent the reaction, the more likely reaction components will be removed prior to complete combustion and, hence, the darker and thicker the smoke from a headfire will result.

II.2 Physics of combustion

The physics involved in the combustion of wildland fuel and its behaviour is, like the chemistry, complicated and strictly dependent on the conditions in which a fire is burning. The primary physical process in a wildland fire is that of heat transfer (Williams, 1982):

The primary physical processes driving the transfer of heat in a wildland fire are that of advection and radiation. In low wind conditions, the dominating process is that of radiation (Weber, 1989). In conditions where wind is relevant is advection that dominates (Grishin *et al.*, 1984). However, in any condition it is reasonable to assume that both mechanisms must be

considered. In attempting to represent the role of advection in wildland fire spread, the application of fluid dynamics is of prime importance.

II.2.1 Advection or Fluid transport

The key aspect of fluid dynamics and its application to understanding the motion of gases is the notion of continuity. Here, the molecules or particles of a gas are considered to be *continuous* and thus behave as a fluid rather than a collection of particles. Another key aspect of fluid mechanics (and physics in general) is the fundamental notion of the conservation of quantities which represent the *equations of motion*.

The continuity equation describes the conservation of mass:

$$\frac{\partial \rho}{\partial t} + \nabla(\rho \bar{u}) = 0 \quad (\text{II.2})$$

where ρ is density, t is time and \bar{u} is the fluid velocity (with vector components u , v , and w) and ∇ is the Laplacian or gradient operator (i.e. in three dimensions $\bar{i} \frac{\partial}{\partial x} + \bar{j} \frac{\partial}{\partial y} + \bar{k} \frac{\partial}{\partial z}$).

In order to solve this equation, the evolution of \bar{u} is needed: this is obtained taking a balance of forces acting on the fluid resulting in the *conservation of momentum* equation:

$$\frac{\partial \rho \bar{u}}{\partial t} + \nabla(\rho \bar{u}) \bar{u} + \nabla p = 0 \quad (\text{II.3})$$

where p is the pressure. However, the evolution of p is then needed to solve the equation and this is frequently done, utilising an equation of state to provide the closure mechanism. In fluid dynamics, the equation of state is generally that of the ideal gas law (e.g. $pV = nRT$).

II.2.2 Buoyancy, convection and turbulence

Heat release from the chemical reaction within the combustion zone results in heated gases, both in the form of combustion products and as ambient heated air. The reduction in density caused by the heating increases the buoyancy of the gas and results in the gas rising which can then lead to turbulence in the flow. Turbulence affects the whole range of scales in the atmosphere, from the scale of flame to the atmospheric boundary layer, and acts to mix heated gases with ambient air and to preheat the unburnt solid phase fuels. The action of turbulence also affects the transport of solid phase combustion, such as that of firebrands, resulting in spotfires downwind of the main burning front.

Suitably formulated Navier-Stokes equations can be used to incorporate the effects of buoyancy, convection and turbulence. Specific methods for numerically solving turbulence within the field of fluid dynamics, including renormalisation group theory (RNG) and large eddy simulation (LES), have been developed.

II.2.3 Radiant heat transfer

Radiant heat is a form of electromagnetic radiation emitted from a hot source and is in the infra-red wavelength band. In flame, the primary source of the radiation is thermal emission from carbon particles, generally in the form of soot (Gaydon and Wolfhard, 1960). The general method of modelling radiant heat transfer is through the use of a radiant transfer equation (RTE), which assumes its simplest form in the Stefan-Boltzmann equation:

$$q = \sigma \cdot T^4 \tag{II.4}$$

where σ is the Stefan-Boltzmann constant ($5.67 \times 10^{-8} \text{JK}^{-4} \text{m}^{-2} \text{s}^{-1}$) and T is the radiating temperature of the surface (K). Usually, the radiant heat flux is approximated as a surface emission from the flame face, but this does not fully capture the volumetric emission nature of the flame (Sullivan *et al.*, 2003) and can lead to inaccuracies in flux estimations. More complex solutions of the RTE can improve the prediction of radiant heat but are, necessarily, more computationally intensive.

The Discrete Transfer Radiation Model (DTRM) solves the radiative transfer equation throughout a domain by a method of ray tracing from surface elements on its boundaries and thus does not require information about the radiating volume itself. Discrete Ordinate Method (DOM) divides the volume into discrete volumes for which the full RTE is solved at each instance and the sum of radiation along all paths from an observer calculated.

The Differential Approximation (or P1 method) solves the RTE as a diffusion equation which includes the effect of scattering but assumes the media is optically thick. Knowledge about the media's absorption, scattering, refractive index, path length and local temperature are required for many of these solutions (Sacadura, 2005; Goldstein *et al.*, 2006)

II.2.4 Firebrands (solid fuel transport)

Spotting ignition by firebrands is a significant mechanism of fire spread, as observed in many large-scale fires. Determination of the transport of solid fuel (i.e. firebrands), which leads to the initiation of spotfires is highly probabilistic (Ellis, 2000). This is due in part to the wide variation in firebrand sources and ignitions and the particular flight paths any firebrand

might take. Maximum distance that a firebrand may be carried is determined by the intensity of the fire, the height at which the firebrand was sourced and the wind profile aloft (Albini, 1979; Ellis, 2000). Whether or not the firebrand lands and starts a spotfire is dependent upon the nature of the firebrand, how it was ignited, its combustion properties and the ignition properties of the fuel in which it lands (e.g. moisture content, bulk density, etc) (Plucinski, 2003).

II.2.5 Atmospheric interactions

The transport of the gas phase of the combustion products interacts with the atmosphere around it, transferring heat and energy, through convection and turbulence. The condition of the ambient meteorological conditions, such as changes in wind speed and direction, moisture and temperature both at the surface and higher in the atmosphere, can have a significant impact on the state of the fuel (moisture content), the behaviour of a fire and its growth.

II.2.6 Topographic interactions

The topography in which a fire is burning also plays a part in the way in which energy is transferred to the unburnt fuel. It has recognised that fires burn faster upslope than they do down, even with a downslope wind. This is thought to be due to increased transfer of radiant heat due to the change in the geometry between the fuel on the slope and the flame; however, recent work (Wu *et al.*, 2000) suggests that there is also increased advection in these cases.

II.3 Physical Models

This section briefly describes some of the physical models developed since 1990 (Table II.3) (Sullivan, 2008). The most distinguishing feature of a fully physical model of fire spread in comparison with one that is commonly identified as quasi-physical is the presence of some form of combustion chemistry. These models determine the energy released from the fuel, and thus the amount of energy which is subsequently transferred to surrounding unburnt fuel and to the other elements in the computational domain. This is done through a model describing the fundamental chemistry of the fuel and its combustion. Quasi-physical models, on the other hand, rely upon a fixed amount of energy released by combustion and on flame characteristics to be known *a priori* making their use generally applicable to specific conditions. This limitation makes them not suitable to be considered a good way for study fire spreading and behaviour.

Different approaches and final purposes characterize the physical models reported in table II.3. Some have continued development, some have been implemented and tested against observations, and others have not. Many are implemented in only one or two dimensions in order to improve computational or analytical feasibility.

Table II.3 *Summary of the physical models (1990-present) discussed*

MODEL	AUTHOR	YEAR	COUNTRY	DIMENSIONS
Weber	Weber	1991	Australia	2
AIOLOS-F	Croba <i>et al.</i>	1994	Greece	3
FIRETEC	Linn	1997	USA	3
Forbes	Forbes	1997	Australia	1
Grishin	Grishin <i>et al.</i>	1997	Russia	2
IUSTI	Larini <i>et al.</i>	1998	France	2
PIF97	Dupuy <i>et al.</i>	1999	France	2
LEMTA	Sero-Guillaume	2002	France	2
UoS	Asensio <i>et al.</i>	2002	Spain	2
WFDS	Mell <i>et al.</i>	2006	USA	3

II.3.1 Weber (1991)

Weber's (1991b) model was an attempt to provide the framework to build a physical model of fire spread, rather than an attempt to actually build one. To this end, he highlights several possible approaches but does not give any definitive answer.

Weber begins with a reaction-transport formulation of the conservation of energy equation, which states that the rate of change of enthalpy per unit time is equal to the spatial variation of the flux of energy plus heat generation. He then formulates several components that contribute to the overall flux of energy, including radiation from flames, radiation transfer to fuel through the fuel, advection and diffusion of turbulent eddies. Heat is generated through a chemical reaction that is modelled by an Arrhenius law which includes heat of combustion. This results in a first cut model that is one dimensional in x plus time.

In a more realistic version Weber determines the solution of the model in two dimensions producing two parametric equations for spatial x and y that yields an ellipse whose centre has been shifted. Weber favourably compares this result with that of Anderson *et al.* (1982), who first formalised the spread of a wildland fire perimeter as that of an expanding ellipse. No performance data are given.

II.3.2 AIOLOS-F (CINAR S.A., Greece)

AIOLOS-F was developed by CINAR S.A., Greece, as a support tool for wildland fire behaviour prediction. It is a model that utilises the 3-dimensional form of the conservation laws to couple the combustion of a fuel layer with the atmosphere to model forest fire spread (Croba *et al.*, 1994). It consists of two components, AIOLOS-T which predicts the local wind field and wind-fire interaction, and AIOLOS-F which models the fuel combustion.

The combustion model is a 3D model of the evolution of enthalpy from which change in solid-phase temperature is determined. A thermal radiation heat transfer equation provides the radiant heat source term. Fuel combustion is modelled through a 3-dimensional fuel mixture-fraction evolution that is tied to a single Arrhenius Law for the consumption of solid phase fuel. The quantity of fuel consumed by the fire within a time interval is an exponential function of the mixture fraction.

Fuel is assumed to be a single layer beneath the lowest atmosphere grid. Fuel is specified from satellite imagery on grids with a resolution in the order of 80 m. No data on calculation time is given, although it is described (Croba *et al.*, 1994; Lymberopoulos *et al.*, 1998) as being faster than real time.

II.3.3 FIRETEC (Los Alamos National Laboratory, USA)

FIRETEC (Linn, 1997), developed at the Los Alamos National Laboratory, USA, is a coupled multiphase transport/wildland fire model based on the principles of conservation of mass, momentum and energy. It is fully 3-dimensional and in combination with a hydrodynamics model called HIGRAD (Reisner *et al.*, 1998, 2000a,b), which is used to solve equations of high gradient flow such as the motions of the local atmosphere.

FIRETEC is described by the author as self-determining, meaning that the model does not use prescribed or empirical relations in order to predict the spread and behaviour of wildland fires, relying solely on the formulations of the physics and chemistry to model the fire behaviour.

The complex combustion reactions of a wildland fire are represented in FIRETEC using a few simplified models, including models for pyrolysis, char burning, hydrocarbon combustion and soot combustion in the presence of oxygen (Linn, 1997).

A peculiar of the FIRETEC model is that the variables that occur in the relative solid and gas phase conservation equations are divided into mean and fluctuating components: this approach is similar to that used for the modelling of turbulence in flows.

The concept of a critical temperature within the resolved volume is used to initiate combustion: once the mean temperature exceeds the critical

temperature, combustion starts and the evolution equations are used to track the solid and gas phase species. The critical temperature is chosen to be 500 K (Linn, 1997).

Because FIRETEC models the conservation of mass, momentum and energy for both the gas and solid phases, it does have the potential to determine the occurrence of ‘spotting’ downwind of the main fire. Running on a 128-node SGI computer with R10000 processors, a simplified FIRETEC simulation is described as running at ‘one to two orders of magnitude slower than realtime’ for a reasonable domain size (Hanson *et al.*, 2000).

II.3.4 Forbes (1997)

Forbes (1997) developed a two dimensional model of fire spread using radiative heat transfer, species consumption and flammable gas production. The basis for his model is observations of eucalypt forest fires which appeared either to burn quiescently or as raging infernos. The main conceit behind the model is a two-path combustion model in which the solid fuel of eucalypt trees either thermally degrades directly and rapidly in an endothermic reaction, or produces flammable ‘eucalypt vapours’ endothermically which then combust exothermically.

Forbes, developing a two-dimensional solution, makes the assumption that the height of the processes involved in the vertical direction (i.e. the flames) is small when compared to the area of the fire (i.e. by some orders of magnitude). This solution produces an elliptical fire shape stretched in the direction of the wind. He suggests improving the model by including fuel moisture. No performance data are given.

II.3.5 Grishin (Tomsk State University, Russia)

Grishin’s model, as described in a number of papers (Grishin *et al.*, 1983; Grishin, 1984; Grishin *et al.*, 1984; Grishin and Shipulina, 2002), is based on analysis of experimental data and developed using the concepts and methods of reactive media mechanics. In this formulation, the wildland fuel (in this case, primarily forest canopy) and combustion products represent a non-deformable porous-dispersed medium (Grishin, 1997). Turbulent heat and mass transfer in the forest, as well as heat and mass exchange between the near ground layer of the atmosphere and the forest canopy, are incorporated. The forest is considered as a multi-phase, multi-storied, spatially heterogeneous medium outside the fire zone. Inside the fire zone, the forest is considered to be a porous-dispersed, seven phase, two-temperature, single-velocity, reactive medium. The six phases within the combustion zone are: dry organic matter, water in liquid state, solid products of fuel pyrolysis

(char), ash, gas (composed of air, flying pyrolytic products and water vapour), and particles in the dispersed phase.

The model takes into account the basic physicochemical processes (heating, drying, pyrolysis of combustible forest material) and utilises the conservation of mass, momentum and energy in both the solid and gas phases. Other equations, in conjunction with initial and boundary conditions, are used to determine the concentrations of gas phase components, radiation flux, convective heat transfer, and mass loss rates through Arrhenius rate laws using experimentally-determined activation energy and reaction rates.

The original formulation was intended only for the acceleration phase from ignition until steady state spread is achieved (Grishin *et al.*, 1983). This was extended using a moving frame of reference and a steady-state rate of spread (ROS) to produce an analytical solution for the ROS which was found to vary linearly with wind speed (Grishin, 1984). The speed of the fire front is taken to be the speed of the 700 K isotherm. The domain used for numerical analysis is in the order of 100-200 m long. Rate of spread is found to be dependent on initial moisture content of the fuel. No performance data are given.

II.3.6 IUSTI (Institut Universitaire des Systemes Thermiques Industriels, France)

IUSTI (Larini *et al.*, 1998; Porterie *et al.*, 1998a,b, 2000) is based on macroscopic conservation equations obtained from local instantaneous forms (Larini *et al.*, 1998) using an averaging method first introduced by Anderson and Jackson (1967). IUSTI considers wildland fire to be a multi-phase reactive and radiative flow through a heterogeneous combustible medium, utilising coupling through exchange terms of mass, momentum and energy between a single gas phase and any number of solid phases. The physico-chemical processes of fuel drying and pyrolysis due to thermal decomposition are modelled explicitly.

Mass loss rates are deduced from Arrhenius-type laws following on from the values used by Grishin *et al.* (1983) and Grishin (1997) and thermogravimetric analysis (Porterie *et al.*, 2000). The pyrolysis products are assumed to be removed out of the solid instantaneously upon release. Mass diffusion of any chemical species is neglected and no chemical reactions occur in the solid phase. A single one-step reaction model in which fuel reacts with oxidant to produce product is implemented.

The formation of soot is modelled as the soot volume fraction which forms mostly as a result of the pyrolysis process and so is assumed to be a percentage of the mass loss rate due to pyrolysis. Drag is included through the drag coefficient which is a function of the Reynolds number of the solid phase. Solid phase particles are treated as spheres. The conductive/convective heat transfer coefficient is expressed using the Reynolds number

for flow around cylinders. The governing equations of conservation in both gas and solid phases are made discrete on a non-uniform grid using a finite-volume scheme. The domain over which the equations are solved is in the order of 1-2 m long by 0.1 m with an average resolution of about 0.01 m. No performance data are given.

II.3.7 PIF97

The detailed work of Larini *et al.* (1998), Porterie *et al.* (1998a) and Porterie *et al.* (2000) provided the framework for the development of a related model, named PIF97 by its authors (Dupuy and Larini, 1999; Morvan and Dupuy, 2001). The aim of this work was to simplify the multi-phase IUSTI model of Larini *et al.* (1998) and Porterie *et al.* (1998a) in order to develop a more operationally-feasible model of wildland fire spread.

PIF97 comes in two parts. The first is a combustion zone model that considers the radiative and convective heat transferred to the fuel bed in front of the flaming zone. The second part of the model is the fire-induced flow in the flaming combustion zone behind the ignition interface. This depends on the ROS of the interface derived from the combustion part of the model.

A later version of PIF97 (Morvan and Dupuy, 2004) was extended to multiple solid phases in order to simulate Mediterranean fuel complexes comprising live and dead components of shrub and grass species, including twigs and foliage. The revised model was implemented as a 2D vertical slice through the fire front as a compromise between the computational time and need to study the main physical mechanisms of the fire propagation. 80×45 control volumes, each 10 cm x 3 cm were used, defining a domain 8 m by 1.35 m. ROS was defined as the movement of the 500K isotherm inside the pyrolysis front. ROS was compared to other models and observations of shrub fires (Fernandes, 2001). The authors summarise their model as producing a ROS relationship for wind $< 3 \text{ m s}^{-1}$ as ‘an increasing function of wind speed’ and then say the ROS reaches a limiting value at a wind speed of about 5 m s^{-1} . The other models and observations showed either linear or power law ($\text{exp} < 1.0$) relationships.

Dupuy and Morvan (2005) added a crown layer to this model resulting in six families of solid phase fuel: three for shrubs (leaves and two size classes of twigs (0-2, 2-6 mm), one for grass, and two for the *P. halepensis* canopy (needles and twigs 2-6 mm). This version implemented a combustion model based on Arrhenius-type laws. Soot production (for the radiation transfer) was assumed at 5% of the rate of solid fuel pyrolysis. The domain was 200 m x 50 m high with, at its finest scale, cells 0.25 m x 0.025 m, average of 0.2 x 0.25 and largest 1.0 x 0.25 m. 200 s of simulation took 48 hours on an Intel Pentium P4 2GHz machine.

II.3.8 LEMTA (Laboratoire d'Énergétique et de Mécanique Théorique et Appliquée, France)

This model, developed by Sero-Guillaume and Margerit (2002) of Laboratoire d'Énergétique et de Mécanique Théorique et Appliquée in France, considers a two-phase model, gas and solid, in three regions of a forest – above the forest, in the forest and below the ground – at three scales: microscopic (plant cell solid/gas level), mesoscopic (branch and leaf level) and macroscopic (forest canopy/atmosphere level). They identify but do not investigate a fourth scale, that of the 'gigascope' or landscape level.

The combustion chemistry is simplified in that only gas-phase combustion is allowed. Solid phase chemistry only considers pyrolysis to gas-phase volatile fuel, char and tar. Soot production is not considered, nor is char combustion. Gas phases include O₂, water, N₂, fuel and inert residue. Conservation of species mass, momentum and energy are derived for mesoscopic gas and solid phase interactions. These are then averaged over the larger macroscopic scale by using distribution theory and convoluting the equations to macroscopic quantities. Extended irreversible thermodynamics is then used to close the system of equations. Arguments about thermal equilibrium are used to further reduce the non-equilibrium equations for temperature and pressure.

The system of equations is then further simplified using assumptions about the nature of the fuel (at rest) and the size and interaction of the fuel particles with the gas phase (i.e. no advection, pressure or porosity variations in the solid phase). Drag is not included. Gas phase equations in the region above the forest do not include solid phase particles and, since soot is not modelled, cannot suitably describe radiant heat from flames.

When simulated on a computer, the model provides a circular shape in no wind/no slope, and an elongated shape under wind. An example burning in real terrain is shown but no discussion of its performance against real fires is given. Mention is made of it operating in real-time on a PC.

II.3.9 UoS (University of Salamanca, Spain)

Asensio and Ferragut (2002) constructed a 2D model of fire spread that used radiation as the primary mode of heat transfer but also incorporated advection of hot gas and convective cooling of fuels. The model (UoS) employed a simplified combustion chemistry model (only two phases: gas and solid, and two species: fuel and oxygen) and utilised only conservation of energy and species mass. It is assumed combustion is fuel limited and thus only one species is conserved. Arrhenius laws for fuel consumption are used. Turbulence is not accounted for directly or explicitly, but a term for advection with a wind velocity vector is included.

No performance data are given.

II.3.10 WFDS (National Institute of Safety Technology, USA)

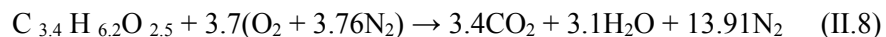
The Wildland Fire Dynamic Simulator (WFDS), developed by the US National Institute of Safety Technology (Mell *et al.*, 2006) and the US Forest Service is an extension of the model developed to predict the spread of fire within structures, Fire Dynamic Simulator (FDS). This model is fully 3D, is based upon a unique formulation of the equations of motion for buoyant flow (Rehm and Baum, 1978) and is intended for use in predicting the behaviour of fires burning through peri-urban/wildlands (what the authors call ‘Community-scale fire spread’ (Rehm *et al.*, 2003; Evans *et al.*, 2003)).

The main objective of this model is to predict the progress of fire through predominantly wildland fuel augmented by the presence of combustible structures. WFDS utilises a varying computational grid to resolve volumes as low as 1.6 m (x) x 1.6 m (y) x 1.4 m (z) within a simulation domain, which can reach the order of 1.5 km² in area and 200 m high. Outside regions of interest, the grid resolution is decreased to improve computational efficiency.

Mell *et al.* (2006) give a detailed description of the WFDS formulated for the specific initial case of grassland fuels, in which vegetation is not resolved in the gas-phase (atmosphere) grid but in a separate solid fuel (surface) grid (which the authors admit is not suitable for fuels in which there is significant vertical flame spread and air flow through the fuel). In the case presented, the model includes features such as momentum drag caused by the presence of the grass fuel (modelled as cylinders) which changes over time as the fuel is consumed. Mechanical turbulence, through the dynamic viscosity of the flow through the fuel, is modelled as a subgrid parameter via a variant of the Large Eddy Simulation (LES) method.

The WFDS assumes a two-stage endothermic thermal decomposition (water evaporation and then solid fuel ‘pyrolysis’). It uses the temperature dependent mass loss rate expression of Morvan and Dupuy (2004) to model the solid fuel degradation and assumes that pyrolysis occurs at 127°C. Solid fuel is represented as a series of layers which are consumed from the top down until the solid mass reaches a predetermined char fraction at which point the fuel is considered consumed.

WFDS assumes that the combustion of pyrolysis coming gases occurs solely as the result of mixing with oxygen in stoichiometric proportion. Char oxidation is not accounted for. The gas phase combustion is modelled using the following stoichiometric relation:



Due to the relatively coarse scale of the resolved computation grids within WFDS, detailed chemical kinetics are not modelled. Instead, the concept of a mixture fraction within a resolved volume is used to represent the mass ratio

of gas-phase fuel to oxygen using a fast chemistry or flame sheet model which then provides the mass loss flux for each species.

The energy release associated with chemical reactions is not explicitly presented but is accounted for by an enthalpy variable as a function of species. The model assumes that the time scale of the chemical reactions is much shorter than that of mixing.

Thermal radiation transport assumes a gray gas absorber-emitter using the P1 radiation model for which the absorption coefficient is a function of the mixture fraction and temperature for a given mixture of species. A soot production model is not used; instead it is an assumed fraction of the mass of fuel gas consumed.

Mell *et al.* (2006) provides simulation information for two experimental grassfires. In the first case, a high intensity fire in a plot 200 m x 200 m within a domain of 1.5 km x 1.5 km and vertical height of 200 m for a total 16 million grid cells, the model, running on 11 processors, took 44 cpu hours for 100 s of simulated time. Another lower intensity experiment over a similar domain took 25 cpu hours for 100 s of simulated time.

II.4 Discussion and summary

According to the final purpose the physical models were intended, they can be divided primarily into two categories; those that are intended for operational or experimental use (or at least field validation) and those that are purely academic exercises. The latter are characterised by the lack of follow-up work (e.g. Weber, Forbes, UoS), although it is possible that components of such models may later find their way into models intended for operational or experimental use. Grishin, IUSTI, and LEMTA were all formulated with the intention of being useful models of fire spread but either due to the complex nature of the models or to the restricted domain over which the model can operate feasibly, their use remains operationally limited.

The remaining physical models, AIOLOS-F, FIRETEC, PIF97 and WFDS have all had extended and ongoing development and each are capable of modelling the behaviour of a wildland fire in a landscape scale (i.e. computational domains in excess of about 100 m). However, in the effort to make this computationally feasible, each model significantly reduces both the resolution of the computational domain and the precision of the physical models implemented. As is the case with any field experiment, it is very difficult to measure all required quantities to the degree of precision and accuracy required by the models. In the case of wildland fires, this difficulty is increased by two or three orders of magnitude. Boundary conditions are rarely known and other quantities are almost never measured at the site of the fire itself.

Table II.5 Summary of the physical models (adapted from Sullivan, 2008)

MODEL	DIMENSIONS	DOMAIN SIZE (X x Y x Z)	RESOLUTIONS (m, s)				CPU No. & TYPE	SIMULATION TIME (s)	COMPUTATION TIME (s)	NOTES
			Δx	Δy	Δz	Δt				
<i>Physical</i>										
Weber	2	?	-	-	-	-	-	-	-	< real time
AIOLOS-F	3	10 x 10 x ? km	-	-	-	-	-	-	-	>> real time
FIRETEC	3	320 x 160 x 61.5m	2	2	1.5	0.002	128 nodes	-	-	
Forbes	2	?	-	-	-	-	-	-	-	
Grishin	2	50 x - x 12 m	-	-	-	-	-	-	-	700 K iso T
IUSTI	2	2.2 x - x 0.9 m	0.02	-	0.09	-	-	-	-	500 K iso T
PIF97	2	200 x - x 50 m	0.25	-	0.25	1 s	P4 2GHz	200 s	48 h	500 K iso T
LEMETA	2	-	-	-	-	-	PC	-	-	~ real time
UoS	2	-	1.88	1.88	-	0.25 μ	-	-	-	
WFDS	3	1.5 x 1.5 x 0.2 km	1.5	1.5	1.4	-	11 nodes	100 s	25 h	>>> real time

IUSTI and PIF97 undertook validation utilising laboratory experiments of suitable spatial scales in which the number and type of variables were strictly controlled. In many laboratory experiments, the standard condition is one of no wind and no slope. The ability to correctly model the behaviour of a fire in such conditions is only one step in the testing of the model. Both IUSTI and PIF97 (as well as a number of the quasi-physical models discussed here) were validated in these conditions of wind and/or slope.

Both FIRETEC and WFDS attempted validation against large scale experimental grassland fires (Cheney *et al.*, 1993) and thus avoided many of the issues of validation against wildfire observations. Table II.5 (Sullivan, 2008) shows a summary of the scope, resolution and computation time available in the literature for each of the models. Here models such as AIOLOS-F, FIRETEC and WFDS stand out from the others because of their stated aim to be a useful tool in fire management.

PIF97 and WFDS give nominal computation times for a given period of simulation. PIF97 and WFDS, using the current level of hardware, are all much greater than realtime (in the order of 450 times realtime for WFDS on 11 processors (Mell *et al.*, 2006)). FIRETEC is described as being 'several orders of magnitude slower than realtime'. The authors of FIRETEC are aware of not being able to predict the behaviour of landscape wildland fires, but mainly suggest that the primary use of purely physical models of fire behaviour is the study of fires under a variety of conditions in a range of fuels and topographies, that is scenarios, which are not amenable to field experimentation. Hanson *et al.* (2000) suggest that the operational fire behaviour models of the future will be reduced versions of the purely physical models being developed today.

It is obvious, from the performance data available in the literature, that the current physical approaches to modelling fire behaviour on the hardware available today are not able yet to provide real-time prediction in order to conduct fire suppression or emergency plans. However, their use in the scientific community has become in the last years very promising especially because they aim to analyze the fire behaviour on a scientific basis. Among the analyzed software only FIRETEC and WFDS found validation under large domain size, considering for their formulation the interaction between fuel and atmosphere: this aspect appears to be a fundamental approach in order to correctly analyze such a phenomena (Linn, 2005).

In this short review, the capabilities of the physically-based models have been highlighted. The softwares FIRETEC and WFDS appear to be the most reliable ones even if some performance tests seems to favourite the second code. WFDS is an extension (to fires in vegetation) of the structural fire simulation tool FDS which is designed for use by practicing fire protection engineers. Feedback from users around the world was used to make FDS a robust simulation tool. FIRETEC, however, was not developed for, and is not used by, a large user community. FIRETEC requires significantly more

computational resources to run. Exploratory simulations on relatively small domains (120 m x 120 m x 200 m; 60 x 60 x 34 grid points) required 3 days and 16 processors for 100 s of simulated time. The same simulation with WFDS ran on a laptop in less than 1 hour, over a factor of 100 faster. Furthermore, some comparisons based on benchmarks carried out for surface fire propagating through grassland (Mell *et al.*, 2005), indicated that WFDS is more efficient in terms of computational time compared with FIRETEC

The validation process of these two softwares is still an ongoing process being, currently, essentially limited to flat grasslands. Their use in more complex domain configurations remains partial and not completely tested: the achievement of this step may provide indication for a wider application of these codes in order to, hopefully, put the basis for carrying out a risk analysis of fire spreading taking into account specific terrain features and vegetative characteristics of a given area. Therefore the analysis of the potentiality of one of these two codes in efficiently describe the fire propagation, under different fuel and boundary conditions, also across not already tested terrains is evident. These domains include slope-changing surfaces and canyons which represent, both, very common geographic configurations. Furthermore, results of a simulation of fire propagation across a real terrain is also presented. According to the previous considerations, to perform the numerical evaluation, the chose of the WFDS code appeared the most suitable one. In the following chapter, details about the physical mechanisms and length scales governing the propagation of wildfires along with the physical and mathematical constraints involved in the modelling are provided. Subsequent sections propose modelling results related to fire spreading in double-slope and canyons configurations and to the fire evolution across a realistic domain

II.5 References

- Albini, F. (1979). Spot fire distance from burning trees—a predictive model. General Technical Report INT-56, USDA Forest Service, Intermountain Forest and Range Experimental Station, Ogden UT.
- Anderson, D., Catchpole, E., de Mestre, N., and Parkes, T. (1982). Modelling the spread of grass fires. *Journal of Australian Mathematics Society, Series B*, 23:451–466.
- Anderson, T. B. and Jackson, R. (1967). Fluid mechanical description of fluidized beds: Equations of motion. *Industrial & Engineering Chemistry. Fundamentals*, 6(4):527–539.
- Asensio, M. and Ferragut, L. (2002). On a wildland fire model with radiation. *International Journal for Numerical Methods in Engineering*, 54(1):137–157.

- Ball, R., McIntosh, A., and Brindley, J. (1999). The role of char-forming processes in the thermal decomposition of cellulose. *Physical Chemistry Chemical Physics*, 1:5035–5043.
- Beall, F. and Eickner, H. (1970). Thermal degradation of wood components: A review of the literature. Research Paper FPL 130, USDA Forest Service, Madison, Wisconsin.
- Cheney, N., Gould, J., and Catchpole, W. (1993). The influence of fuel, weather and fire shape variables on fire-spread in grasslands. *International Journal of Wildland Fire*, 3(1):31–44.
- Croba, D., Lalas, D., Papadopoulos, C., and Tryfonopoulos, D. (1994). Numerical simulation of forest fire propagation in complex terrain. In *Proceedings of the 2nd International Conference on Forest Fire Research, Coimbra, Portugal, Nov. 1994. Vol 1.*, pages 491–500.
- di Blasi, C. (1998). Comparison of semi-global mechanisms for primary pyrolysis of lignocellulosic fuels. *Journal of Analytical and Applied Pyrolysis*, 47(1):43–64.
- Dupuy, J. and Larini, M. (1999). Fire spread through a porous forest fuel bed: a radiative and convective model including fire-induced flow effects. *International Journal of Wildland Fire*, 9(3):155–172.
- Dupuy, J. L. and Morvan, D. (2005). Numerical study of a crown fire spreading toward a fuel break using a multiphase physical model. *International Journal of Wildland Fire*, 14(2):141–151.
- Ellis, P. (2000). *The aerodynamic and combustion characteristics of eucalypt bark: A firebrand study*. PhD thesis, The Australian National University School of Forestry, Canberra.
- Evans, D., Rehm, R., and McPherson, E. (2003). Physics-based modelling of wildlandurban intermix fires. In *Proceedings of the 3rd International Wildland Fire Conference, 3-6 October 2003, Sydney*.
- Fernandes, P. (2001). Fire spread prediction in shrub fuels in Portugal. *Forest Ecology and Management*, 144(1-3):67–74.
- Forbes, L. K. (1997). A two-dimensional model for large-scale bushfire spread. *Journal of the Australian Mathematical Society, Series B (Applied Mathematics)*, 39(2):171–194.
- Gerhards, C.C. (1979). Effect of high-temperature drying on tensile strength of Douglas-fir 2x4's. *For. Prod. J.*, 29(3):39-46
- Gerhards, C.C. (1982). Effect of moisture content and temperature on mechanical properties of wood: an analysis of immediate effects. *Wood Fiber* 14(1):4:36
- Gerhards, C.C. (1983). Effect of high-temperature drying on the bending yellow-poplar 2x4's. *For. Prod. J.*, 33(2):61-67
- Goldstein, R. J., Ibele, W. E., Patankar, S. V., Simon, T. W., Kuehn, T. H., Strykowski, P. J., Tamma, K. K., Heberlein, J. V. R., Davidson, J. H., Bischof, J., Kulacki, F. A., Kortshagen, U., Garrick, S., and Srinivasan,

- V. (2006). Heat transfer: A review of 2003 literature. *International Journal of Heat and Mass Transfer*, 49(3-4):451–534.
- Grishin, A. (1984). Steady-state propagation of the front of a high-level forest fire. *Soviet Physics Doklady*, 29(11):917–919.
- Grishin, A. (1997). *Mathematical modeling of forest fires and new methods of fighting them*. Publishing House of Tomsk State University, Tomsk, Russia, english translation edition. Translated from Russian by Marek Czuma, L Chikina and L Smokotina.
- Grishin, A. and Shipulina, O. (2002). Mathematical model for spread of crown fires in homogeneous forests and along openings. *Combustion, Explosion, and Shock Waves*, 38(6):622–632.
- Grishin, A., Gruzin, A., and Gruzina, E. (1984). Aerodynamics and heat exchange between the front of a forest fire and the surface layer of the atmosphere. *Journal of Applied Mechanics and Technical Physics*, 25(6):889–894.
- Grishin, A., Gruzin, A., and Zverev, V. (1983). Mathematical modeling of the spreading of high-level forest fires. *Soviet Physics Doklady*, 28(4):328–330.
- Hanson, H., Bradley, M., Bossert, J., Linn, R., and Younker, L. (2000). The potential and promise of physics-based wildfire simulation. *Environmental Science & Policy*, 3(4):161–172.
- Koch, P. (1985). Drying southern pine at high temperature – a summary of research at Pineville, LA from 1963-1982. In: Mitchell P.H. (ed.) 1985. *Proc. North American Drying Symp.* Mississippi State University, pp. 1-38.
- Larini, M., Giroud, F., Porterie, B., and Loraud, J. (1998). A multiphase formulation for fire propagation in heterogeneous combustible media. *International Journal of Heat and Mass Transfer*, 41(6-7):881–897.
- Linn, R. and Cunningham, P. (2005). Numerical simulations of grass fires using a coupled atmosphere-fire model: Basic fire behavior and dependence on wind speed. *Journal of Geophysical Research*, 110 (D13107):19 pp.
- Linn, R. R. (1997). A transport model for prediction of wildfire behaviour. PhD Thesis LA-13334-T, Los Alamos National Laboratory. Reissue of PhD Thesis accepted by Department of Mechanical Engineering, New Mexico State University.
- Lymberopoulos, N., Tryfonopoulos, T., and Lockwood, F. (1998). The study of small and meso-scale wind field-forest fire interaction and buoyancy effects using the aiolos-f simulator. In *III International Conference on Forest Fire Research, 14th Conference on Fire and Forest Meteorology, Luso, Portugal, 16-20 November 1998. Vol 1.*, pages 405–418.
- Mell W, Charney JJ, Jenkins MA, Cheney Ph, Gould J (2005) Numerical simulations of grassland fire behaviour from the LANL-FIRETEC and

- NIST-WFDS models. Proceeding of East FIRE conference, George Mason University, Fairfax, VA, 11–13 May 2005
- Mell, W., Jenkins, M., Gould, J., and Cheney, P. (2006). A physics based approach to modeling grassland fires. *International Journal of Wildland Fire*, 15(4)
- Morten, G. G., Varhegyi, G., Di Blasi, C. (2002). Thermogravimetric Analysis and Devolatilization Kinetics of Wood. *Ind. Eng. Chem. Res.*, 41, 4201-4208
- Morvan, D. and Dupuy J.L. (2004). Modeling the propagation of a wildfire through a Mediterranean shrub using a multiphase formulation. *Combustion and Flame* 138(2004): 199-210.
- Morvan, D. and Dupuy, J. (2001). Modeling of fire spread through a forest fuel bed using a multiphase formulation. *Combustion and Flame*, 127(1-2):1981–1994.
- Plucinski, M. P. (2003). *The investigation of factors governing ignition and development of fires in heathland vegetation*. PhD thesis, School of Mathematics and Statistics University of New South Wales, Australian Defence Force Academy, Canberra, ACT, Australia.
- Porterie, B., Morvan, D., Larini, M., and Loraud, J. (1998a). Wildfire propagation: A two-dimensional multiphase approach. *Combustion Explosion and Shock Waves*, 34(2):139–150.
- Porterie, B., Morvan, D., Loraud, J., and Larini, M. (1998b). A multiphase model for predicting line fire propagation. In *III International Conference on Forest Fire Research, 14th Conference on Fire and Forest Meteorology, Luso, Portugal, 16-20 November 1998. Vol 1.*, pages 343–360.
- Porterie, B., Morvan, D., Loraud, J., and Larini, M. (2000). Firespread through fuel beds: Modeling of wind-aided fires and induced hydrodynamics. *Physics of Fluids*, 12(7):1762–1782.
- Rehm, R. G. and Baum, H. R. (1978). The equations of motion for thermally driven, buoyant flows. *Journal of Research of the National Bureau of Standards*, 83(3):297–308.
- Rehm, R., Evans, D., Mell, W., Hostikka, S., McGrattan, K., Forney, G., Boulding, C., and Baker, E. (2003). Neighborhood-scale fire spread. In *Fifth Symposium on Fire and Forest Meteorology, 16-20 November 2003, Orlando, Florida*. paper J6E.7 8pp, unpaginated.
- Reisner, J. M., Bossert, J. E., and Winterkamp, J. L. (1998). Numerical simulations of two wildfire events using a combined modeling system (HIGRAD/BEHAVE). In *Second Symposium on Fire and Forest Meteorology, 11-16 January 1998, Phoenix, Arizona*, pages 6–13. American Meteorological Society.
- Reisner, J., Knoll, D., Mousseau, V., and Linn, R. (2000a). New numerical approaches for coupled atmosphere-fire models. In *Third Symposium on*

- Fire and Forest Meteorology, 9-14 January 2000, Long Beach, California.*, pages 11–14. American Meteorological Society.
- Reisner, J., Wynne, S., Margolin, L., and Linn, R. (2000b). Coupled atmospheric-fire modeling employing the method of averages. *Monthly Weather Review*, 128(10):3683–3691.
- Sacadura, J. (2005). Radiative heat transfer in fire safety science. *Journal of Quantitative Spectroscopy & Radiative Transfer*, 93:5–24.
- Sero-Guillaume, O. and Margerit, J. (2002). Modelling forest fires. Part I: A complete set of equations derived by extended irreversible thermodynamics. *International Journal of Heat and Mass Transfer*, 45(8):1705–1722.
- Shafizadeh, F. (1982). Introduction to pyrolysis of biomass. *Journal of Analytical and Applied Pyrolysis*, 3(4):283–305.
- Sullivan A.L. (2008) Wildland surface fire spread modelling, 1990–2007. 1: Physical and quasi-physical models. *International Journal of Wildland Fire* 18(4) 349–368
- Sullivan, A., Ellis, P., and Knight, I. (2003). A review of the use of radiant heat flux models in bushfire applications. *International Journal of Wildland Fire*, 12(1):101–110.
- Weber, R. (1989). Analytical models of fire spread due to radiation. *Combustion and Flame*, 78:398–408.
- Weber, R. (1991b). Toward a comprehensive wildfire spread model. *International Journal of Wildland Fire*, 1(4):245–248.
- Williams, F. (1982). Urban and wildland fire phenomenology. *Progress in Energy Combustion Science*, 8:317–354.

Chapter III

Forest fire modelling: basic equations and numerical constraints

This part of the work is an outline of the physical mechanisms and length scales governing the propagation of wildfires. One of the objectives is to describe the physical and mathematical constraints in the modelling of wildfires when using a fully physical model. The literature highlights two regimes in the propagation of surface fires, i.e. wind-driven fires and plume-dominated fires, which are governed by radiation and convective heat transfer, respectively. This division leads to the identification of two governing length scales: the extinction length characterising the absorption of radiation by vegetation, and the integral turbulent length scale characterising the interaction between wind and canopy. A short outline of the mathematical background, necessary to describe the physical and chemical aspects involved in the fire phenomena along with its numerical implications, is also provided.

III.1. Physical mechanisms and characteristic length scales

In wildfires, two basic mechanisms contribute to heat transfer between the flame and the unburned vegetation: radiation coming from soot particles located in the flame, and convective heat transfer between the hot gases coming from the burning zone and vegetation located ahead of the fire front (Pagny and Peterson, 1973; Whelan, 1995). The relative importance of these two heat transfer mechanisms depends on the competition between two forces: inertia due to wind flow, and buoyancy resulting from the density gradient between the hot plume above the fire and ambient air (Whelan, 1995; Morvan *et al.*, 2008). The balance between these two contributions can be quantified by introducing the Byram convective number N_C , defined as the ratio between the rate of heat released from the fire and transferred vertically inside the plume versus the power of the inertial force due to the lateral wind flow (Byram, 1959; Nelson, 1993; Sullivan, 2007):

$$N_C = \frac{2gI_B}{\rho C_p T_0 (U_w - ROS)^3} \quad (III.1)$$

where g , ρ and C_p designate the acceleration of gravity, the density and the specific heat of the gas, respectively, and T_0 is the ambient temperature; U_w , I_B and ROS are the wind speed velocity, the fire line intensity and the rate of spread of the surface fire, respectively.

The fire line intensity, I_B (kW/m), representing one of the most representative parameter of fire severity, can be evaluated using the Byram formula, as follows:

$$I_B = W * H * ROS \quad (III.2)$$

using the following notation: W for weight of fuel consumed per unit area in the active flaming zone (kg/m^2), H for heat of combustion of solid fuel (kJ/kg) and ROS for rate of spread (m/s). Taking into account that part of the energy released by the fire is lost by radiation, the most usual value retained for H is $18,000 \text{ kJ/kg}$.

When $NC \gg 1$, the behaviour of the fire is mainly governed by the dynamics of the thermal plume. In this case the trajectory of flames is nearly vertical and the convective column is well developed. The fire spread is mainly influenced by the fire itself and weakly by the wind. During propagation of the fire, one can observe strong updrafts characterised by rapid growth, followed by strong downdrafts after air is cooled in the upper part of the atmosphere. This phenomena promotes rapid descending air flow, which can cause collapse of the plume, with possible formation of a whirlwind. This fire configuration can promote high potential for spotting (more or less long-distance transport of burning particles, causing secondary ignition). This fire regime is referred to in the literature as plume dominated (Pyne *et al.*, 1996) and the heat transfer between the flames and vegetation is mainly supported by radiation.

When $NC \ll 1$, the behaviour of fire is mainly controlled by wind flow. In this case, the thermal plume and flames are strongly deflected by the wind, and the variations of rate of spread are nearly linear in wind speed. This regime of fire propagation is referred to in the literature as wind driven (Pyne *et al.*, 1996) and propagation of the fire is mainly sustained by convective heat transfer; i.e. the hot gases coming from the burning zone are pushed by the wind flow, toward unburned fuel.

In considering the physical phenomena that lie at the origin of these two mechanisms of heat transfer, i.e. soot particles and the Stefan–Boltzmann σT^4 law for radiation, and local velocity magnitude and gas temperature T for convection, the second regime of propagation (namely wind-driven flow) is less affected by nonlinear mechanisms. Consequently, it is not surprising that the behaviour of such fires is more easily predictable, very often exhibiting linear dependence on wind speed velocity.

Because their behaviour are less predictable, plume-dominated fires are less studied experimentally. Nevertheless, this regime of fire propagation is also of great interest, to understand their erratic behaviour which can potentially cause injuries to firefighters, during prescribed burning operation or suppression fire operations (Morvan *et al.*, 2009a and 2009b).

To summarise, two mechanisms contributing to fire behaviour are clearly identified: wind flow, i.e. atmospheric boundary layer (ABL) flow, and radiative heat transfer between the flame and vegetation. These two physical phenomena can be characterised by two length scales: the turbulent integral length scale l_T for ABL and the extinction length δ_R characterising the penetration of radiative heat transfer inside the vegetation layer.

The roughness layer, representing the part of the ABL located between zero and three times the height of the canopy (H_{Fuel}), is mainly affected by coherent structures resulting from the shear interaction (Kelvin–Helmholtz instability), induced by the presence of the vegetation, with the wind flow. Consequently, l_T is strongly correlated with the height of the canopy ($l_T \sim H_{Fuel}$ horizontally and $l_T \sim H_{Fuel}/3$ vertically) (Finnigan, 2000; Kaimal and Finnigan, 1994; Raupach and Thom, 1981)

The extinction length scale δ_R is directly related to two physical characteristics of the vegetation layer: the surface-area-to-volume ratio σ_s and the packing ratio (i.e. the volume fraction occupied by the vegetation) α_s (Table III.1):

$$\delta_R = \frac{4}{\alpha_s \sigma_s} \quad (III.3)$$

To calculate the radiation intensity field I (W/m²/str), necessary to evaluate the radiative heat transfer, the following radiation transfer equation (RTE) must be solved (Modest, 2003)

$$\frac{d\alpha_G I}{ds} = \alpha_G \sigma_a \left(\frac{\sigma T^4}{\pi} - I \right) + \sum_k \left[\frac{\alpha_s \sigma_s}{4} \left(\frac{\sigma T_s^4}{\pi} - I \right) \right]_k \quad (III.4)$$

where the following notations are introduced: gas volume fraction α_G , gas + soot mixture extinction coefficient σ_a , temperature of the gas T and temperature of solid fuel particles T_s . The two terms on the right-hand side in Eq. III.4, represent the contributions from the gas and the solid fuel particles (the k -summation is carried out over the whole set of solid fuel families) to the radiative heat transfer. The same terms (with opposite sign) must appear as source/sink terms in the energy balance equations for the gas mixture and the solid fuel particles.

The combustion process occurring in fire phenomena is turbulent in nature: in this case the Damkohler number (D_a) corresponding to the ratio of chemical time scale τ_c and turbulent time scale τ_t indicates that fire

characterised by high D_a are mainly controlled by the mixing process and very weakly by the kinetic process (Borghi and Champion, 2000).

Table III.1 *Typical attenuation length scale for various ecosystems*

FUEL	BOREAL FOREST	MEDITERRANEAN PINE FOREST	SHRUBS	GRASS	FUEL BED
δ_R	4.75	0.25	0.15	0.15-0.5	0.025

Let us now consider the physical phenomena occurring inside the vegetation layer and contributing also to the final behaviour of a propagating fire. First, it is necessary to define the level of detail necessary to describe the fuel complex layer. Except for some particular situations (homogeneous fuel bed or grassland for example), real vegetation, at landscape scale, is highly heterogeneous, being composed of various species, each structured by different solid fuel elements (foliage, twigs, trunk etc.). The question can be formulated as follows: how can one represent these very complex and heterogeneous structures? A part of the answer can be found in the physical properties characterising the vegetation and contributing effectively to the propagation of fires. These parameters are more or less identified: the fuel moisture content, the surface-area-to-volume ratio, the packing ratio (volume fraction) and the fuel density. Using this set of physical properties, it is possible to define classes (or families) of solid fuel particles representing the variability of fuel elements (foliage, twigs) composing a vegetation layer.

Experimental fires carried out in the laboratory (in dead fuel bed, on a flat terrain, without wind), propagating through homogeneous fuel beds, showed that the fire residence time (defined as the ratio between fire front depth and

rate of spread: $\tau_{\text{Fire}} = \frac{L_{\text{Fire}}}{\text{ROS}}$ increased sharply when the thickness of the

solid fuel particles exceeded 6 mm. Considering that the fire residence time reflects also the response time characterising each solid fuel elements composing a fuel complex when submitted to the thermal stress induced by a fire front, it seems reasonable to consider this value as a threshold for the finest fuel particles in the vegetation description (i.e. coarser fuel particles do not respond quickly enough to contribute actively to fire propagation).

Under the action of the thermal stress resulting from the heat released by the fire, the state of the vegetation located just ahead of the fire front exhibited the following evolution (see also Figure III.1):

1. If the local temperature exceeds a threshold value equal to 373 K, the foliage and the twigs dehydrate (step I);
2. Between 400 K and 500 K, the dry solid fuel is subjected to a chemical reaction (pyrolysis) and is transformed into gas products (mainly CO, CO₂ and CH₄) and charcoal (step II);

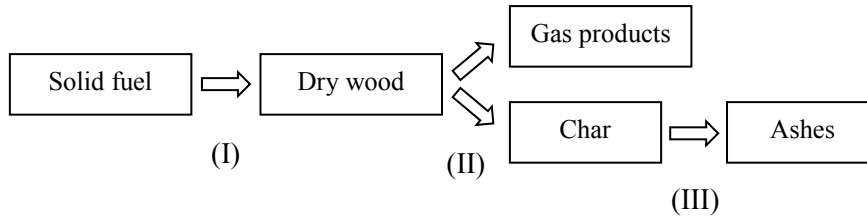


Figura III.1 *Mechanisms of thermal degradation of vegetation*

3. Above 700 K and under the action of ambient air, the surface of char is oxidized (step III).

To follow the evolution of the vegetation state, a set of solid fuel families representing the fuel complex were introduced in the model, each characterised using three mass fractions: water content, dry fuel and charcoal, complemented with a mass fraction representing residual ash.

III.2 Fundamental equations

A fully physical wildfire model is a model based on the solution of the equations governing the evolution of the coupled system formed by the vegetation and the surrounding atmosphere. Models of this class are all based on a multiphase formulation. Of course, all physical scales cannot be directly calculated, as some of them (flame depth, individual fine fuel particles) must be simulated using a physical model.

Generally, in this kind of approach the evolution of the state of the coupled system formed by the vegetation and the surrounding atmosphere is calculated by solving two problems, the first one in the gas phase and the second one in the set of solid particles representing the vegetation.

The problem in the solid phase (vegetation) is formulated assuming that the vegetation stayed at rest and that the thickness of solid fuel particles is sufficiently small (<6 mm), and consequently that the energy balance equation can be solved assuming that the solid fuel particles can be considered as thermally thin (i.e. the temperature distribution inside each solid fuel particles can be considered as locally homogeneous). Two mechanisms of energy exchange with the gas mixture are introduced: convective exchange between the hot or cold gas and the vegetation, and radiative heat transfer. Concerning the thermal degradation of solid fuel particles, the reaction rates reproducing the three steps described previously (drying, pyrolysis and surface oxidation) are evaluated using a Heaviside function for drying or two Arrhenius laws for pyrolysis and surface oxidation.

The problem in the gas phase is formulated by introducing two levels of averaging. A first one in space was introduced to homogenise the contribution resulting from the interaction between the vegetation and the wind flow. One consequence of this first step is the introduction of additional source/sink terms in the momentum and turbulence equations representing the average effect resulting from drag forces induced by the presence of solid fuel particles (foliage, branches, twigs) composing the vegetation. The second step, of time or space averaging, constituted the classical TRANS (Eq. III.7) or LES (Eq. III.8) filtering treatment.

Using a mass average procedure (Favre), the continuity (Eq. III.5), momentum (Eq. III.6), turbulent (or sub-grid scale) kinetic energy (Eq. III.7 and III.8) energy (Eq. III.9) and chemical species (Eq. III.10) balance equations can be written as follows:

$$\frac{D\bar{\rho}}{Dt} = \sum_{\alpha} \bar{M}_{\alpha}^{(S)} \quad (\text{III.5})$$

$$\frac{D\bar{\rho}\tilde{u}_i}{Dt} = \frac{\partial(\alpha_g \bar{\sigma}_{ij})}{\partial x_j} - \frac{\partial(\overline{u_j u_i})}{\partial x_j} + \bar{\rho}g_i - \rho C_D \frac{\alpha_s \sigma_s}{2} \|\tilde{U}\| \tilde{u}_i \quad (\text{III.6})$$

$$\frac{D\bar{\rho}K}{Dt} = \frac{\partial}{\partial x_j} \left(\frac{\mu_{\text{eff}}}{\sigma_K} \frac{\partial K}{\partial x_j} \right) + \bar{\rho}P - \bar{\rho}\varepsilon + \rho C_D \frac{\alpha_s \sigma_s}{2} \|\tilde{U}\| \left(\|\tilde{U}\|^2 - \beta_D K \right) \quad (\text{III.7})$$

$$1 \leq \beta_D \leq 5$$

$$\frac{D\bar{\rho}K}{Dt} = \frac{\partial}{\partial x_j} \left(\frac{\mu_{\text{eff}}}{\sigma_K} \frac{\partial K}{\partial x_j} \right) + \bar{\rho}P - \bar{\rho}C\varepsilon \frac{K^{3/2}}{L_{\text{SGS}}} - 2\rho C_D \frac{\alpha_s \sigma_s}{2} \|\tilde{U}\| K \quad (\text{III.8})$$

$$C\varepsilon = 0.93$$

$$\frac{D\bar{\rho}\tilde{h}}{Dt} = \frac{\partial \bar{q}_j}{\partial x_j} - \frac{\partial}{\partial x_j} (\overline{u_j h}) - \overline{Q_{\text{CONV}}^{(S)}} \quad (\text{III.9})$$

$$\frac{D\bar{\rho}\tilde{Y}_{\alpha}}{Dt} = \frac{\partial}{\partial x_j} \left(\rho D \frac{\partial \tilde{Y}_{\alpha}}{\partial x_j} \right) - \frac{\partial(\overline{u_j Y_{\alpha}})}{\partial x_j} + \bar{W}_{\alpha} + \bar{M}_{\alpha}^{(S)} \quad (\text{III.10})$$

using the following notation:

- ρ Bulk density of the gas phase ($q = \text{agqg}$)
- α_g Volume fraction of the gas phase
- α_s Volume fraction of the solid phase (vegetation)
- u_i i -th component of the velocity vector
- σ_s Average value of surface-area-to-volume fraction (SA/V) of solid fuel particles representing the vegetation
- σ_{ij} Stress tensor

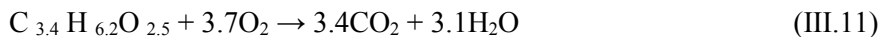
- g_i Acceleration of gravitation
- h Enthalpy
- q_j Heat flux (molecular diffusion and radiation)
- Y_a Mass fraction of chemical species
- T Gas temperature
- μ Dynamical viscosity
- K Turbulent kinetic energy (TKE)

All last terms on the right-hand side of these equations represent the additional terms coming from the interaction between ambient atmosphere and vegetation (gas production due to pyrolysis reaction, drag force, heat transfer by convective exchange etc.). Concerning the effects of drag force upon the turbulence budget (Eq. III.7 and Eq. III.8), the source term (proportional to U^3) represents the production of wake turbulence due to the presence of branches, twigs and foliage inside the canopy.

III.3 Simulation conditions

Dealing with the representation of real fuel complex (fully heterogeneous vegetation), most of the physics-based code are able to take into account the presence of various solid fuel particles types inside the same grid cell, representing the local variability in size (surface-area-to-volume ratio) and state (moisture content, density) inside the vegetation layer. This characteristic is particularly interesting for studying the interaction between dead and living fuel, as occurs for a fire propagating in a fully heterogeneous fuel complex (such as in chaparral) or for studying surface-to-crown fire transition in forest fires.

Concerning with the composition of pyrolysis products, based on experimental analysis (Grishin, 1997), it varies according to the software. In WFDS, the gas phase combustion is modelled using the following stoichiometric relation (assumed to occur at 500 K)



Consequently, the heat release rate of the fire is obtained by multiplying the fuel consumption rate by the heat of combustion.

In the solid phase, the start of the burning process is defined by the identification of an ignition source and this is accomplished by the definition of a surface belonging to the calculation domain to which a thermal power (HRR) is associated. Furthermore, also a function characterizing the HRR time evolution is needed in order to define the initial and final time when the thermal source is active.

Concerning the density/pressure/velocity coupling, WFDS is formulated using a low-Mach-number approximation, while FIRETEC uses a fully compressible formulation. This choice (fully compressible/low Mach) has a large effect on the numerical efficiency of these models (Mell *et al.*, 2005);

i.e. for subsonic flow, a simulation carried out using a fully compressible formulation needs to solve the problem using a time step significantly smaller than the same simulation performed using a low-Mach-number approximation, the ratio between the two time steps being approximately equal to the Mach number as indicated in the Eq. III.12.

$$\frac{\Delta t (\text{Full compressible})}{\Delta t (\text{Low Mach})} = \text{Mach} \quad (\text{III.12})$$

III.3.1 Domain meshing

The mesh size Δ has to be able to catch the fuel heterogeneity and cannot be chosen without taking into account some physical considerations. Keeping in mind that both the atmospheric boundary layer/canopy turbulence and the radiative heat transfer play an important role in propagation of fires, Δ have to, at least, satisfy the following constraint (III.13):

$$\Delta < \min\left(\frac{H_{Fuel}}{3}, \frac{4}{\sigma_s \alpha_s}\right) \quad (\text{III.13})$$

If this criteria cannot always be verified, mainly for CPU time reasons (3D calculations), it must be compensated by introducing a sub-grid model and this is the case, for example of WFDS.

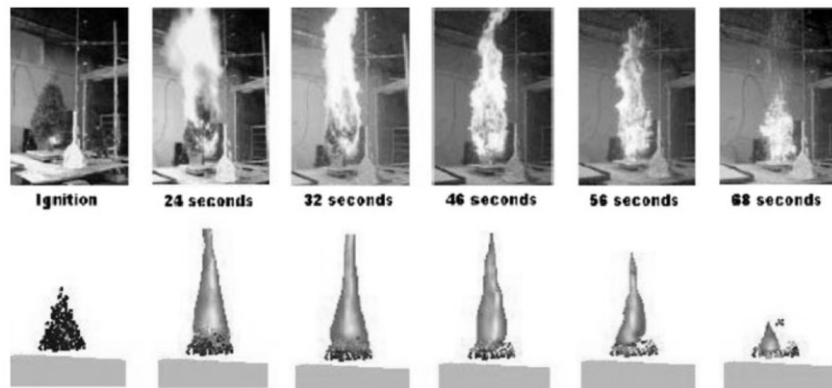


Figure III.2 *Experimental fire and simulation (using WFDS) carried out in a tall Douglas fir (Mell et al., 2009)*

When the surface fuel cannot be fully represented for large scale simulations it is replaced by a “boundary fuel element” option (the energy balance inside the surface fuel layer is treated separately and the result of

this sub-model is then introduced as source terms in the problem concerning the gaseous phase). Of course, in this case a part of the physics is lost (here the details of the flow inside the surface fuel layer are not fully reproduced), but this is certainly the price to pay for solving such problems in a reasonable CPU time. In particular, the boundary fuel element model was applied to model fire propagating in grassland (Mell *et al.*, 2007), while the fuel element model was adopted to simulate fire carried out in a single, 2 m high Douglas fir at the Building and Fire Research Laboratory (BFRL-NIST) (Mell *et al.*, 2009). The experiments were performed for various fuel (needles) moisture content, ranging from 10% to 50%. As shown in Figure III.2, the dynamics of the two fires (experimental and simulated) were quite similar. The curves representing the time histories of mass loss rates and incident radiant heat fluxes (obtained numerically) compared fairly well with experimental data measured in similar conditions (Mell *et al.*, 2009) both in amplitude and in dynamics, confirming that the agreement between experimental and numerical results was not only qualitative but also quantitative.

However, when dealing with pool fires, entrainment and compartment fires, the main parameter that can be used as scaling factor may be deduced by the Equation III.14 (Zukoski, 1995):

$$Q^* = \frac{\dot{Q}}{\rho_\infty C_p T_\infty (gD)^{1/2} D^2} \quad (\text{III.14})$$

where \dot{Q} is the energy release rate issued from the combustion process and ρ_∞ , C_p and T_∞ are the ambient air density, specific heat and temperature, respectively. g is the gravity vector and D is the diameter or characteristic length scale of the fire. Q^* represents the ratio between the energy provided by the combustion reaction and the energy associated with the induced buoyant flow. The relation between D and the buoyantly induced velocity (u_b) is defined as $u_b = \sqrt{gD}$ with the assumption that the pool diameter is the characteristic length scale of the problem. A different approach consists in considering Q^* equal to one and extract the characteristic length scale (D) from Equation III.14:

$$D = \left(\frac{\dot{Q}}{\rho_\infty C_p T_\infty \sqrt{g}} \right)^{2/5} \quad (\text{III.15})$$

The length scale D can then be successfully used to scale the characteristic flame diameter at the axis of a pool fire, but it implies that motion is purely dominated by buoyancy. Therefore, it is limited when either fuel injection velocity (jets), geometry (confinement) or length scale (flow instabilities) introduce other driving forces to the problem. The quantity D/δ_x

can be considered as the number of computational cells spanning the characteristic diameter of the fire; values for D/δ_x , useful to get a good resolution of the calculation, ranges from 4 to 16 (McGrattan *et al.*, 2010).

Extension of fire models to relatively large-scale configurations, studying the behaviour and effects of fires upon structures in wildland–urban interface (WUI), is underway. This issue can be considered as particularly important, considering the surfaces concerned and the number of habitation units located in the WUI (Radeloff *et al.*, 2005). One of the most advanced tools to study this problem seems to be WFDS and all the specific models initially developed for WFDS only have now been implemented in FDS: Fire Dynamics Simulator (<http://fire.nist.gov/fds/>). This new scientific frontier, concerning wildfire modelling, can be considered as highly strategic, to quantify the emissions of wildfires (green gases, aerosols, smoke etc.) and their impacts on carbon cycle and global warming, risks to health and micro-meteorology.

III.4 References

- Borghi R, Champion M (2000) Modélisation et théorie des flammes, TECHNIP edn
- Radeloff VC, Hammer RB, Stewart SI, Fried JS, Holcomb SS, McKeefry JF (2005) The wildland-urban interface in the United States. *Ecol Appl* 15(3):799–805
- Byram G (1959) In: Davis K (Ed) *Forest fire control and use*. McGraw-Hill, New York, pp 90–123
- Finnigan JJ (2000) Turbulence in plant canopies. *Ann Rev Fluid Mech* 32:519–571
- Grishin AM (1997) In: Albini F (Ed) *Mathematical modelling of forest fires and new methods of fighting them*. Tomsk State University, Tomsk
- Kaimal JC, Finnigan JJ (1994) *Atmospheric boundary layer flows*. Oxford University Press, Oxford
- McGrattan K., Hostikka S., Floyd J., Baum H., Rehm R., Mell W., McDermott R.: “Fire Dynamics Simulator (Version 5) Technical Reference Guide - Volume 1: Mathematical Model”. NIST Special Publication 1018-5, (Available at: <http://www.fire.nist.gov/fds/>), (2010)
- Mell W, Charney JJ, Jenkins MA, Cheney Ph, Gould J (2005) Numerical simulations of grassland fire behaviour from the LANL-FIRETEC and NIST-WFDS models. *Proceeding of East FIRE conference*, George Mason University, Fairfax, VA, 11–13 May 2005
- Mell W, Jenkins MA, Gould J, Cheney Ph (2007) A physics-based approach to modelling grassland fires. *Int J Wildland Fire* 16(1):1–22
- Mell W, Maranghides A, McDermott R, Manzello SL (2009) Numerical simulation and experiments of burning Douglas fir trees. *Combust Flame* 156:2023–2041

- Modest MF (2003) Radiative heat transfer, 2nd edn. Academic, London
- Morvan D, Hoffman Ch, Rego F (2009b) Numerical simulation of the interaction between two fire fronts in the context of suppression fire operations. -In: 8th Symposium on fire and forest meteorology, Kalispell, MT-USA, 13–14 October 2009
- Morvan D, Méradji S, Accary G (2008) Wildfire behavior study in a Mediterranean pine stand using a physically based model. *Combust Sci Tech* 180(2):230–248
- Morvan D, Me´radji S, Accary G (2009a) Physical modelling of fire spread in Grasslands. *Fire Safety J* 44:50–61
- Nelson RM (1993) Byram’s derivation of the energy criterion for forest and wildland fires. *Int J Wildland Fire* 3(3):131–138
- Pagny PJ, Peterson TG (1973) Flame spread through porous fuel. *Proc Combust Instit* 14:1099–1107
- Pyne SJ, Adreus PL, Laven RD (1996) Introduction to wildland fire, 2nd edn. Wiley, New York
- Raupach MR, Thom AS (1981) Turbulence in and above plant canopies. *Annual Rev Fluid Mech* 13:97–129
- Sullivan AL (2007) Convective Froude number and Byram’s energy criterion of Australian experimental grassland fires. *Proc Combust Instit* 31:2557–2564
- Whelan RJ (1995) The ecology of fire. Cambridge University Press, Cambridge
- Zukoski E.E.: “Properties of Fire Plumes”, Chapter 3, *Combustion fundamentals of Fire*, G. Cox Editor, Academic Press, Pp.101-220, 1995.

Chapter IV

Fire propagation on flat and sloped surface. Role of the surface fuel in generating a crown fire

In this chapter the way by which the wind and terrain inclination affect the fire propagation across a homogeneous fuel bed was investigated, putting in evidence the role these two parameters have in affecting the fire rate of spread. Furthermore the role of the surface bulk density in generating a crown fire in a domain characterized also by the presence of trees was also studied

IV.1 Introduction

In this chapter the way by which the wind and terrain inclination affect the fire propagation across a homogeneous fuel bed was investigated. The role played by these two parameters in the fire behaviour was studied by the WFDS code. The analysis showed that wind velocity affects the rate of spread more strongly than the terrain slope. The evolution of the fire front was also analysed and the comparison between the simulated rates of spread and those obtained from laboratory and field experiments was performed. In the case of fires moving on a flat surface without wind, a well defined constant rate of spread was obtained, while under steep slopes and strong wind conditions the rate of spread decreased in time. The possibility of the occurrence of a transient regime even under constant geometric and ambient conditions was also addressed. Furthermore the role played by the understory vegetation on the development of a crown fire was also

investigated. In the performed 3D simulations, a heterogeneous surface fuel under a linear stand of trees was considered. The bulk density of the understorey vegetation affects the fuel burnout time and, therefore, the time the trees remain exposed to the heat generated by the combustion of the surface fuel. Simulation results showed that surface fuel management oriented in reducing the biomass accumulated on the ground can limit the fire intensity and the severity of the crown fire. A reduction in the load of the vertical fuel can also influence the fire dynamics: the lowering of the fire front temperatures and the cooling of the fuels involved may be promoted leading to the fire extinguishment.

In the simulations, vegetative fuel is arranged as beds of pine needles and fire propagates across them according to wind intensity and terrain inclination. The relative magnitude of these two parameters modules the position of the flame with respect to the unburnt fuel, affecting, in this way, the rate of flame propagation. The constancy of ambient conditions (wind and terrain slope) does not generally imply a constant rate of spread of the flame: the existence of a transient whose length cannot be defined in advance is also highlighted in the work

IV.2 Simulation conditions

IV.2.1 Flat and sloped terrain

To study the fire propagation rate on flat and sloped surfaces, a grassland domain was considered. The surfaces used in the simulations were 30 m long (x) and 40 meters wide (y). The physical characteristics of the grass adopted in the simulations are those based on NIST experiments on Australian grass (F19 in Mell et al, 2005). Grass was ignited along a 1 meter-wide line located in correspondence of the beginning of the grass and having length equal to the domain size. The maximum heat flux release rate associated to the ignition source was set to 500 kW/m². In order to investigate the influence of the terrain slope three different runs with sloped domains of 0°, 15° and 30° were simulated. In all the case, however, the fire was ignited on a flat surface, 3 meters before the beginning of the inclination of the terrain. Simulations were run with different wind velocity, i.e. 0, 2, 3, 4 and 5 m/s. Domain meshing was performed according to the Eq. III.15. The quantity D^*/δ_x was set equal to 16 for all the simulations. In this way a maximum mesh size of 0.27 m in all direction was obtained. Simulations were performed on a single CPU core and each was completed in about 4 h on an Intel Xeon E5630 at 2.53 GHz CPU with 6 GB ram.

IV.2.2 Forest stand domain

In this case the numerical simulations were performed to study the propagation of a fire through a wildland configuration consisting of trees and understory vegetation, composed by a mixture of shrub and grass, as shown in Figure IV.1. The trees canopies consisted of pine crowns. The base three-dimensional resolved domain was 28 m long (x -direction) 6 m high (z -direction) and 6 m wide (y -direction). The surfaces between $x=-4$ and $x=0$, between $y=2.4$ and $y=3$ and between $x=22$ and $x=24$ were left free of vegetation. The grid mesh was set to $0.20 \times 0.20 \times 0.20$ m³ in the whole domain. In all the simulations, wind was set to blow along the x direction at a velocity of 5 m/s. Ignition was started after a time sufficient to establish a steady state condition in the gas phase.

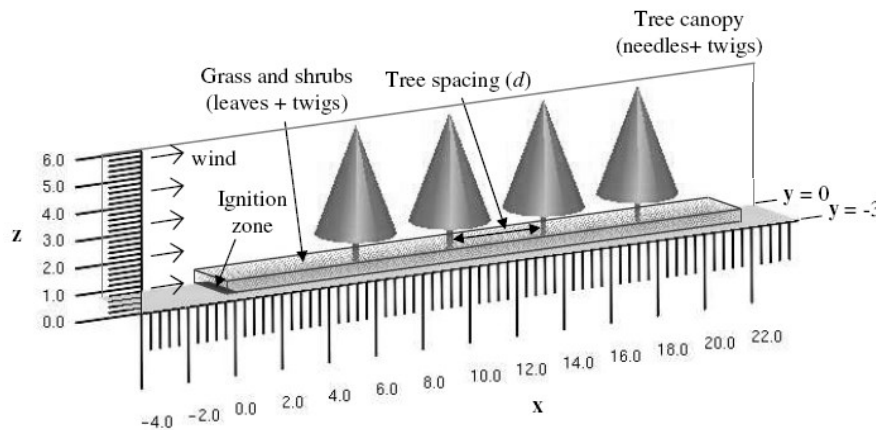


Figure IV.1 Configuration of the computational forest domain. d is the distance between the tree trunks. Wind is constant at the boundary surface (\rightarrow) and blows along x at 5 m/s.

In the forest stand, the vegetation was structured as follows: the depth of the shrub layer was equal to 0.60 m, the height of grass was equal to 0.40 m, the tree crowns were cones 4 m high, with a 3.16 m diameter base, located at 1 m from the terrain. For $0 < x < 5$ m only surface fuel was considered. Five solid fuel families were introduced to represent the vegetation: one for the grass, two for the shrub (consisting of leaves and twigs) and two for the trees (formed by needles and twigs). The physical properties of the fuel families, summarized in Table IV.1, were those reported in the works of Morvan (2007) and Dupuy and Morvan (2004) who limited the description of the vegetation to thin solid fuel particles (< 6 mm). Such a choice arises from previous experimental studies (Call and Albini,

1997) showing that, during the propagation of a wildfire through a living fuel bed (moisture content on dry basis $\approx 100\%$), the main part of the burned fuel has thickness lower than 6 mm.

Table IV.1 *Physical properties of the fuel families in the forest domain*

FUEL FAMILY	DENSITY OF DRY MATERIAL (kg/m ³)	BULK DENSITY (kg/m ³)	SURFACE AREA TO VOLUME RATIO (m ² /m ³)	MISTURE CONTENT ON DRY BASIS (%)
Grass	400	0.40-0.80-1.20	10000	5.0
Shrub leaves	820	1.23-2.46-3.69	4000	70.0
Shrub twigs	900	0.90-1.80-2.70	4000	70.0
Tree needles	850	0.255	10000	100.0
Tree twigs	900	0.180	1000	100.0

Table IV.2 *Numerical simulations set in the forest domain*

SIMULATION	TREE SPACING (d , m)	GRASS BULK DENSITY (ρ_g) (kg/m ³)	SHRUB LEAVES BULK DENSITY (ρ_l) (kg/m ³)	SHRUB TWIGS BULK DENSITY (ρ_s) (kg/m ³)	SURFACE FUEL BULK DENSITY (ρ_F) (kg/m ³)
A1	3	0.40	1.23	0.90	0.90
A2	3	0.80	2.46	1.80	1.80
A2	3	1.20	3.69	2.70	2.70
B1	2	0.40	1.23	0.90	0.90
B2	2	0.80	2.46	1.80	1.80
B3	2	1.20	3.69	2.70	2.70
C1	4	0.40	1.23	0.90	0.90
C2	4	0.80	2.46	1.80	1.80
C3	4	1.20	3.69	2.70	2.70

The fire was ignited in the shrub and in the grass introducing a transient heat source lasting 12 s: the ignition source was represented by a surface, 4.80 m long and 0.20 m wide, located at $x=0$ (red area in Figure 1) to which a maximum heat release rate per unit surface of 4000 kW/m² was associated. Such a power corresponds to about 46000 kJ, i.e. equal to the energy produced by the combustion of about 1.3 L of diesel fuel. In order to investigate how the interaction between the understorey vegetations and the trees affects the fire propagation, nine simulations were performed: this was accomplished by changing the surface fuel bulk density (ρ_F) and the trees spacing (d) as shown in Table 2. Since the base of the cone representing each tree canopy has a 3 m diameter, 2 meter tree spacing, reported in Table IV.2,

stands for canopies that overlap each other by 1 meter; ρ_F is the average surface fuel bulk density calculated as:

$$\sum \rho_i \cdot X_i \quad (i = g, l, s) \quad (IV.1)$$

where X represents the volumetric fraction of each family of fuel (grass, shrub leaves, shrub twigs).

IV.3 Results and discussion

IV.3.1 Flat and sloped terrain

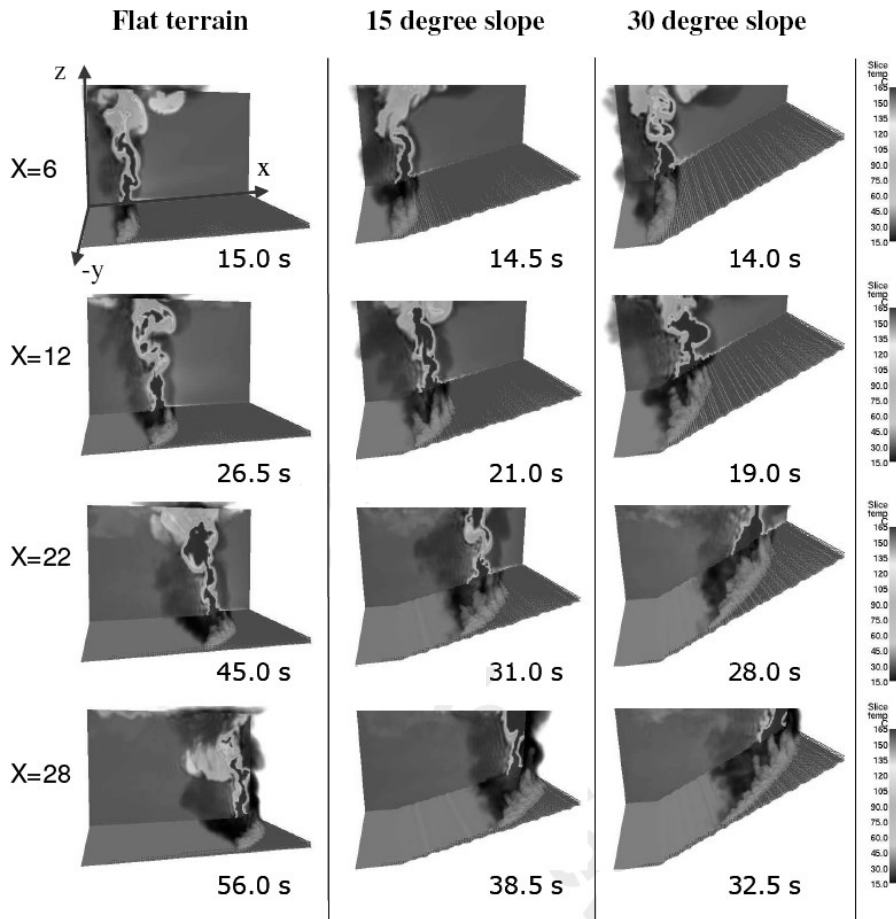


Figure IV.2 Fire spreading on flat and sloped terrains in the absence of wind. Colourbar for the temperatures in the gas phase (in correspondence of $y=0$) is reported on the right.

Figure IV.2 shows the results of the simulations in the absence of wind for different plane inclinations. In particular, for flat and sloped terrains the Figure shows pictures, obtained by working out results of simulations, representing four positions of fire fronts and the times from the fire start necessary to reach those positions. The flame axis is almost vertical for both cases of flat and inclined terrains; the gas flow in the vicinity of the fire front is mainly affected by the expansion of the hot gases above the combustion zone and this buoyancy flow (plume dominated fires) induces the entrance of fresh air from both side of the fire. The presence of a sloped surface induces an increase in the flame front propagation rate: all the domain burns in about 39 s and 33 s for the 15° and 30° inclinations, respectively, while it takes about 60 s in the case of the flat surface.

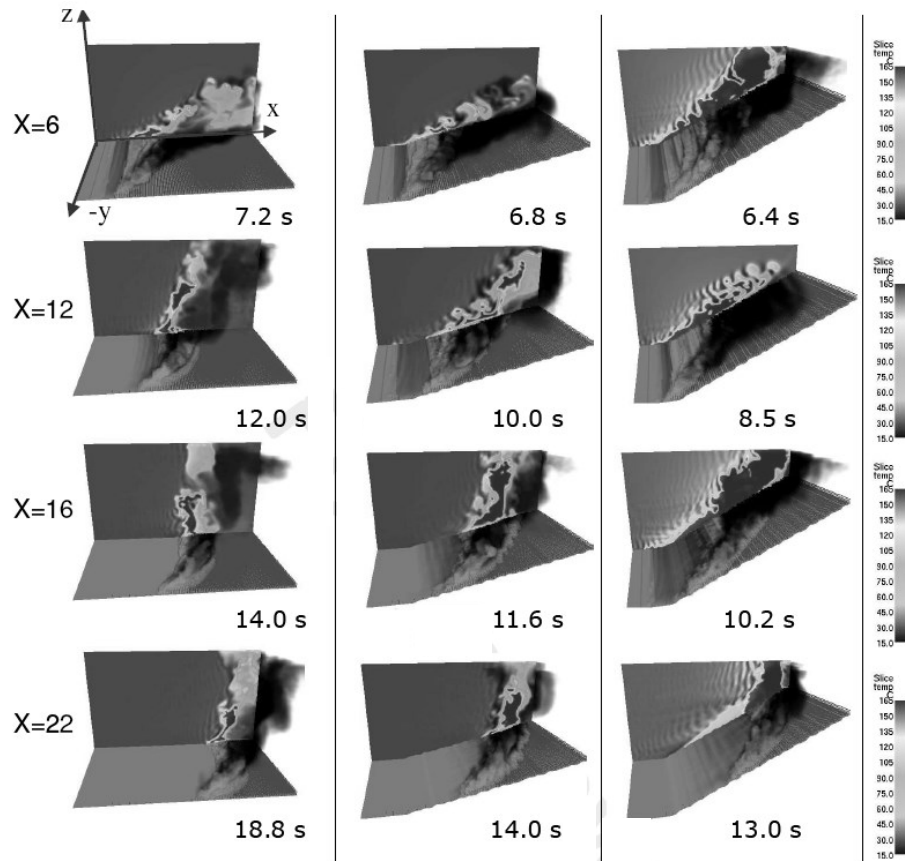


Figure IV.3 Fire spreading on flat and slope terrains for wind blowing at 5 m/s along x. Colourbar for the temperatures in the gas phase (in correspondence of $y=0$) is reported on the right.

Results of simulations, carried out in the presence of wind, are reported in Figure IV.3. Even in this case, for flat and sloped terrains the Figure shows pictures, obtained by working out results of simulations, representing four positions of the fire front and the times from the fire start necessary to reach those positions.

With respect to the results presented in Figure IV.2, those in Figure IV.3 highlight the effect of the wind on the fire propagation characteristics: in this case the wind deviates significantly the axis of the flames inducing the ignition of the fuel located far ahead the fire front. This effect is also visible in some snapshots of Figure 3 where the fire fronts span a far larger surface with respect to the case without wind. Under strong wind conditions (Figure IV.3), the shape of the fire deviates markedly from the vertical (wind driven fires), inducing a shearing and a tilting of the flame at the top of the fuel layer. The action of the wind on the fire dynamics is also shown by the formation of fingers of flame impinging alternatively on the fuel surface (top and central snapshots in Figure IV.3).

The evolution in time of the fire fronts shows the development of parabolic transverse profiles due to the effect of different boundary conditions establishing at the plane $y=0$ (no thermal dissipation) and at the external edge. In order to evaluate the rate of spread (ROS) of the flames, defined as the surface area burned out per unit time, it was necessary to monitor the area spanned by the fire front in time. The position of the fire front at a given time was obtained from the space profiles of the net thermal power flux (kW/m^2) produced by the grass combustion: it represents the locus of the x-y coordinates where, at a given time, there are the maxima of generated power. In this way the areas spanned by the fire in time could be evaluated. Results of these calculations are shown in Figure IV.4 (a and b) where the burned area of the grassland domain is reported as a function of time. For each simulation data were interpolated by linear and quadratic curves through the following equations:

$$\text{- Linear equation: } x_l = a_l \cdot t + b_l \quad (\text{IV.2})$$

$$\text{with correlation coefficient } r_l^2 \text{ and derivative } R_l = a_l \quad (\text{IV.3})$$

$$\text{- Quadratic equation: } x_q = a_q \cdot t^2 + b_q \cdot t + c_q \quad (\text{IV.4})$$

$$\text{with correlation coefficient } r_q^2 \text{ and derivative } R_q = 2a_q \cdot t + b_q \quad (\text{IV.5})$$

It is worth noting that the derivatives R_l and R_q coincide with ROS, as defined above. Equations IV.2 and IV.3 correspond to a constant rate of spread (R_l) while the quadratic form - Equations IV.4 and IV.5 - produces a variable rate of spread (R_q). In the last case, depending on the sign of a_q , R_q results decreasing or increasing in time. Table IV.3 summarizes the values of the parameters in equations from IV.2 to IV.5 for each test. The correlation coefficient for the quadratic form was generally greater than that for linear fitting. In all the cases the values of r_l and r_q were very similar and very close

to unity and, hence, a constant rate of spread can be reasonably assumed. However, it is worth noting that the time length for each simulation was always limited within 60 s and, probably, longer times are required to discriminate between the considered trends.

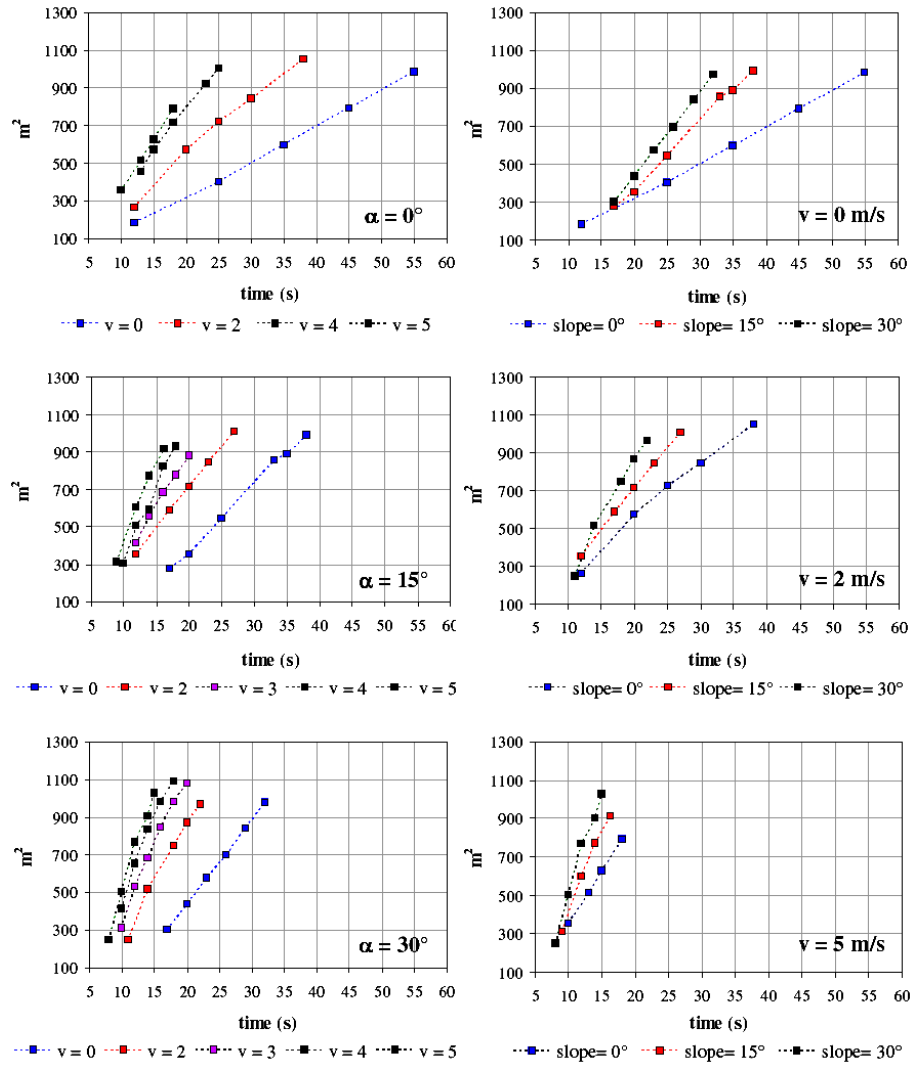


Figure IV. 4a (left column) Surfaces (m^2) spanned by the fire in time (s) at fixed domain inclinations (α) for different wind velocities (v in m/s)

Figure IV.4b (right column) Surfaces (m^2) spanned by the fire in time (s) at fixed wind velocities (v) for different domain inclinations (slope)

Results in Figure IV.4 agree with those found by Viegas (2004a), who performed experimental tests on flat and inclined surfaces in order to study the existence of a steady state regime. The test surface in his work had an area of 9 m² (3 m x 3 m) and could be inclined at any desired angle between 0° and 40°; the vegetative bed was made of *Pinus pinaster* needles with a fuel load in the range between 0.6 and 1.0 kg/m² and a moisture content in the range 8-13% (on dry basis). Time length in these tests did not exceed 300 s.

Table IV.3 Parameters of Equations IV.2 to IV.5 obtained through linear and quadratic fitting

TEST n°	α	v (m/s)	a_l (m ² /s)	r_l^2	a_q (m ² /s ²)	b_q (m ² /s)	r_q^2
A0	0	0	18.796	0.9990	0.0351	16.445	0.9996
A2	0	2	29.956	0.9879	-0.3673	48.323	0.9987
A4	0	4	45.210	0.9972	-0.7671	74.506	0.9997
A5	0	5	54.560	0.9997	0.2481	47.614	0.9998
B0	15	0	35.107	0.9970	-0.0887	39.976	0.9972
B2	15	2	43.656	0.9989	-0.2862	54.792	0.9999
B3	15	3	58.175	0.9923	-2.0432	123.560	0.9992
B4	15	4	78.202	0.9835	-0.8921	103.180	0.9842
B5	15	5	84.909	0.9933	-3.2358	165.380	0.9999
C0	30	0	44.830	0.9997	0.0551	42.128	0.9997
C2	30	2	64.250	0.9887	2.1174	133.590	0.9981
C3	30	3	76.525	0.9860	-3.0471	167.940	0.9993
C4	30	4	84.314	0.9772	-5.4164	235.970	0.9997
C5	30	5	108.920	0.9882	-4.8596	221.050	0.9956

In accordance with tests A0 and B0 in Table IV.3, Viegas found negligible differences between linear and quadratic fitting for 0° < α < 20° and for a linear ignition source. Furthermore, the effect of wind in decreasing the rate of spread on a flat surface (tests A2 and A4, $a_q < 0$) was also confirmed. Results reported by Viegas were limited to tests where the combined effect of wind and slope was not investigated, limiting the attention to flat surfaces with wind and to sloped surfaces without wind.

Results in Table IV.3 extend such experimental findings showing that wind has, generally, a decreasing effect on Rq in time not only on flat surfaces, but even on inclined domains ($a_q < 0$ in tests from B0 to B5 and from C3 to C5 in Table IV.3). The effect of wind in decreasing the rate of spread on a flat surface (tests A2 and A4 in Table IV.3) was also pointed out by Morvan and Dupuy (2004), who found that for moderate wind conditions (up to 3 m/s) the ROS linearly increases with wind speed. On the contrary, they found that for higher velocities (up to 10 m/s) the wind does not have the same effect upon fire propagation, the ROS reaching a limiting value. At high wind speeds, the mixing of the fresh air, carried by the wind, with the hot gases results in cooling of the flaming zone, reducing the magnitude of

the heat flux between the flame and the unburnt vegetation and, consequently, affecting negatively the rate of spread as well.

The simultaneous influence of wind and terrain slope on ROS (i.e., $R_l = a_l$) is shown in Figure IV.5 where R_l vs. the slope at fixed velocities (Fig. IV.5a) and R_l vs. wind velocity at fixed plane slopes (Fig. IV.5b) are displayed. From Figure IV.5 it clearly appears that R_l increases at increasing both slope and wind velocity even though the effect of wind velocity is more marked. This result may be explained since the increase of both quantities reduces the distance between flames and fuel ahead of it. Also these results were confirmed by Viegas (2004a) who showed that the dimensionless experimental rate of fire spreading (defined as the ratio between the actual rate of spread and that calculated for a flat surface without wind) at 5 m/s on a flat surface was 16 higher (~35) than that obtained when operating on a sloped surface (45°) without wind (~18).

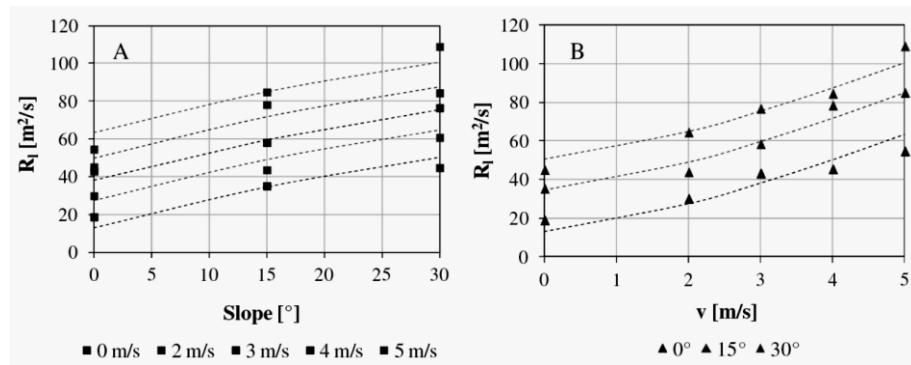


Figure IV.5a (left) Influence of the terrain slope on the rate of spread (ROS= R_l) in (m/s) at different wind velocities (0, 2, 3, 4, 5 m/s from bottom to top)

Figure IV.5a (right) Influence of wind velocity on the rate of spread (ROS= R_l) in (m/s) at different terrain slopes (0°, 15°, 30° from bottom to top). Symbols stand for results of simulations while curves are calculated by Eq. IV.6.

According to the literature (Rothermel, 1972; Boboulos, M., Purvis, 2009; Viegas, 2004b) and considering the linear form of the rate of spread (Equations IV.1 and IV.2), the dependence of R_l on wind velocity and slope can be expressed as a sum of these two contributions. For our simulations, results were correlated ($r^2 = 0.9586$) by the following expression:

$$R_l = a + b \cdot v^{1.36} + c \cdot \alpha^{0.8} \quad (\text{IV.6})$$

where a is the reference spreading rate at $v = \alpha = 0$, v is the wind velocity and α is the inclination of the domain. Values of R_l calculated from Equation IV.6 are reported in Figure IV.5 for comparison with the values obtained from the simulations. The parameters a , b and c in the Equation IV.6 are equal to 12.996, 5.607 and 2.570, respectively. Equation IV.6 shows an almost linear dependence of R_l on α (Fig. IV.5a) and a more than linear contribution of the wind velocity (Fig. IV.5b). Such a relationship between R_l and wind velocity is also confirmed by Boboulos and Purvis (2009). These authors, performing laboratory tests for studying the fire propagation across pine needles beds, concluded that wind effect is decisive for the fire spread, particularly for bed slopes up to 10 degrees; furthermore, the wind effect becomes more significant for velocities above 2 m/s and 20 degrees of bed slope.

In literature, it is common to express the rate of spread of flames in m/s (here this quantity will be indicated as ROS_l) instead than in m^2/s (ROS). In the first case the rate of fire propagation is assumed as a vector, whose intensity is the maximum rate of spread, measured, usually, along a symmetry plane. This way to express the rate of fire propagation appears limited due to the consideration that fire is a phenomenon occurring on a surface and the evolution in time of ROS_l and ROS may not always follow the same trend. The knowledge of both ROS and ROS_l and their comparison can be an interesting way to analyze the fire spreading because in this way it is possible to obtain indications about the evolution in the time of the shape of the surface, which is burning.

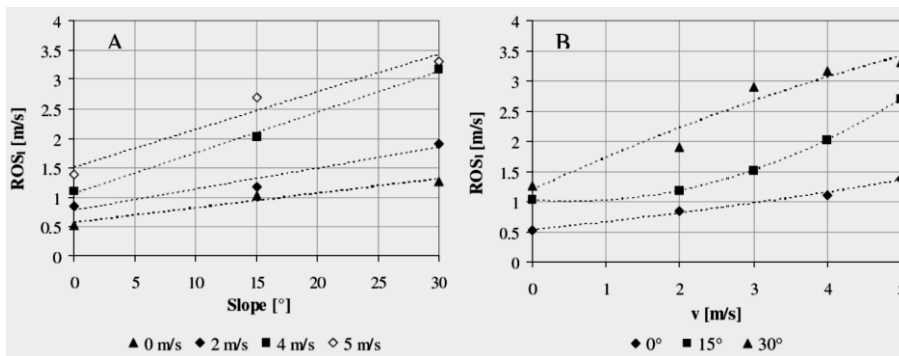


Figure IV.6a (left) Influence of the terrain slope on the rate of spread (ROS_l) in (m/s) at different wind velocities.

Figure IV.6b (right) Influence of wind velocity on the rate of spread (ROS_l) in (m/s) at different terrain slopes. Symbols stand for results of simulations. Lines represent the interpolating curves.

Figure IV.6 reports the values of ROS_I obtained by simulations that yielded the results presented in Figure IV.5. Comparing figure IV.5b and IV.6b, it can be noticed that in the case of a terrain slope of 30° and for wind velocities above 2 m/s ROS and ROS_I show different trends as the wind velocity increases: a weak grow of ROS_I and a strong grow of ROS . This means that a steep slope (30°) in combination with a moderate wind velocity (3 m/s) may result in a burning surface tending to become larger rather than longer.

As known, the heat release rate (HRR) represents the total thermal power generated by the fire. It is worth noting that the feature of its time profile is strictly related to the fire spreading characteristics. For instance, the two HRR profiles reported in Figure IV.7 were obtained by the elaboration of the results of two of the simulations listed in Table IV.3 for the flat geometry, i.e. tests A0 and A4. The HRR pertaining to the first test, carried out in the absence of wind, is practically constant during the run and corresponds to an almost constant rate of spread (test A0: a_q (m^2/s^2) close to zero (Table IV.3)) while the HRR of the second test, performed under windy conditions ($v = 4m/s$), presents a decreasing trend and corresponds to a decreasing rate of spread (test A4: a_q (m^2/s^2) negative and high absolute value (Table IV.3)), confirming that the HRR trend can be associated to the description of steady or unsteady-state fire spreads, both accelerating or decelerating.

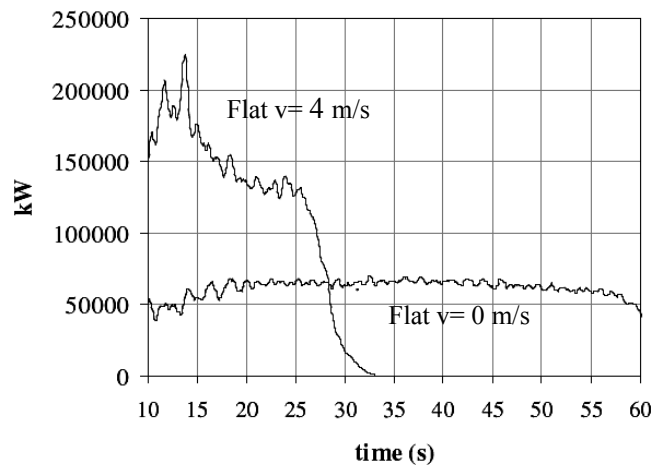


Figure IV.7 Time evolution of HRR for flat domain under calm ($v=0$ m/s) and windy ($v=4$ m/s) conditions.

IV.3.2 Forest stand domain

Surface fuel bulk density and tree spacing markedly influence the fire spreading rates across the domain. Figure IV.8 shows the time evolution of the position of the fire front at ground level.

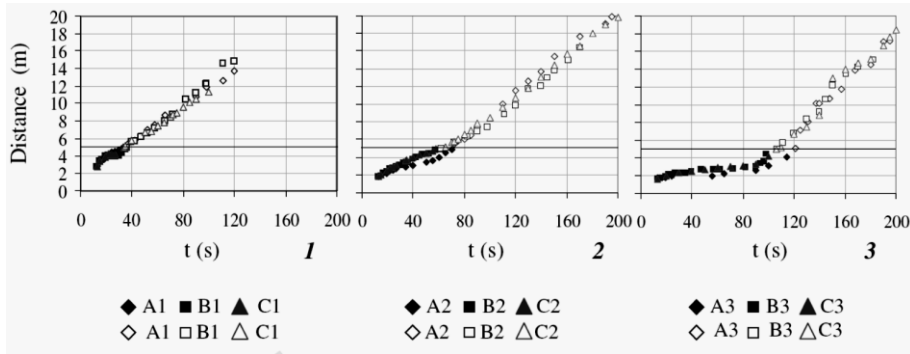


Figure IV.8a Distance spanned by the fire front at the ground level at different d for fixed ρ_F (1: $\rho_F=0.90$; 2: $\rho_F=1.80$; 3: $\rho_F=2.70$) (cfr. Table IV.2). Black lines mark the separation ($x=5$ in Figure IV.1) between the zone where only surface fuel existed and that where both fuels were present.

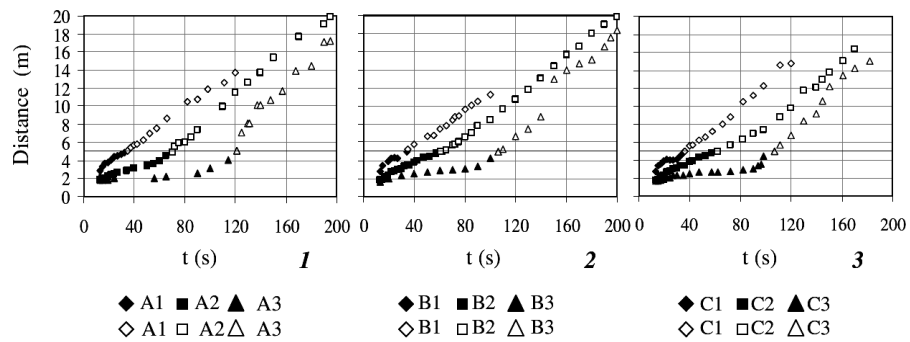


Figure IV.8b Distance spanned by the fire front at the ground level at different ρ_F for a fixed d (1: $d=0$; 2: $d=-1$; 3: $d=1$) (cfr. Table 2). Black lines mark the separation ($x=5$ in Figure 1) between the zone where only surface fuel existed and that where both fuels were present.

The positions in time of the fire front were tracked by recording the values in time of the coordinate x where the isotherms at 340 K intersect the $y=0$ plane, at $z=0$; the hot pockets that may appear more or less far ahead the fire front were ignored. It is worth noting that the slope of the curves in

Figure IV.8 represents just ROS_I (m/s), as defined in the previous paragraph. Figure IV.8 evidences that the distance spanned in time by the fire front was more dependent of the surface fuel bulk density (ρ_F) rather than of the tree spacing (d): at fixed ρ_F a variation of d did not produce significantly different ROS_I (Figure IV.8a), while at fixed d an increase of ρ_F resulted in markedly dissimilar rates of spread (Figure IV.8b).

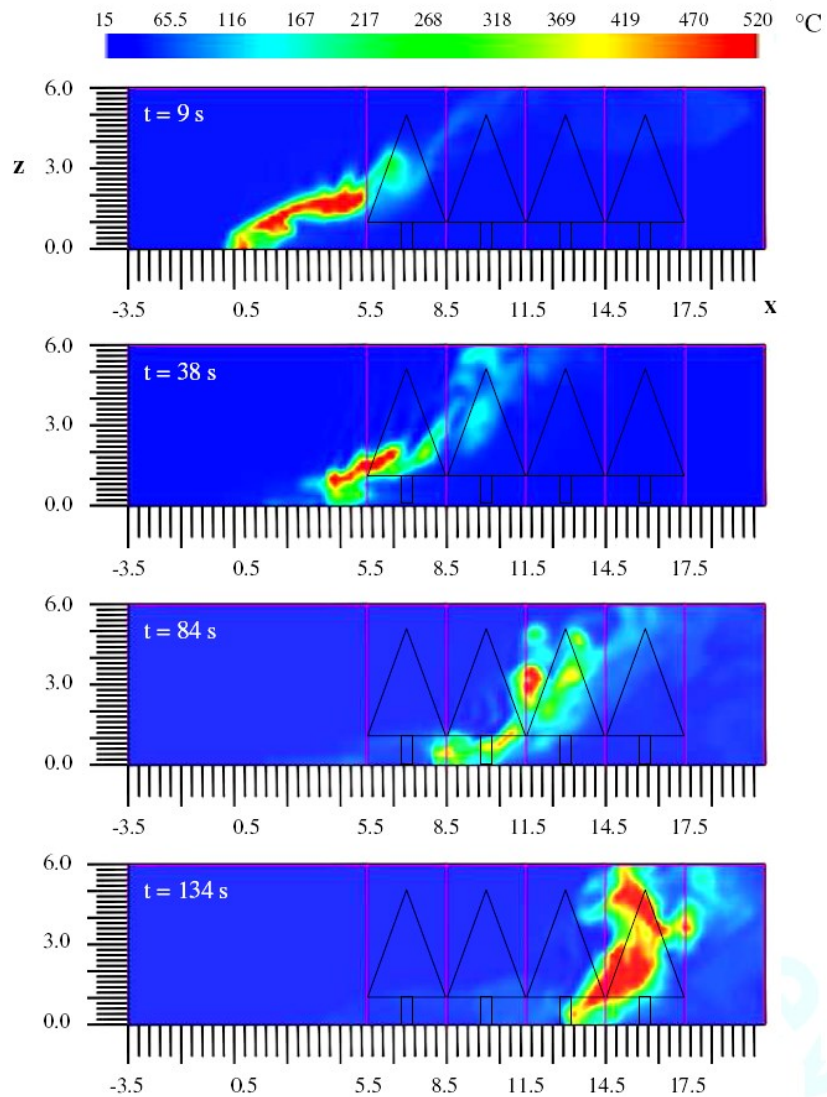


Figure IV.9 Time evolution of the temperature space profiles on the $y=0$ plane, for the case A1 of Table IV.2, during a surface to crown fire transition. Colourbar on the top is the same for each time step

A variation in the fire spreading rate (i.e. significant change of line slope) roughly took place in correspondence of the beginning of the vertical fuel ($x=5$ m), where the transition from surface fire to crown fire occurred. Such a variation in the fire dynamics, on the $y=0$ plane, was mainly evidenced by an increase in the flame height; furthermore, the flow of air inside the canopies was slowed down by the presence of the unburnt fuel, resulting in a change of the flame inclination which tended to become less slanted towards the ground. This behaviour was evident in all the simulations carried out and in Figure IV.9 such a fire evolution is represented for the case A1 of Table IV.2.

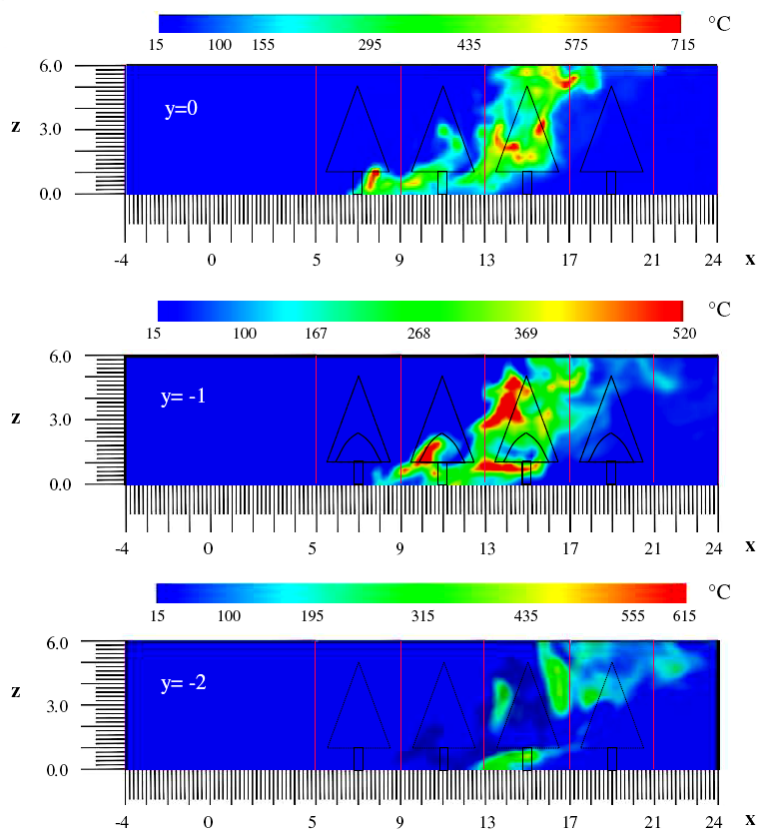


Figure IV.10 Temperature space profiles at $t=143.4$ s on the $y=0$, $y=-1$ and $y=-2$ planes (cfr. Figure IV.1) for the case C2 of Table 2. Solid lines represent the sections of the tree stand cut by the y planes

In all the investigated cases, the first tree of the row, reached by a flame tilted by the wind, resulted less dehydrated and burned with respect to the others.

ROS_i values computed in the part of the domain where only surface fuel existed ($0 < x < 5$ m), were different from those measured in the area where both fuels were present ($x > 5$ m). In the cases 1, 2 and 3 in Figure IV.8a, in the first five meters the rates of spread decreased at increasing surface fuel bulk density being about 0.085, 0.060 and 0.023 m/s at ρ_F equal to 0.90, 1.80, 2.70 kg/m³, respectively; later on, despite the drag effect due to the presence of the vertical fuel, the ROS_i went up to about 0.11 m/s in the first two conditions and 0.14 m/s in the third case. This was due to the development of a velocity field also along the y direction: according to Figure IV.1, the fluid flow was slowed in correspondence of the tree stand ($y=0$) but remained unaffected where no vertical obstacles were present ($y=-3$), resulting in flames tending to surround the trees. In Figure IV.10, this situation is shown for the case C2 of Table 2 reporting, for a fixed time, the temperature profiles in correspondence of different y planes. The heat transport along the y direction enhances strongly the dehydration and the burning processes of the trees affecting positively the ROS_i. It is important to remark that the increase in the rate of spread due to the presence of the vertical fuel cannot be correctly simulated in a 2D approach. In this case, in fact, the drag effect due to the presence of the trees can be considered, but the heat transport across the transverse direction cannot; such a consideration could explain why previous authors, working on a bi-dimensional geometry, found a decrease in the fire propagation rate in correspondence of the tree stand (Dupuy and Morvan, 2004).

The amount of vertical fuel burned by the fire resulted strongly dependent on the bulk density of the surface fuel: at low ρ_F (case 1 of Figure IV.8a), when looking at the results for the two families of fuel particles in the canopy, the needles of the trees reached by the flames were completely burned, but a significant part of twigs remained unburned (>85%); on the contrary, when considering high ρ_F (case 3 of Figure 8a), both families of fuel in the canopy were consumed. In addition, at low ρ_F also the tree spacing affected the behaviour of fire spreading: a tree spacing of 4 m resulted in a fire extinguishment after the second tree, while this event did not occur at d equal to 3 m and 2 m. This could be due to a different amount of fuel available to sustain the flames and also to a different cooling effect of the vegetation by the local wind dynamics. In fact, Figure IV.11 shows that, in the case $d=4$ m, because of the lower density of the vertical fuel, the fluid velocities in correspondence of the canopy base ($z=1$ m) are higher than in the other two conditions. Therefore, under specific domain configurations ρ_F and d may act synergistically in reducing the flame temperature up to lead to the fire extinguishment. Higher ρ_F values correspond to higher fire propagation rates in the tree stand but the time the fire remains in contact with the tree crowns is longer. In fact, increasing the surface vegetative fuel bulk density, the time length during which the surface fuel continues to burn after the flaming front has passed, increases.

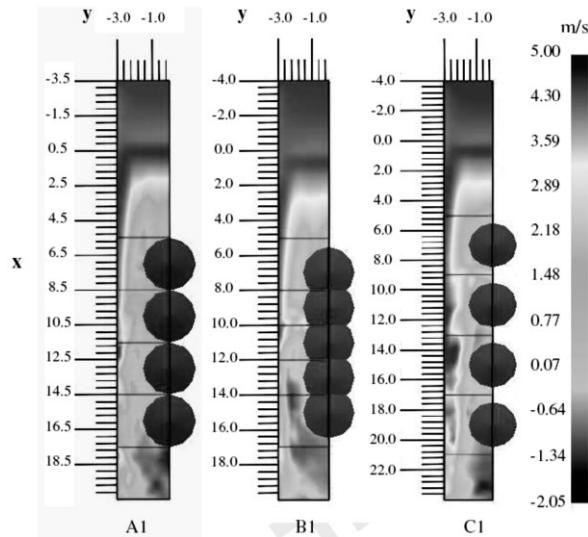


Figure IV.11 *x*-component of the velocity field at 80 s in correspondence of the base of the tree canopies ($z=1m$). (left): $d= 3$ m (case A1 of Table IV.3), (centre): $d= 2$ m (case B1 of Table IV.3) and (right): $d= 4$ (case C1 of Table IV.3).

In Figure IV.12 the difference in the shape of the flame fronts is shown for two values of ρ_F corresponding, respectively, to the cases A1 ($\rho_F = 0.90$ kg/m³) and A3 ($\rho_F = 2.70$ kg/m³) of Table IV.2. Although the combustion of the surface fuel was in both cases complete, fire did not affect the tree twigs in the case A1 while did it in the case A3. This was due to the longer fuel burnout time in the case A3: here fire moved first as elongated fronts propagating along the x direction on the part of the domain covered only by surface fuel and, then, moved towards the inner of the domain reaching the trees

The power (HRR) coming out from the calculation domain, in the two cases of the Figure IV.12 is shown in Figure IV.13 as a function of the time: it is evident how the net power generated reflects the trend observed for the area reached by the fire (Figure IV.12). In particular, in the case of $\rho_F = 0.90$ kg/m³, apart from a short initial transient, the net power coming out of the domain is practically constant. In this condition, in fact, the crown fire involves only the tree needle and the energy associated to the fire has a trend similar to that found for fire spreading across surface fuel only. If we associate the lower $\rho_F = 0.90$ kg/m³ value to an understorey treatment, aimed to reduce the fuel (made of deposited dead tree branches or leaves) available for burning, it is immediately clear how this work of maintenance can reduce the risk of transition to a crown fire

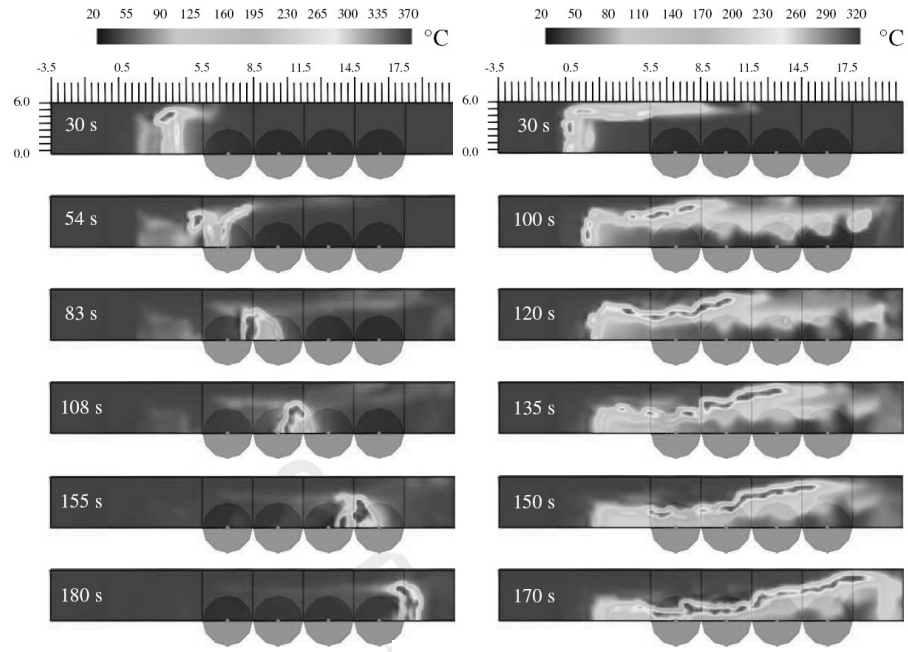


Figure IV.12 Time evolution of the temperature space profiles on the $z=0$ plane. $d=3$ m. (left) $\rho_F=0.90$ kg/m³ (case A1 of Table IV.3) and (right) $\rho_F=2.70$ kg/m³ (case A3 of Table IV.3).

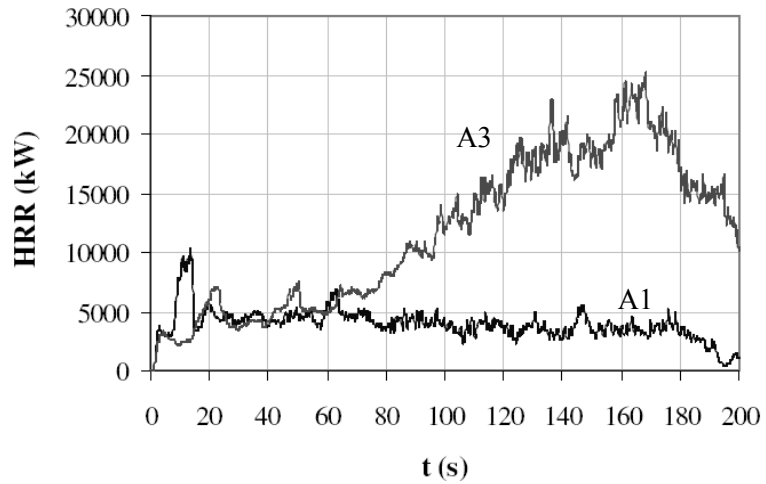


Figure IV.13 Time evolution of HRR at $d=3$ for $\rho_F=0.90$ kg/m³ (case A1 of Table IV.3) and $\rho_F=2.70$ kg/m³ (case A3 of Table IV.3)

IV.4 Conclusions

The performed simulation study on flames spreading across grassland mains confirmed the strong dependence of the propagation rate on the wind velocity and on the terrain slope. Their effect on the propagation of the fire was expressed through a simple relationship, which takes into account the contribution of these two parameters: the ROS resulted to have a stronger dependence on wind velocity than on the terrain slope. ROS, expressed as surface spanned per unit time by the fire, is not always sufficient to fully describe the fire propagation features because it does not yield information about the shape the fire assumes during the spread. In this respect, the calculation of ROS_i , besides ROS, is very helpful.

The dynamic behaviour of the fire was also analyzed; this is not generally done in classical models, which assume that a fire in a homogeneous fuel bed with uniform slope will propagate with a constant rate. The fire transient behaviour was little evident in sloped terrain where the simulation times (not exceeding 60 s) were probably too short to correctly catch the fire behaviour evolution. However, the general decreasing effect of wind on ROS, found in this case and observed also in experimental tests reported in literature, depends on the mixing of the fresh air, carried by the wind, and the hot gases from combustion that cools the flaming zone so reducing the ROS.

The propagation of a wildfire through a tree stand was also simulated in 3D geometry. The numerical results showed the ability of this approach to simulate the fire propagation through a heterogeneous forest fuel, and to check the role of the surface fuel bulk density (ρ_F) in regulating the transition from a surface fire to a crown fire. For the conditions tested (wind and tree arrangement) the crown fire could not propagate if it was not supported by a suitable surface fire. Consequently, by reducing ρ_F and, therefore the biomass at the ground level, the intensity of the simulated surface fire was reduced and crowning was arrested or remained limited to the tree needles. The fire rate of spread involving a crown fire was higher than the fire propagation rate across the surface fuel only. This is due to the development of fluid flow gradient in the transverse direction able to increase the dehydration and burning processes of the trees. To reduce the intensity and the risk of transition from a surface fire to a crown fire, the best solution is to reduce the intensity of the surface, by removing part of the biomass accumulated on the ground (reduction of ρ_F). Furthermore, an increase in the tree spacing may decrease the temperature of hot gases originated from the surface fire: an increased wind speed, arising in such a condition, reduces the time of convective heating and, therefore, the net energy transfer to the crown fuel. The rate of spread in such an environment is not enough to correctly describe the fire dynamics. The surface fuel bulk density regulates the fire burnout time, which is responsible of the destructive effect in term of fuel burned in a real forest environment.

Numerous are the parameters affecting fire propagation in these two kind of environment and more results and further studies are needed in this direction to collect information and data helpful forest fire management safety.

IV.5 References

- Morvan, D. (2007). A numerical study of flame geometry and potential for crown fire initiation for a wildfire propagation through shrub fuel. *Int. Journal of Wildland Fire*, **16**, 511-518.
- Dupuy JL and Morvan D, (2004) Modeling the propagation of a wildfire through a Mediterranean shrub using a 19 multiphase formulation. *Combustion and Flame*, **138**, 199–210.
- Call PT, Albini FA (1997) Aerial and surface fuel consumption in crown fires. *International Journal of Wildland Fire*, **7**, 259-264.
- Viegas, DX (2004a) On the existence of a steady state regime for slope and wind driven fires. *International Journal of Wildland Fire*, **13**, 101-117.
- Viegas, DX (2004b) Slope and wind effect on fire propagation. *International Journal of Wildland Fire*, **13**, 143-156.
- Rothermel C. (1972) A mathematical model for predicting fire spread in wildland fuel in: Research Paper INT-115: US Department of Agriculture, Forest Service, Intermountain Forest and Range Experiment Station, Ogden, UT, p. 40.
- Boboulos M, Purvis MRI (2009) Wind and slope effects on ROS during the fire propagation in East-Mediterranean pine forest litter. *Fire Safety Journal*, **44**, 764–769.

Chapter V

Fire propagation across double-slope and canyon configurations

In this chapter an investigation of the ability of the WFDS code in describing the fire propagation across double-slope and canyon configuration is presented. In the first case the main objective is to understand the main parameters affecting the variation of fire propagation in correspondence of the changing of the slope of the domain. In the second case the main objective is to verify the ability of the computational code in correctly describing the so-called eruptive behaviour, typical for fire moving in this kind of domain, characterized by an exponential increase in the fire propagation rate promoted by the particular domain configuration the fire is moving across. When available a comparison between experimental and model results is also provided.

V.1 Introduction

The effect of geometry on flame propagation was investigated by many authors who focused their attention especially on flame moving on flat or sloped surfaces under calm and windy conditions (Morvan and Dupuy, 2004; Malangone *et al.*, Viegas, 2004a; Rothermel, 1972, Boboulos and Purvis, 2004, Viegas, 2004b): in these cases the fire spreading rate results substantially constant when the main parameters governing the phenomenon (domain inclination, vegetation and meteorology) remain unchanged. However, recent works (Viegas *et al.*, 2010, Viegas and Pita, 2004) showed that such a condition is not true when particular geometric configurations are considered (i.e. valley, canyon): even in absence of wind, the fire rate of spread may become not constant in the time nor uniform in the space making the actual fire propagation rate more complex to identify and less predictable.

The time evolution of the fire propagation over a terrain configuration like a canyon is usually represented by an eruptive behaviour. Such a

condition is characterized by a low fire spreading rate during the initial stage, followed by a sudden increase of the fire propagation and intensity. In canyons, this phenomenon is mainly due to the rapid preheating of fuels located ahead of the fire front and to the induced strong convective mass transport which continuously draw air at the base of the canyon feeding the fire itself. This evolution in the fire dynamics occurs without any change in the main parameters governing the fire propagation such as wind and ambient temperature, vegetation type and moisture content. Evidences of such a fire behaviour are reported in a number of articles available in the literature (Viegas, 2002; Viegas, 2004; Viegas, 2006; Viegas and Pita, 2004; Viegas *et al.*, 2005; Viegas *et al.*, 2006). In particular, Viegas and his co-workers (Viegas and Pita, 2004) demonstrated and discussed the transient nature of the fire spread and proved the existence of the eruptive fire behaviour in laboratory experiments by considering several symmetrical canyon-like configurations. In these tests the authors used a rig with two faces inclined at a fixed angle attached to a structure that could be differently inclined ($0^\circ < \alpha < 40^\circ$) and an ignition source located in correspondence of the intersection line of the two faces of the canyon (defined as water line). They showed that at inclinations slope (α) of 0° and 10° the rate of spread remained relatively constant, with only small variations over time, while for canyons inclined at 30° and 40° the fire fronts accelerated significantly. Viegas (2005) introduced and discussed also a mathematical model designed to account for eruptive fire behaviour. In this model heat produced by the flames promotes air intake which intensify the combustion process and the rate of fire spread. The increase in fire intensity further enhances the induced air movement leading to an accelerated fire growth. Even if the model is able to predict the eruptive fire behaviour under certain conditions, it does not have an explicit dependence on the topographic characteristics of the terrain. Recent work from the same authors (Viegas *et al.*, 2010a) approached also the study of the effect of an ignition located at the lower external corner of a canyon (asymmetric ignition) on the fire propagation characteristics. The acceleration in the fire spreading rate, arising in conjunction with the passage of the fire from the canyon flank where it started to the next one, may be faster than that observed for an ignition point located at the same position where the fire crosses the water line. This behaviour is due to the effect promoted by the convection induced by the flank, which, in the asymmetric ignition case, is much higher than that one, caused by symmetric ignition.

This part of the thesis aims to investigate the ability of WFDS to adequately simulate experimental results and to correctly reproduce the way fire spreads across two different terrain configurations (double-slope domains and canyon) in the absence of wind; this was accomplished by comparing the results of the model simulations with findings from experimental tests available in the literature [Viegas *et al.*, 2010b; Viegas

and Pita, 2004). In the simulations, the vegetative fuel is arranged in beds of different inclinations and fire propagates across them according to terrain inclination and shape. The combined contribution of these two parameters determines the position of the flame with respect to the fuel: an abrupt change in slope makes the rate of flame propagation dependent also on the fire evolution history, while a canyon configuration induces a transient rate of spread whose duration cannot be defined *a priori*.

One of the main parameters considered to discuss the results is the Rate Of Spread (ROS, m/s) which has to be indented as the distance run by the fire front in time along the symmetry axis of the geometry where the fire propagates.

The mesh resolution was set according to Eq. III.15, by the dimensionless ratio D/δ_x (Mcgrattan *et al.*, 2010). A value of about 16 of such a ratio was chosen for the canyon simulations implying a maximum mesh size of 0.03 m. In the double-slope domains simulations, instead, the D/δ_x ratio was set to about 9 giving a maximum mesh size of 0.05 m: in this case, a further grid refinement up to 0.025 m caused much longer computational times but only small variations in the measured rate of spread (<10%). Such a mesh definition complied also with the restraints imposed by the Eq. II.13. Simulations, using the WFDS code were performed by adopting the fuel element model.

V.2 Simulation conditions

V.2.1 Double-slope domain

The study of the effect of the terrain slope on the fire propagation rate was already accomplished by the present author (Malangone *et al.*, 2011a, 2011b). Results of simulations showed that flames propagate on an inclined surface with a practically constant rate of spread (ROS) and that the ROS increases as the terrain inclination increases.

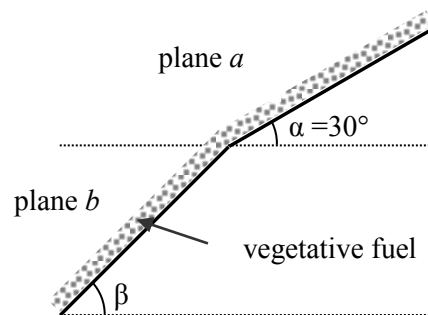


Figure V.1 Double-slope plane configuration.

The double-slope plane geometry gives the possibility to analyze the behaviour of a fire front when it moves on a surface which undergoes a sudden variation in the inclination.

To validate the capability of WFDS to simulate the fire propagation in such a condition, simulations have been compared with experimental results obtained by Viegas et al. (Viegas *et al.*, 2010b)] with a dihedral plane; the configuration, used in the experiments and reproduced in the simulations, of the two planes forming a double-slope surface is shown in Figure V.1. The actual dihedral table (4m x 4m each plane) used in the experiments is shown in Figure V.2. It can form a ridge, a plane slope of constant inclination or a valley that, as the ridge, can be either symmetric or asymmetric. In the fire tests performed by Viegas et al. (Viegas *et al.*, 2010b), a load of 0.6 kg/m² of straw, having an average moisture content of 6%, was used as vegetative fuel. These data were used in the model while the physical properties of the fuel were deduced from elsewhere (Zhou *et al.*, 2005). In particular, it was assumed a bulk density of 6 kg/m³ implying a 10 cm thick fuel bed.



Figure V.2 Dihedral plane during a fire test (Viegas 2010b)

In the experimental tests, to ignite the straw a line fire was lighted at the edge of the plane *b* (Figure V.1) using a wool thread soaked in a mixture of diesel and petrol fuels, in a 3 to 1 proportion, to assure a practically instantaneous ignition. In the simulations a linear 15 cm wide ignition source lasting about 12 seconds at the edge of the plane *b* was considered: maximum heat flux release rate associated to the ignition source was set to 1000 kW/m². needles and straw both with a fuel load of 0.6 kg/m². In order to study the variation of ROS on the plane *a* due the changing of the angle β , in the experimental tests α had a fixed value (30°), while β was varied in the range from -40° to +40°. Negative angles for the plane *b* correspond to a valley configuration.

V.2.2 Canyon configuration

For the modelling of a fire developing in a canyon, a geometry built with two adjacent planes (1.5 m x 3 m each) was considered. As shown in Figure V.3, each plane was oriented in such a way to form with the horizontal plane two angles (β and δ). δ represents the steepness of the canyon while β indicates how open/closed it is. Varying β and δ , different configurations can be obtained. The terrain surfaces are plane, without any curvature. The intersection line of the two faces is the canyon water line. The physical characteristics of the vegetative fuel (*Pinus Pinaster* needles) covering this surface were taken from the works of Viegas and Pita (2004) and Mell *et al.* (2006).

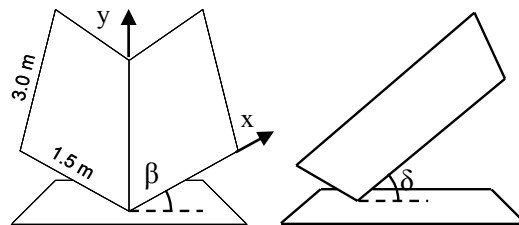


Figure V.3 Canyon Configuration ($\beta=\delta=40^\circ$)

Pine needles were ignited in correspondence of the symmetry plane of the canyon by a pseudopunctual source ($3.6 \cdot 10^{-3} \text{ m}^2$) at about 1 m from the lower external edge. Fuels having different moisture content (MC) of 0.04, 0.08 and 0.13 on dry basis were considered in the simulations; the maximum heat release rate associated to the ignition source was set equal to 500 kW/m² when the moisture contents were 0.04 and 0.08, and equal to 2000 kW/m² when MC was 0.13. All the simulations were run in the absence of wind.

V.3 Results and discussion

V.3.1 Double-slope domain

The comparisons between the experimental and modelled results are shown in Figures V.4 and V.5. In particular, Figure V.4 reports the rate of spread (ROS_B) on the plane *b* evaluated as linear distance run in the time by the fire front along the longitudinal axis of the plane; Figure V.5 shows the variation in the rate of spread on the plane *a* (ROS_A), which has a constant inclination (30°), as a function of the slopes adopted in the preceding plane *b*. Figure V.4 shows a good agreement between the experimental and model values when a fuel load of 0.6 kg/m^2 was assumed.

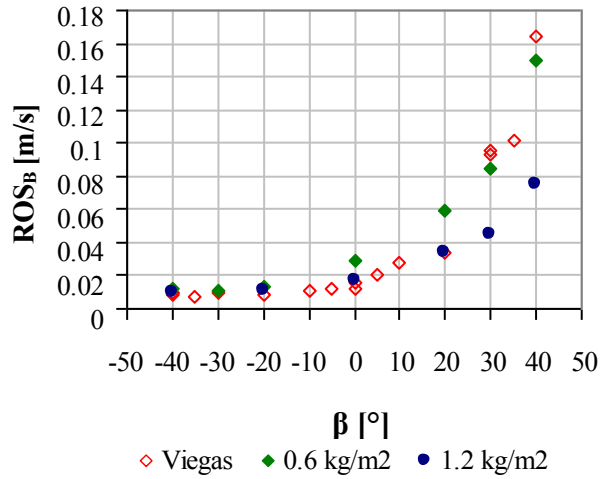


Figure V.4 Comparison between the experimental and simulated rate of spread for flames moving on plane *b*

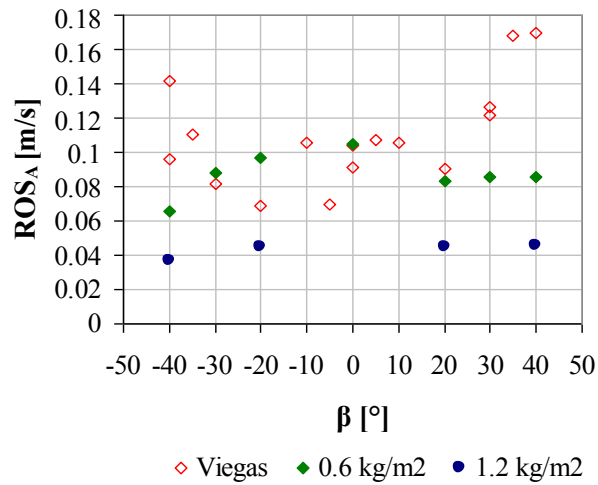


Figure V.5 Comparison between the experimental and simulated rate of spread for flames moving on plane *a*

With a heavier vegetative load (1.2 kg/m²) the ROS had the same behaviour for negative values of the *b* slope, while lower rates of spread with respect to the previous case were found at zero and positive *b* plane inclinations. Figure V.3 also shows that ROS_B increases at increasing slope. However, when the flames move downwards ($\beta < 0^\circ$) both the predicted and the observed rate of spread yielded small variations: in these cases the

flames are tilted backward and are unable to pre-heat the unburnt fuel. As a result, the experimental rate of spread at $-40^\circ < \beta < -10^\circ$ exhibits an average constant value of about 0.01 m/s and predictions match this value.

The comparison between simulated and experimental results (Figure V.5), assuming a 0.6 kg/m^2 fuel load, shows some differences for $\beta < -30^\circ$ and $\beta > 20^\circ$. Actually, experimental results are quite scattered in the whole range of considered inclination angles but they seem to suggest that the ROS_A increases either as β increases or as β decreases with respect to the value measured at $\beta \approx 0$. Instead, the values of ROS_A derived from the simulations increase in the range of β from -40° to 0° and are almost constant in the range $20^\circ < \beta < 40^\circ$.

In order to elucidate these findings in Figure V.6 the predicted fire front shapes, represented by the 300°C isotherms, are shown: the flame profiles are symmetrically represented with respect to the longitudinal axis (y) and are depicted according to a top view considering an orthographic projection on flat surface (x - y). They show an increasing distortion over time as the fire travels along the combustion table, more pronounced at higher β values. It is also evident how the sudden change of slope, when it occurs, produces a variation of the shape of the fire perimeter.

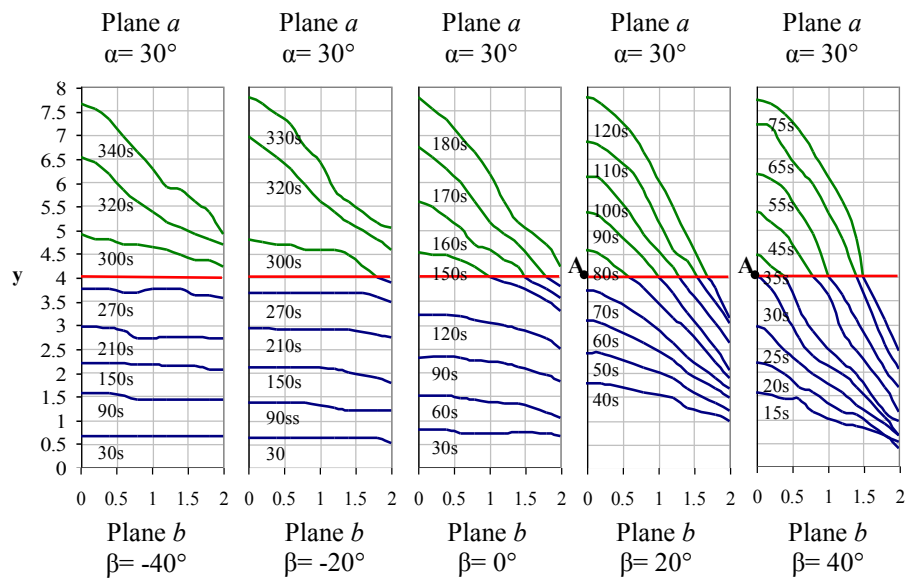


Figure V.6 Evolution in time of the fire profiles. Red line marks the changing in slope between the two faces forming the dihedral table. Time in seconds is reported for each profile.

The slope of the plane b strongly affects the way the plane a becomes ignited: for $-20^\circ < \beta < -40^\circ$ the transverse flame profile is almost flat before

entering the plane a while at $20^\circ < \beta < 40^\circ$ a sort of point ignition source, originating in the centre of the edge of the plane a , (point A in Figure V.6) is produced. Due to the different β , the heat sources which ignited the plane a are characterized by different shapes and intensities and, therefore, originate different ROS_A , as observed in Figure V.5.

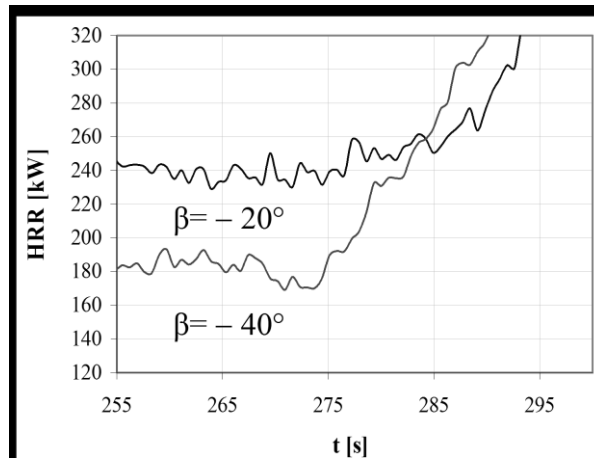


Figure V.7 Heat Release Rate (HRR) vs. time on the plane a for $\beta = -20^\circ$ and -40° .

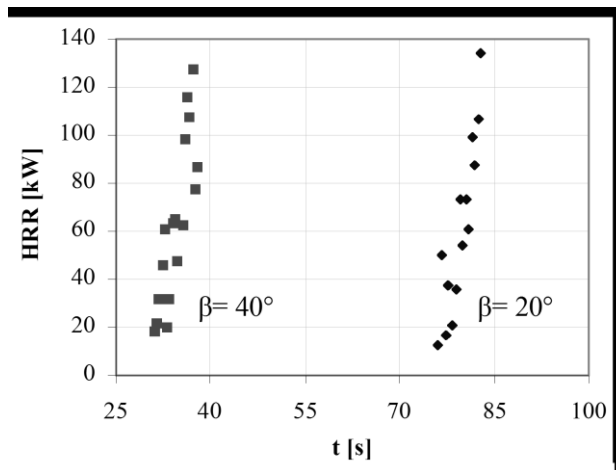


Figure V.8. Heat Release Rate (HRR) vs. time on the plane a , at $\beta = 20^\circ$ and 40° . Plane a ignition time: 30s and 75s at $\beta = 40^\circ$ and 20° , respectively

In Figure V.7 the heat released by the fire before moving on the plane a is shown for $\beta = -20^\circ$ and -40° : it can be seen how the energy generated when β is -20° is higher than when it is -40° , explaining the lower ROS_A calculated in this latter case. Instead, when β is equal to 20° or 40° (Figure V.8) the

ignition source originating on the centre of the edge of the plane a (position A in Figure V.5) generates nearly the same energy variation (about 14 kW/s) for about 10 seconds after the flame has reached the plane a . Therefore, in both cases a very similar heat source ignited the plane a , justifying the same ROS_A (Figure V.5). When $\beta=0^\circ$ the result is in between the two previous being the heat source induced on the plane a represented by a line that ignites only the central part of plane.

It can be concluded that small variations in the shape of the flame before the plane transition can have important consequences on ROS_A , hence, the discrepancies between the experimental and simulated fire contours seem to justify the different value of rate of spread on plane a found by simulations and experiments especially at very steep slopes.

V.3.2 Canyon configuration

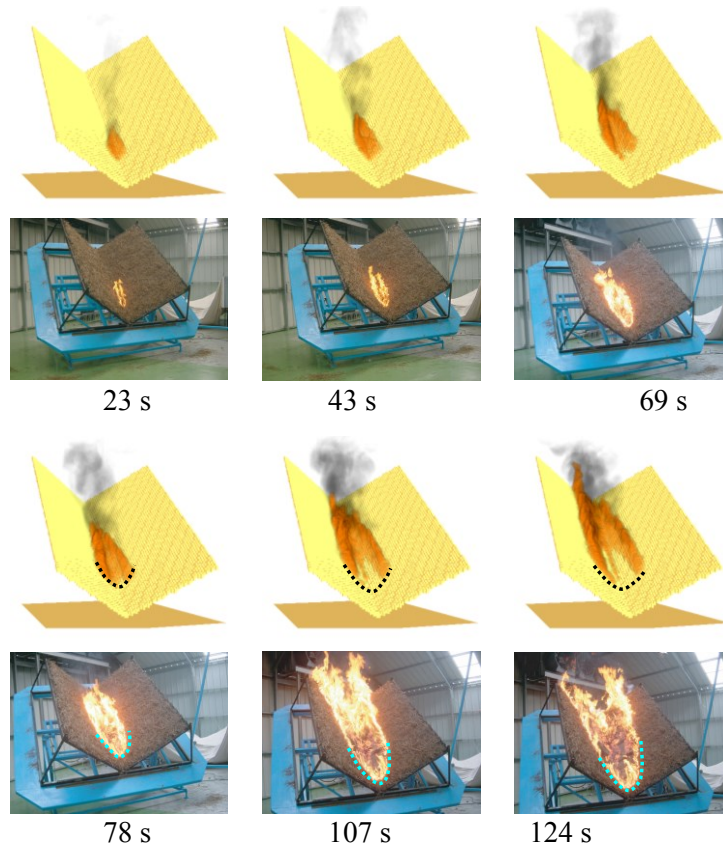


Figure V.9 Comparison between experimental and simulation results ($MC=0.13$). Dotted lines, at 78, 107 and 124 s, evidence the different fire contours between the experimental and simulation results.

In Figure V.9 a comparison between the simulation and experimental

(Viegas and Pita, 2004) results, obtained with a vegetative fuel having $MC=0.13$ and $\beta=\delta=40^\circ$ is shown.

Figure V.9 shows that there are differences between the evolution in the time of the shape of the fire fronts calculated by WFDS and that determined by visual observations and reported in the literature (Viegas and Pita, 2004). Specifically, WFDS yields a fire perimeter with an “U” profile, while a “V” shape can be observed from the pictures. However, such a difference could be due to the limitation to display data generated by the computational code. Indeed, the fire shape was obtained from the simulation results considering only the heat released by the burning fuel, i.e. neglecting the visible light radiation present in the actual combustion phenomenon.

A more quantitative comparison between the experimental and the simulation results is presented in Figure V.10 in terms of burnt area growth versus time. In this case the burnt areas, calculated from the isosurfaces of the heat release rate (20 kW/m^3) at ground level, approximate quite well the experimental profile when $MC=0.13$ and $MC=0.08$ (Figure V.10). Furthermore, it has to underline that in the work of Viegas and Pita (2004) the number of available parameters for defining the vegetative fuel characteristics was limited and, therefore, further information about the fuel characteristics required by the software were taken from a different reference (Mell et al., 2006)

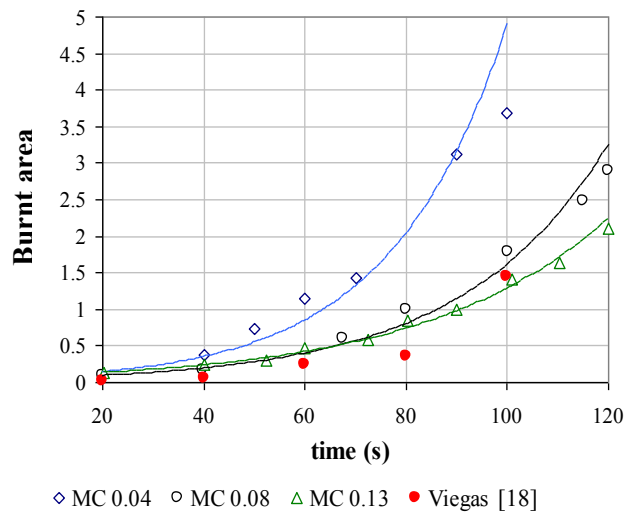


Figure V.10 Comparison of burnt area growth in canyon configuration between the experimental tests and the simulated results at different moisture contents. Exponential fitting curves are represented by solid lines.

Besides the results above, Figure V.10 shows other two features of the

system investigated. The first is the effect of fuel moisture content on the calculated ROS. Indeed, the Figure indicates that the fuel humidity level heavily influences the ROS. Therefore, the lack of accurate information on the values of parameters employed in the experiment could give rise to large differences between modelling and experimental results. The second is that the fire propagation rate has a not linear trend versus time. This can be also appreciated from Table V.1 where the parameters of the exponential curve fitting the burnt area values and shown in Figure 10 are reported. This finding agrees with the result of Viegas and Pita (2004) who experimentally proved that in this domain configuration the fire has a peculiar dynamic behaviour: the rate of spread increases continuously, even in the absence of wind, causing the well known phenomenon of blow-up associated with real canyon fires.

Table V.1 Parameters for the fitting curves in figure 7

Fitting equation: $Area = a \cdot e^{b \cdot t}$ (Area [=] m² t [=] s)			
	<i>a</i>	<i>b</i>	<i>R</i> ²
MC= 0.04	0.062	0.0438	0.9572
MC= 0.08	0.0497	0.0349	0.9868
MC= 0.13	0.0802	0.0278	0.991

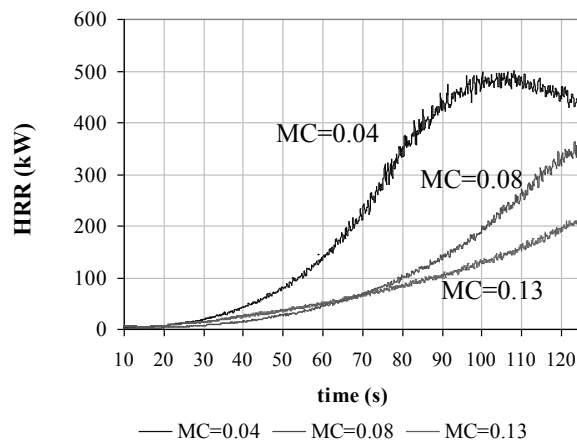


Figure V.11 Heat release rate profiles for canyon geometry at different moisture content (MC)

In Figure V.11 the heat release rate versus time is reported for fuels at different moisture contents. The heat release rate (HRR) represents the total amount of heat produced by the fire in the time and is directly related to the fire spreading rate. It is shown that the net heat generated by the fuel, due to

the particular geometrical configuration, is not balanced by heat losses.

Therefore, the tendency of the ROS to increase indefinitely is not stopped until the whole surface available for burning is consumed. In these conditions the pre-heating of the fuel ahead of the flame is strongly promoted, increasing the fire propagation rate; this mechanism, according to the literature (Velez, 2000), appears to be a reasonable way to explain the results.

Moreover, Figure V.11 shows that HRR decreases at increasing fuel moisture content: this effect is due to a reduction in the amount of fuel available and to a complementary increase in the quantity of water to be evaporated.

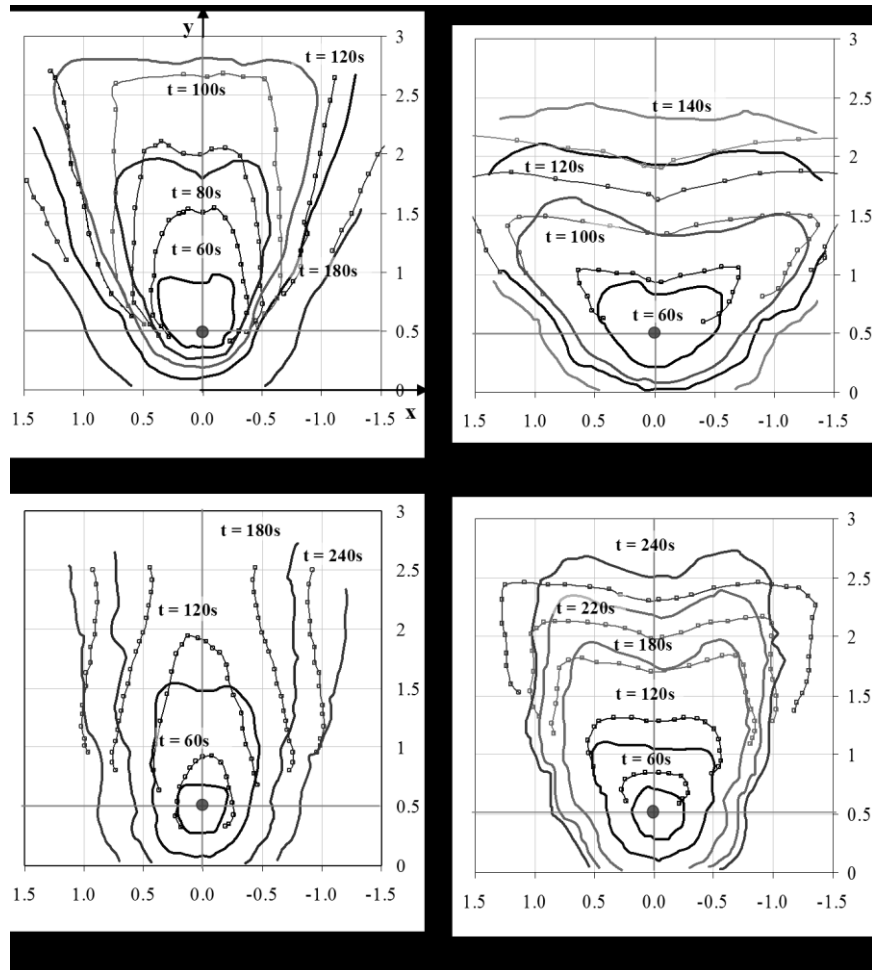


Figure V.12 *Pinus needles: Comparison between experimental (solid line) and simulated results (solid+squares line)*

Further comparison between experimental (Viegas and Pita, 2004) and model results were performed with the same kind of fuel having a moisture content of 10%. In this case the ignition source, was located on the symmetry plane of the canyon at 0.5 m from the lower external edge and the heat release rate associated to it was set equal to 1600 kW/m². The comparison between the experimental and the modelled results are presented in Fig. V.12. Here, the lines represent the positions in time of the external edge of the fire front, which were tracked by recording the values of the isotherms at 227°C.

The surfaces limited by these lines were assumed as completely burned. The comparison in Figure V.12 shows a fair agreement between experiments and model results although these latter were not able to describe the backfire propagation, which probably requires a spatial resolution much higher than that employed and/or a different ignition source. For instance, this last parameter was estimated through a trial and error procedure because no clear information about its energy and size is reported in the reference literature.

The major discrepancy between the experimental and the simulated values occurs in conjunction with high δ values and short times after fire ignition. Such a discrepancy, however, tends to fade at longer times when the influence of the ignition source characteristics on the fire behaviour becomes less effective. If the δ value influences the fire propagation rate along the y direction, the β angle influences the extension of the fire boundary along the x axis. In correspondence of the same δ value, quite narrow shapes arise at $\beta=20^\circ$, while wider profiles come up when $\beta=40^\circ$ is assumed. The values of these two angles control the fire shape evolution, regulating the possibility for the flames to evolve in a bifurcation of the fire front. Such a condition arises at $\delta=20^\circ$ where the fire propagation along the x direction is faster than that along y direction. An opposite effect is observed at $\delta=40^\circ$ where the fire fronts, originating on the two canyon ridges, tend to merge at the water line in a single head during their propagation along the y direction.

V.3.2.1 Effect of the position of the ignition source

This section covers the situation in which the origin of the fire was placed at the lower edge of the water line, or line of symmetry (symmetric ignition), and in correspondence of the right bottom corner of the canyon (asymmetric ignition); respect to the previous cases the extension of the study of the forest fire propagation in canyons to other ignition positions can provide a significant aid in understanding the dynamics of eruptive behaviour. In this case the fuel bed was composed by straw with a fuel load of 0.6 kg/m². The fuel physical properties were taken from the literature (Viegas and Pita, 2004; Mell *et al.*, 2006; Zhou *et al.*, 2005). For the mesh and ignition conditions the same parameter of the previous section were applied.

V.3.2.1.1 Symmetric vs. asymmetric ignition: qualitative comparison

The fire patterns arising for symmetric and asymmetric ignitions are very different and in Figure V.13 and V.14 a qualitative trend is shown in the case of $\delta = \beta = 40^\circ$.

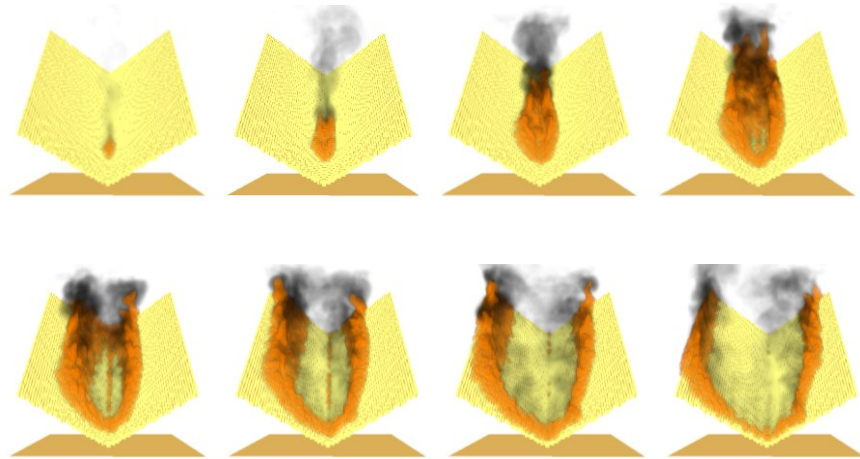


Figure V.13 Fire simulation for the symmetric ignition. Frame times: 5s; 20s; 40s; 60s; 80s; 100s; 120s; 140s

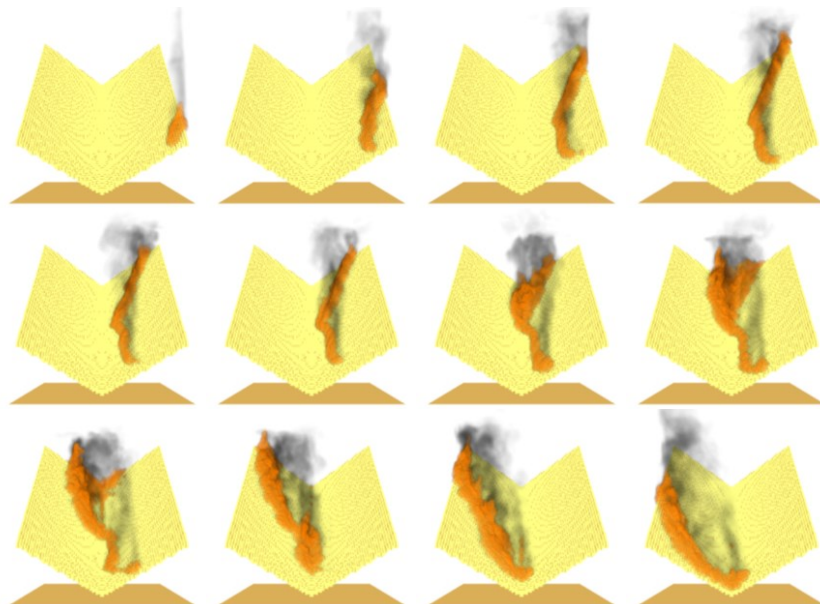


Figure V.14 Fire simulation for the asymmetric ignition. Frame times: 50s; 130s; 210s; 280s; 320s; 340s; 380s; 400s; 420s; 460s; 500s; 550s.

In the case of symmetric ignition (Figure V.13) a high rate of spread and fire intensity is associated to the fire propagation due to the strong convection, which determine the pre-heating of the fuel. In the case of the asymmetric ignition (Figure V.14), instead, the fire progression is different: flames move initially under the influence of the slope of the canyon flank where they started towards the canyon water line, where a sudden increase in the fire propagation rate occurs, causing an abrupt extension of the fire front also on the opposite canyon face. The time evolution of the fire spreading may also be obtained from the heat release rate (HRR) time profiles shown in Figure V.15. HRR represents the total thermal power associated to the fire. It is evident from Figure V.15 that in the case of symmetric ignition point it increases rapidly and continuously until the fire has consumed the majority of the available fuel. Instead, in the case of asymmetric ignition point the HRR grows slowly until the canyon water line is reached, where it abruptly increases when the fire front crosses the canyon water line continuing its propagation on the opposite flank

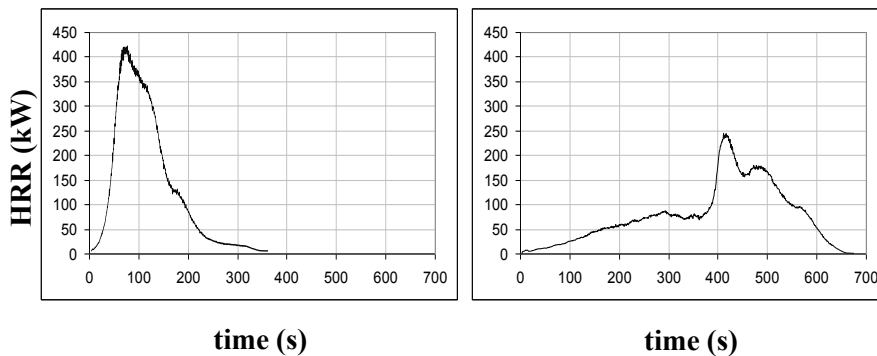


Figure V.15 Time profiles of HRR for the cases of symmetric (right) and asymmetric (left) ignition source.

V.3.2.1.2 Symmetric vs. asymmetric ignition: quantitative comparison

The value of the angles δ and β strongly affects the fire path as shown in Figures V.16 and V.17 where the time evolution of the fire boundaries for various canyon configurations are displayed. The way to obtain the fire contours is the same used for the *pinus* needles simulations. The *pinus* fuel is characterized by a lower surface to volume ratio ($s = 4100 \text{ m}^{-1}$) with respect to the straw ($s = 13300 \text{ m}^{-1}$): such a condition generates in the *pinus* needles fire propagation rates lower than those measured for the finer fuels with the same geometric configuration. As expected, the fire front time profiles in Fig. V.16 tends to remain symmetric with respect to the water line while in figure V.17 they evolve differently according to the canyon inclination angles.

For the symmetric case the computation of the rate of spread (ROS), which is defined as the distance run by the fire front per unit time, was accomplished. ROS can be easily obtained from the data of Fig.V.16 considering the distance run in time by the fire front along the y axis. Results indicate that the ROS remains roughly constant for $\delta=0^\circ$ and $\delta=20^\circ$ and has the values of $7 \cdot 10^{-3}$ m/s and $1.5 \cdot 10^{-2}$ m/s, respectively. For $\delta=40^\circ$ ROS is not constant and the fire front undergoes an acceleration (a) depending on how closed the canyon is: for $\beta=20^\circ$ and $\beta=40^\circ$, a is $2 \cdot 10^{-4}$ m/s² and $5 \cdot 10^{-4}$ m/s², respectively.

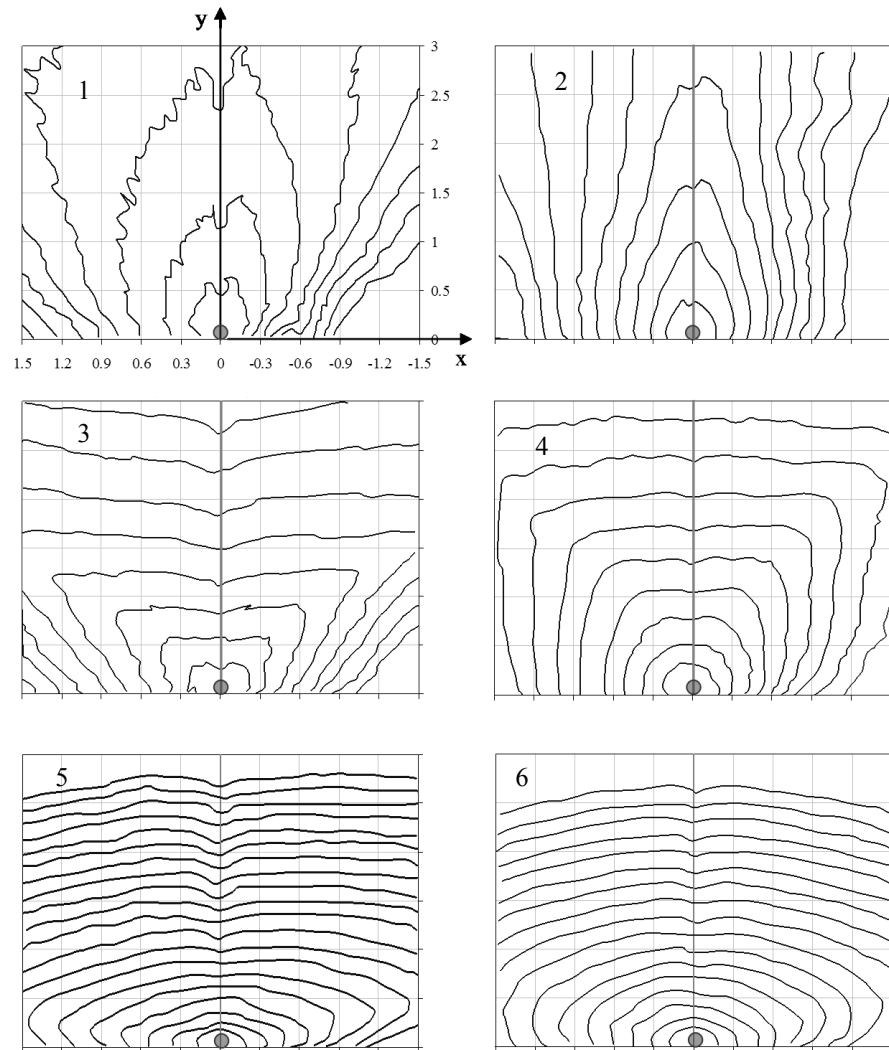


Figure V.16 Fire shape evolution in time for symmetric ignition (grey dot). Time step between lines is 20 s. Left: $\beta=40^\circ$ - Right: $\beta=20^\circ$. From top to bottom $\delta=40^\circ$, $\delta=20^\circ$, $\delta=0^\circ$

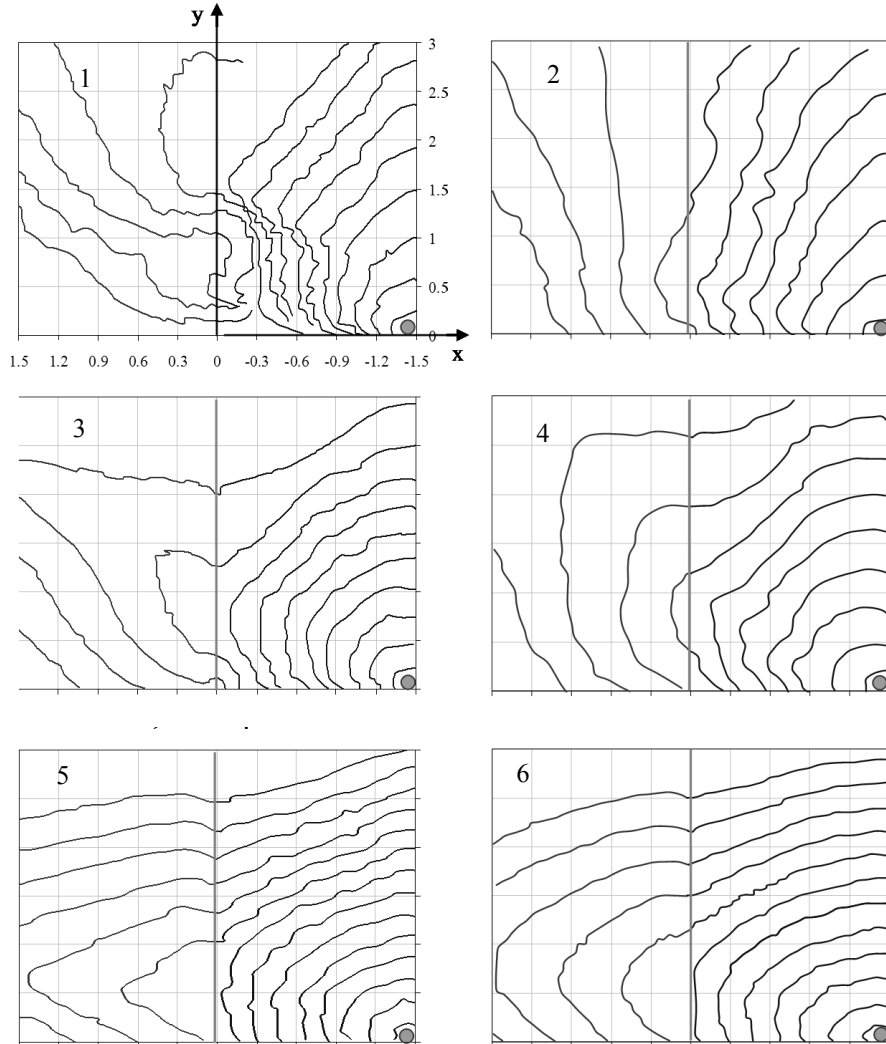


Figure V.17 Fire shape evolution in time for asymmetric ignition (grey dot). Time step between lines is 40 s. First fire profile is at 20 s. Left: $\beta=40^\circ$ - Right: $\beta=20^\circ$. From top to bottom $\delta=40^\circ$, $\delta=20^\circ$, $\delta=0^\circ$

Although useful, ROS may be lacking in describing fire propagation characteristics in canyons. For instance, at a given time for the case $\delta=20^\circ$ the position reached by the fire front on the y axis is practically the same independently of β , but the area spanned for $\beta=40^\circ$ is larger than in the case $\beta=20^\circ$. In this conditions a parameter, useful to analyze the fire propagation feature, may be the surface cumulative area spanned in time by the fire. It is obtained by computing the surface area inside the lines representing the fire

boundaries in time and is reported in Figure 8 for the cases of symmetric ignition.

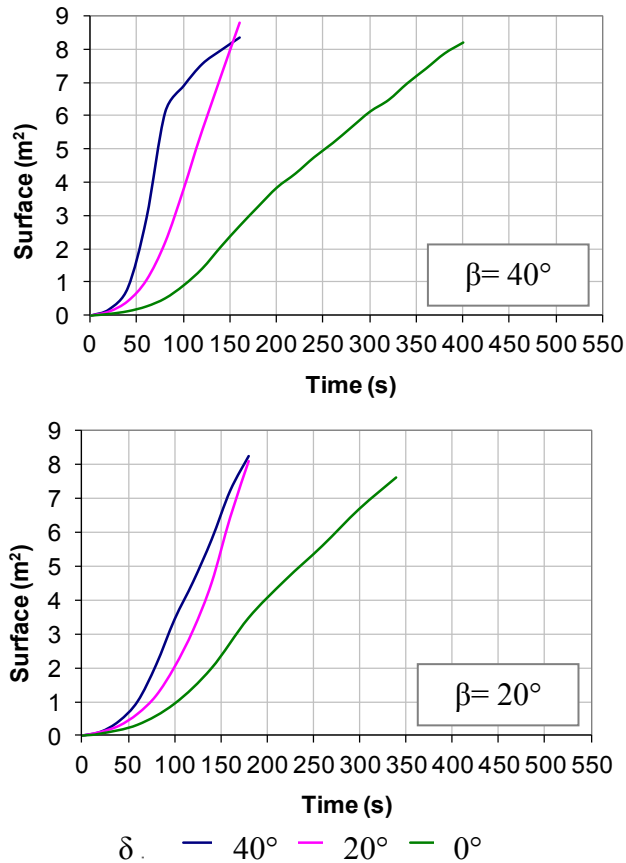


Figure V.18 Surface evolution in time for symmetric ignition ($\beta=40^\circ$ top, $\beta=20^\circ$ bottom)

Figure V.18 shows that with symmetric ignition and for a given β angle, after a slow initial growth the cumulative surface area spanned by the fire increases steadily and reaches an almost constant rate of change (that is the time derivative (R_s) of the curves in Fig.s 8), which results higher the higher δ . However, the change of R_s is strong by varying δ from 0° to 20° while it is much weaker by varying δ from 20° to 40° . Moreover, the shape of canyon (β) seems to play differently on the rate of increase of surface area involved in fire. Indeed, for $\delta = 0^\circ$ the highest R_s verifies at $\beta = 20^\circ$, while for δ equal to 20° or 40° it verifies when $\beta = 40^\circ$. The knowledge of both ROS and R_s gives a complete understanding of the fire features during its propagation through the canyon. Indeed, larger extension of the fire perimeter along the x direction is therefore expected at the higher value of β , as can be seen

from the comparison of the sketches 3) and 4) in Figure V.16. Similar considerations can be made for $\delta=0^\circ$ comparing sketches 5) and 6) in Figure V.16.

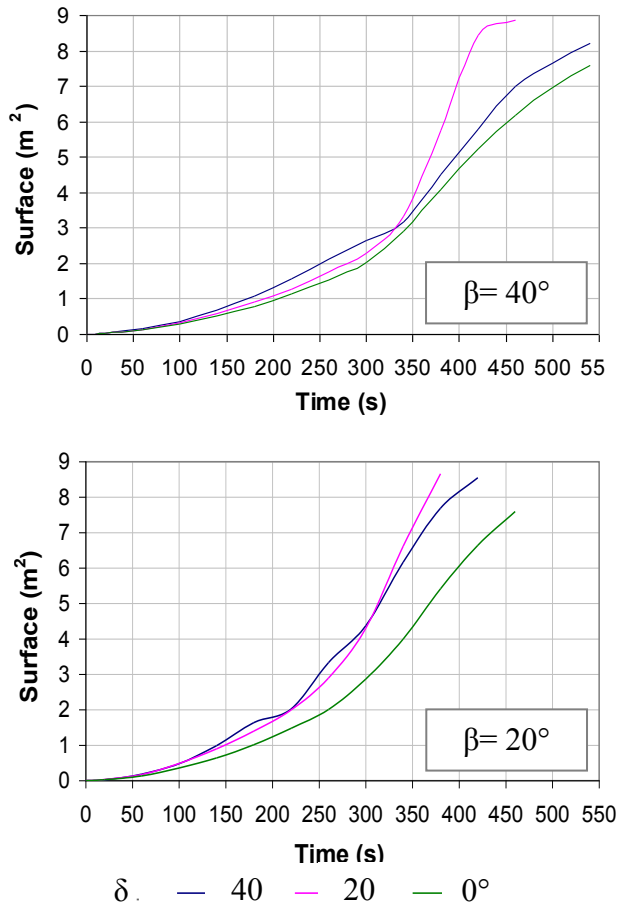


Figure V.19 Surface evolution in time for the asymmetric ignition ($\beta=40^\circ$ top, $\beta=20^\circ$ bottom)

For the asymmetric case, Figure V.17 shows that at high δ values the fire propagates preferentially upwards rather than towards the water line. This occurs likely because the canyon orientation promotes the heating of the unburned fuel located above the position of fire ignition. In addition, for the same δ angle, the fire progression towards the canyon water line is slower at increasing β angle, because the heating of the fuel located laterally with respect to the position of the fire ignition becomes less effective. For instance at $\delta=20^\circ$ and $\delta=0^\circ$ the fire front reaches the opposite flank after about 290s and 220s when β is 40° and 20° , respectively. With respect to the

symmetric ignition case in the present case fire has not a preferential way of propagation and, therefore, the calculation of the ROS appears not applicable.

The surface cumulative areas spanned in time by the fire front in the case of asymmetric ignition are reported in Figure V.19. With respect to the case of symmetric ignition they appear significantly different. In particular, they smoothly increase in time and their derivatives R_S do not approach constant values nor reach values so high as those calculated in the previous case. In addition, the differences between the profiles obtained varying δ from 0° to 20° and between 20° to 40° are practically the same. The comparison between the profiles obtained at $\beta=20^\circ$ and at $\beta=40^\circ$ in figure 9 shows that the surface evolution has a similar trend in time except for the case $\beta=40^\circ$ and $\delta=20^\circ$ where the simulation results seem to evidence the presence of two distinct slopes (before and after 320 s) that could be related each to the fire propagation across one of the two canyon flanks.

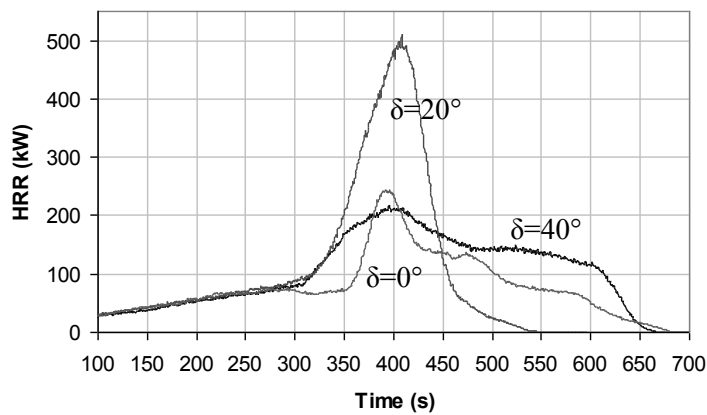


Figure V.20 *HRR time evolution for the asymmetric ignition ($\beta = 40^\circ$)*

When an asymmetric ignition occurs, the way through which the fire propagates on the opposite canyon face changes according to the canyon angles. In fact, the propagation from one face to the other in correspondence of the canyon water line may develop in two distinct fronts as in the case $\delta=40^\circ$ - $\beta=40^\circ$ (Fig. V.17(1)) or in a single front as in the other cases. Furthermore, also the thermal power associated to these propagation ways is different. Indeed, the HRR time profiles calculated for the three cases of asymmetric ignition and $\beta=40^\circ$ (Fig.10) may support this issue justifying also the higher R_S value for the case $\delta=20^\circ$ - $\beta=40^\circ$ with respect to the other two cases of Figure V.20. In this case, in fact, the total thermal power generated by the fire in correspondence of the passage of the fire front on the opposite canyon flank is the highest.

V.4 Conclusions

The physically-based model WFDS- specifically designed to simulate the fire behaviour – was found to be an effective tool to correctly study the way the flame spread across different kinds of terrains (double-slope domains and canyon).

The results obtained for the double-inclination domain showed that the fire spreading rate on a plane is dependent not only on the fuel bed properties and the terrain slope but also on the boundary conditions, namely the fire spread properties, at the edge of the given fuel bed. Indeed, the change in inclination of the behind plane (*b*) produced ignition sources having different shapes and energies, which originated different rates of spread on the forward plane (*a*). The agreement between experimental and simulated results was satisfactory, but failed partially when considering high inclination (both positive and negative): in these cases dissimilarities between the real fire contour and how it is modelled by the software may explain the differences between the simulated and experimental values.

The dynamic behaviour of the fire was also observed; this effect is not generally predicted in classical model, which assume that fire in a homogeneous fuel bed and in a uniform slope will propagate with a constant rate of spread. In the canyon configuration it was observed that the fire growth is relatively slow at the beginning, and then increases very rapidly and the time lag for this transition depends on the moisture content and/or the fuel properties in general. In this case, the pre-heating of the unburnt fuel is strongly promoted because the net heat generated by the fuel is not balanced by a proper amount of heat loss and, hence, this affects the fire phenomenon by accelerating its rate of spread. In this case also the time becomes an important factor in describing the fire behaviour and its role in correctly define the flame propagation rate needs to be considered along with the topography, vegetation and meteorology parameters.

Furthermore also the dynamic propagation of the fire in canyon according on whether there is symmetric or asymmetric ignition was studied. In particular, in the second case the fire growth is relatively slow at the beginning and, then, increases very rapidly and the time lag for this transition depends on the fuel properties and on the characteristics on the canyon (angles δ and β). An acceleration in the surface spanned in time by the fire occurs just in correspondence of the reaching of the canyon water line. In this position fire becomes a new heat source for the next ridge but its intensity and shape cannot be deduced easily. A quantitative analysis of the results indicated that the classic approach, which consider the ROS as the main parameter, is not sufficient in describing fire spreading especially in all the cases where a preferential path of fire propagation is missing. The extension of the study to other geometries and ignition conditions can

provide a significant aid in understanding the factors that can influence the fire behaviour, giving a large contribution to increment personal safety during fire suppression activities.

V.5 References

- Boboulos, M., Purvis, M.R.I.: “Wind and slope effects on ROS during the fire propagation in East-Mediterranean pine forest litter”, *Fire Safety Journal*, 44: 764–769 (2009).
- Malangone, L., Russo, P., Vaccaro, S., Effects of wind and terrain slope on flames propagation in a vegetative fuel bed, XXXIV Meeting of the Italian Section of the Combustion Institute, Roma, 24-26 October 2011b.
- Malangone, L., Russo, P., Vaccaro, S., The role of the terrain geometry on the flames propagation through a vegetative fuel bed, MCS 7 Chia Laguna, Cagliari, Sardinia, Italy, September 11-15, 2011a
- McGrattan K., Hostikka S., Floyd J., Baum H., Rehm R., Mell W., McDermott R.: “Fire Dynamics Simulator (Version 5) Technical Reference Guide - Volume 1: Mathematical Model”. NIST Special Publication 1018-5, (Available at: <http://www.fire.nist.gov/fds/>), (2010)
- Mell, W.E., Manzello, S.L. and Maranghides, A.: “Numerical modeling of fire spread through trees and shrubs”. *Proc. V International Conference on Forest Fire Research*, Viegas Ed., 2006.
- Morvan D., Dupuy J.L.: “Modeling the propagation of a wildfire through a Mediterranean shrub using a multiphase formulation”, *Combustion and Flame* 138: 199–210 (2004).
- Rothermel C.: “A mathematical model for predicting fire spread in wildland fuels”, in: Research Paper INT-115: US Department of Agriculture, Forest Service, Intermountain Forest and Range Experiment Station, Ogden, UT, 1972, p. 40.
- Velez R.: “La defensa contra incendios forestales – Fundamentos y experiencias”, McGraw Hill Interamericana de España: Madrid, Spain (in Spanish), 2000.
- Viegas D. X., Rui Figueiredo A., Pita L.P., David D., Rossa C.: “Analysis Of The Changes Of Boundary Conditions In A Slope”. *Proc. VI International Conference on Forest Fire Research*, D. X. Viegas (Ed.) (2010b).
- Viegas, D.X., A mathematical model for forest fires blow-up, *Combustion Science and Technology*, 177, 2005, pp. 27-51.
- Viegas, D.X., On the existence of a steady state regime for slope and wind driven fires, *International Journal of Wildland Fire*, 13, 2004, pp. 101-117.
- Viegas, D.X., Parametric study of an eruptive fire behaviour model, *International Journal of Wildland Fire*, 15, 2006, pp. 169-177.

- Viegas, D.X., Pita, L.P., Caballero, D., Rossa, C., Palheiro, P., Analysis of accidents in 2005 fires in Portugal and Spain. 9th International Wildland Fire Safety Summit, April 25-27, Pasadena, CA, 2006.
- Viegas, D.X., Pita, L.P., Fire spread in canyons, *International Journal of Wildland Fire*, **13**, pp. 253-274, 2004.
- Viegas, D.X., Pita, L.P., Ribeiro, L., Palheiro, P., Eruptive fire behaviour in past fatal accidents, 8th International Wildland Fire Safety Summit, April 26-28. Missoula, MT, 2005.
- Viegas, D.X., Pita, L.P., Santiago, L., Fire Behaviour in Canyons as a Consequence of Asymmetric Ignitions, 6th International Conference on Forest Fire Research, 2010a.
- Viegas, D.X., Fire line rotation as a mechanism for fire spread on a uniform slope, *International Journal of Wildland Fire*, **11**, 2002, pp. 11-23.
- Viegas, Domingos X.: "On the existence of a steady state regime for slope and wind driven fires", *Int. J. of Wildland Fires*, 13, 101-117 (2004a).
- Viegas, Domingos X.: "Slope and wind effect on fire propagation". *Int. J. of Wildland Fires*, 13: 143-156 (2004b).
- Zhou H., Jensen A.D., Glarborg P., Jensen P.A., Kavaliauskas A., Numerical modeling of straw combustion in a fixed bed, *Fuel*, **84**, pp. 389-403, 2005.

Chapter VI

Simulation of fire spread within a relatively large scale domain with complex geometry

In this section the numerical code WFDS is used to study the behaviour of a fire propagating over a relatively large area with a real surface configuration. In particular, the code is able to provide information to deduce the fire front shape profiles and terrain area burned in time. The proposed method of employment of the simulation software is compared with data, available in the literature, concerning a piloted fire accident occurred in central Portugal in 2001. The comparison between the experimental and the modelled results shows a good agreement and may suggest that this model may serve as the basis for an on going prediction method.

VI.1 Introduction

Previous sections investigated the behaviour of fire propagating across small domains. Even if some peculiar features characterizing the fire behaviour can be observed and studied also at small scale (Viegas and Pita, 2004), the tendency to extend such a results to a large domain can be hazardous. Fire experimentalists are aware of the difficulty in extrapolating data from bench scale type tests to large scale events even if data from bench scale tests should provide a reasonable prediction about the interaction of known potential ignition sources and fuels and fire spread based on the characteristics of the environment (e.g., geometry, ventilation, fuel load, etc).

Computational codes, enabling three-dimensional simulations of fire spread, are, generally, used only for small area domains or for laboratory scale experiments. In the first case in order to limit the computational costs, and in the second case because, when used for validation purposes, the small

scale is simpler to control. Currently, for large scale fires ($>10 \text{ km}^2$) GIS-based fire simulators are adopted, which work in conjunction with a GIS platform able to provide information about the heterogeneity of the terrain and of the vegetation fuel. Such an exchange of information between the GIS platform and the computational code is not always so straightforward and often requires high specific GIS competences and skills in order to first build the specific database representing the domain to investigate and, then, to convert this organized information in an input data usable by the computational code. In particular, to represent the morphology of the terrain the DEM (Digital Elevation model) model is considered in GIS; it is a type of data which represents the three-dimensional nature of the domain through a sort a matrix in which to every position in the plane (x and y coordinates) is associated an elevation (z coordinate). Database of DEM file exists, but usually they are not free and are available at a coarse resolution, therefore unable to satisfactory represent the morphology of limited-surface domains. In this chapter to represent the morphology of the domain the GIS approach was not considered; the use of a different software able to build the DEM data starting from free available elevation data of a domain (iso-level curves) (i.e., i.e. <http://maps.google.it/>, terrain mode) was considered.

VI.2 Simulation conditions

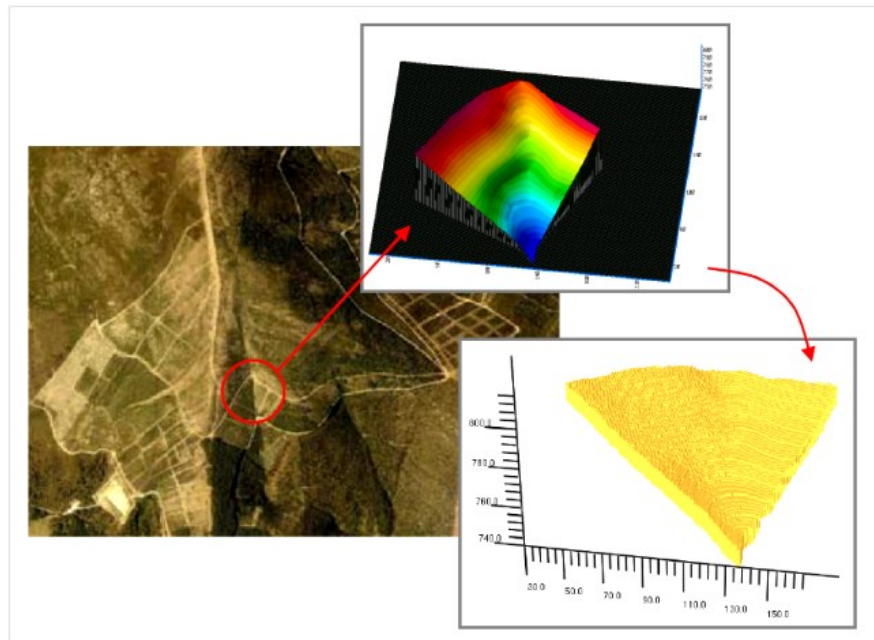


Figure VI.1 Aerial view of the Lousã area (left), its visualization in SURGE software (top) and its conversion in WFDS code (right).

The calculation domain was derived from a real terrain with the configuration of the canyon shown in Figure VI.1. Its conversion into the format recognized by the computational code was first performed by turning the domain into a xyz table, using the free software SURGE (<http://surgeweb.sweb.cz/surgemain.htm>), then the matrix representing the height (z) of the surface in correspondence of each point (x,y) of the plane was converted in the final format recognized by WFDS using common editing programs (Microsoft Word and Excel). The iso-level curves available in the literature (Viegas and Pita, 2004), were used as starting point to build the elevation model of this domain.

Figure VI.1 represents one of the plots (circled) in which the area of Lousã, located in central Portugal, was divided from 1998 to 2002 in order to perform fire tests in open field (Viegas *et al.*, 2002; Viegas and Pita, 2004). Those experiments were designed to generate input data to be used in fire behaviour models and to support the development of new models and their validation. All the cited experiments were made in good weather conditions with wind below a certain threshold that would have made unsafe the experiments. For this reason simulations were carried out in the absence of wind.

The computational domain is 145 m long (x), 162 m wide (y) and 92 m tall (z) and has a surface area of about 25.2 ha. The whole computational domain was divided into 23 computational meshes: to limit the calculation load, the back side of the canyon, where no event occurs, was kept out of the simulation. Each computational mesh had the resolution of 1 m in the x and y direction and 0.8 m in the z axis. According to this domain meshing only two calculation points in the fuel bed were considered. Simulation was performed on a single CPU core and was completed in about 60 h on an Intel Xeon E5630 at 2.53 GHz CPU with 6 GB ram.

The vegetative fuel was assumed to cover uniformly the domain and was represented by three shrubs species, *Erica umbellata*, *Erica australis* and *Chamaespartium tridentatum* with an average height of 1.0 m and a fuel load of 3.7 kg/m². However, in the real domain such a vegetative species corresponded to the 85% of the total cover with some heterogeneity in the respect to the shrub height as well. In general, near the top of the hill, the shrubs are lower and more disperse and some fuel breaks exist. The vegetation gets more dense and very high near the bottom where shrubs 2 m high could be found. The physical characteristics of the fuel, implemented in the computational code, were taken from the literature (Barboutis and Philippou, 2007). Shrubs were ignited at three points near the water line at the base of the canyon. The maximum heat flux release rate, associated with the ignition source, was set equal to 12000 kW/m². As said, simulations were run in the absence of wind.

VI.3 Results and discussion

Results, reported in Figure VI.2, show the time profiles of the fire front during its propagation along the canyon.

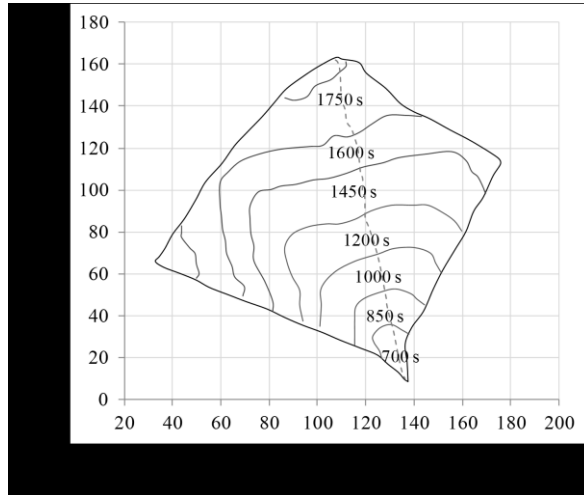


Figure VI.2 Time shape profiles. Dashed line: canyon water line

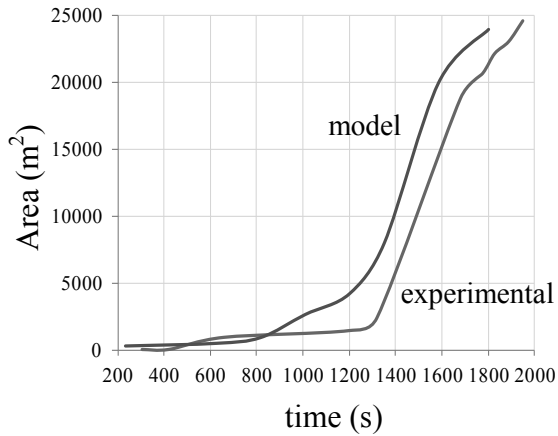


Figure VI.3 Area growth in the field experiment compared with the modelled results

The fire contour at each time step was evaluated as the isotherm at 100°C. Under the assumption of no external factors (i.e., no wind field, uniform fuel density, etc.) a fire front on a flat surface would propagate at the same rate in all directions, creating concentric fronts; on the contrary, in

this case the fire propagates following the surface irregularities and, then, the fire front moves slower in the canyon water line than along its flanks (Fig. VI.2) (Malangone *at al.*, 2012).

Figure VI.3 reports the comparison between the calculated and the experimental values of the cumulative area spanned by the fire as a function of time. Due the irregularities in the domain configuration difficulties arose in the calculation of burned surfaces at each time step: according to the cited reference this calculation was simplified assumed that the canyon can be considered as quite regular forming the angles of 25° (δ) and 31° (β) with the horizontal (see Fig. III.8). Figure VI.3 shows that a) the canyon surface becomes completely burned in about 1800 s; b) initially, the area spanned by the fire increases in time at a relatively low rate but after about 1200 s from the fire start there is a strong acceleration and such a rate becomes more than 10 times higher; c) the experimental and the calculated values of the spanned area in time have similar trends although the calculated values resulted shifted upward of about 100 s with respect to the experimental results; d) toward the end of the test the rate of increase of the cumulative burned area decreases because of both a lower amount of fuel available and a slight reduction in the inclination in the canyon (Malangone *at al.*, 2011).

The feature described under the point b) above is typical for this kind of domains (canyons). Indeed, the concave shape of the terrain is able to generate, even in the absence of wind, a sudden change of the fire behaviour (eruptive fire) because it favours the pre-heating of the fuel located ahead of the fire front and promotes the continuous intake of fresh air at the base of the canyon (chimney effect) (Viegas and Pita 2004). The minor discrepancy between experimental and calculated data, underlined under the point c), could be due to incorrect assumptions (power and or position) of the ignition source in the numerical model, which could give rise to an anticipated fuel ignition with respect to the real case. Furthermore, the assumption to consider the fuel bed as uniform does not represent correctly its actual distribution. Indeed, detailed information about the fuel load and the ignition source used in the experiments were not available. This aspect needs to be further investigated.

VI.4. Conclusions

Results showed that the use of the physics-based model, WFDS, may be effective in studying the way fire spreads across a real domain with a complex configuration. Results confirm the strong dependency of the terrain heterogeneity on the time profiles of the fire front.

At the level of resolution adopted, WFDS was not able to directly resolve the fire behaviour details in the grass fuel bed, but the fire/domain interactions that occur over scales on the order of a few meters could be resolved. This level of resolution of the fire physics was sufficient to capture

the dynamics of the fire perimeter and also to highlight the role of the domain geometry (canyon) in generating an eruptive fire behaviour. Results of the cumulative area spanned in time by the fire also showed a good agreement between experimental and calculated values, while minor differences between results are probably due to a wrong estimation of the ignition source (in power and/or position) and to a not accurate definition of the fuel distribution. Results provide a basis to carry out a risk analysis of fire spreading taking into account specific terrain features and vegetative characteristics of a given geographic area.

VI.5. References

- Viegas D.X., Cruz M.G., Ribeiro L.M., Silva A.J., Ollero A., *et al.*: Gestosa fire spread experiments. In 'Proceedings of the IV International Conference on Forest Fire Research and Wildland Fire Safety', Luso, Portugal, 18–23 November (2002).
- Barboutis J.A., Philippou J.L.: "Evergreen Mediterranean hardwoods as particle board raw material" *Building and Environment*, 42(3) 1183–1187 (2007).
- Malangone L., Russo P., Vaccaro S.: "Fire behaviour in canyons due to symmetric and asymmetric ignitions". International Congress *Fire Computer Modeling* October 18-19 Santander (Spain) (2012).
- Malangone L., Russo P., Vaccaro S.: "The role of the terrain geometry on the flames propagation through a vegetative fuel bed", *MCS 7 Chia Laguna*, Cagliari, Sardinia, Italy, September 11-15 (2011).
- Viegas, D.X., Pita, L.P., Fire spread in canyons, *International Journal of Wildland Fire*, **13**, pp. 253-274, 2004.

Chapter VII

Conclusions

In this PhD thesis the forest fire phenomenon was investigated by means of the physical model WFDS. The results here presented showed the ability of the model to provide information in order to deduce the rate of spread and the area spanned in time by the fire in some particular terrain configurations.

The performed simulation study on flames spreading across grasslands confirmed the strong dependence of the fire propagation rate on the wind velocity and the terrain slope. Their effect on the propagation of the fire was expressed through a simple relationship, which takes into account the contribution of these two parameters: the ROS resulted to have a stronger dependence on wind velocity rather than on the terrain slope. However, the need to adopt a further parameter which gives information also about the area spanned by the fire in time was also pointed out.

The analysis of the propagation of a wildfire through a tree stand offered the possibility to study the main parameters affecting the development of a crown fire. In particular, the role of the surface fuel bulk density (ρ_F) in regulating the transition from a surface fire to a crown fire was evidenced. By reducing ρ_F and, hence, the biomass at the ground level, the intensity of the fire is reduced and the crown fire is arrested or only limited to the tree needles without affecting the woody part of the tree canopies. Therefore, the surface fuel bulk density regulates the fire burnout time, which is responsible of the destructive effect in term of fuel burned in a real forest environment.

The results obtained for the double-inclination domain showed that the fire spreading rate on a plane is dependent not only on the fuel bed properties and its slope but also on the boundary conditions, namely the fire spread properties at the edge of the given fuel bed. Indeed, the change in inclination of a plane originates ignition sources having different shapes and energies on the plane located just ahead of it. The agreement between experimental and simulated results was satisfactory, but failed partially when considering high inclination (both positive and negative) with respect to the horizontal plane.

The dynamic behaviour of the fire was also observed in canyon configuration where the fire growth is relatively slow at the beginning, and then increases very rapidly and the time lag for this transition depends on the moisture content and/or the fuel properties. In this case, the pre-heating of

the unburnt fuel is strongly promoted: this affects the fire phenomenon by accelerating its rate of spread. The study of fire propagation in canyons was extended considering also the role played by the position of the burning source, namely symmetric and asymmetric ignition. In the second case the fire growth is relatively slow at the beginning and, then, increases very rapidly and the time lag for this transition depends on the fuel properties and on the characteristics on the canyon. An acceleration in the surface spanned in time by the fire occurs just in correspondence of the canyon water line. In this position fire becomes a new heat source for the next ridge but its intensity and shape cannot be deduced easily. A quantitative analysis of the results indicated that the classic approach, which consider the ROS as the main parameter in describing fire spreading is not sufficient in this case and in all the conditions where a preferential path of fire propagation is not present.

Application of WFDS to study how the fire spreads across a real domain with a complex configuration confirmed a strong dependency of the terrain heterogeneity on the time profiles of the fire front. At the level of resolution adopted, WFDS was not able to directly resolve the fire behaviour details in the grass fuel bed, but the fire/domain interactions that occur over scales on the order of a few meters could be resolved. This level of resolution of the fire physics was sufficient to capture the dynamics of the fire perimeter and also to highlight the role of the domain geometry (canyon) in generating an eruptive fire. Results of the cumulative area spanned in time by the fire also showed a good agreement between experimental and calculated values, while minor differences between results were probably due to a not adequate simulation of the ignition source (in power and/or position) and to a not accurate definition of the fuel distribution, since the limited information on experimental procedure.

The extension of this kind of study to other geometries and ignition conditions can provide a significant aid in understanding the factors that can influence the fire behaviour, giving a large contribution to increment personal safety during fire suppression activities. Results provided a basis to carry out a risk analysis of fire spreading taking into account specific terrain features and vegetative characteristics of a given geographic area. However, due to their computational requirements, it is unlikely that in the near future the code adopted, and probably the other physically-based codes as well, at least in their present form, will replace present day operational models and approaches. With respect to empirical models they have the potential to provide reliable and detailed predictions of the behaviour and effects of fire over a much wider range of conditions. Therefore, it is desirable that the near term research applications will include their use in the assessment of the effect of fire on vegetation during prescribed burns, the response of a fire to a given fire break or thinning strategy and understanding of the behaviour and spread of fires through the intermix of structural and vegetative fuels

that characterize wildland-urban interfaces. Furthermore, also the complex way to implement all the information needed for the numerical simulation may limit the use of these computational codes. For instance, in WFDS a user graphic interface is missing and all the data required for the execution of the calculation have to be provided through a text file structured as command lines: this step is a very long time consuming activity and requires advanced skills and competence. Therefore it is justified its classification as a preventive tool for the investigation of fire behaviour rather than a real-time instrument for fire safety and emergency management